ABSTRACT

Title of Document: EVALUATION OF OPTICAL SENSOR PLATFORMS FOR MULTIPLEXED DETECTION OF PROTEINS

Samantha Anne Spindel, Doctor of Philosophy, 2014

Directed By: Adjunct Professor, Kim E. Sapsford-Medintz, Fischell Department of Bioengineering

This work investigated optical sensor platforms for protein multiplexing, the ability to analyze multiple analytes simultaneously. Multiplexing is becoming increasingly important for clinical needs because disease and therapeutic response often involve the interplay between a variety of complex biological networks involving multiple, rather than single, proteins. Moreover, one biomarker may be indicative of more than one disease, similar diseases can manifest with similar physical symptoms, and monitoring a disease requires the ability to detect subtle differences over time. Multiplexing is generally achieved through one of two routes, either through spatial separation on a surface (different wells or spots) or with the use of unique identifiers/labels (such as spectral separation – different colored dyes, or unique beads – size or color). We looked into combining both spatial separation and unique labels to further expand the multiplexing capabilities of surfaces. Our original research resulted in one of the few demonstrations of reactive semiconductor nanocrystal

immunoassays for multiplexed analysis within a single well on a microtiter plate. Innovative planar surface fluorescent immunoassays were developed for both spatial and spectral multiplexing using Quantum Dots and prospective incorporation into a Point-of-Care (POC) device involving an evanescent wave scanner. These assays used standard microscope slides combined with flow cells and were designed to markedly reduce the amount of sample and reagents needed as compared to standard 96-well plate assays. The platform was optimized for detecting Chicken IgG and Staphylococcal Enterotoxin B (SEB); SEB is commonly used in the literature to characterize the performance of biosensor platforms. The planar surface fluorescent immunoassays were applied to a real-world public health need to detect renal injury. Two emerging novel biomarkers, Kidney Injury Marker-1 (KIM-1) and Neutrophil Gelatinase Associated Lipocalin (NGAL), were investigated for their potential to detect injury earlier and with more specificity than current methods using serum creatinine (SCr). Detecting these medically-relevant markers using planar surface fluorescence immunoassays could potentially allow for more rapid diagnosis of acute kidney injury (AKI), among other uses.

EVALUATION OF OPTICAL SENSOR PLATFORMS FOR MULTIPLEXED DETECTION OF PROTEINS

By

Samantha Anne Spindel

Dissertation submitted to the Faculty of the Graduate School of the
University of Maryland, College Park, in partial fulfillment
of the requirements for the degree of
Doctor of Philosophy
2014

Advisory Committee:
Dr. Kim Sapsford-Medintz, Chair
Dr. Ian White, Co-Chair
Dr. Robert Briber (Dean's Representative)
Dr. Yu Chen
Dr. Benjamin Fisher
Dr. Alan Huston

Dedication

This work is dedicated to the memory of my grandparents, Florence and Herbert Spindel and Maria and Alfredo Purificacion, and my Great-Aunt Lourdes Z. Nisce.

Acknowledgements

I wholeheartedly thank my advisor, Laboratory Leader, and Chair of my committee, Dr. Kim E. Sapsford-Medintz for her help and guidance throughout the past few years. Her direction, wisdom, and support made this work possible. I appreciate Dr. Benjamin Fisher for his encouragement and support as Deputy Director of the Division of Biology, but also for continuing to provide guidance while serving in a new capacity at the Food and Drug Administration. I thank Dr. White, the Co-Chair for my committee, for serving in this role and for providing helpful feedback with regard to the Ph.D. process. I thank Dr. Alan Huston and our other collaborators at the Naval Research Laboratory for providing materials and valuable ideas. I thank Dr. Yu Chen for serving on my committee and for providing valuable feedback regarding my research. I acknowledge the assistance from my Division Director, Dr. Marilyn Lightfoote, who provided me with the opportunity to work at the Food and Drug Administration and who has supported my academic endeavors. I thank Dr. Peter Goering, Mr. Ronald Brown, and Dr. Qin Zhang for the rat samples used in these studies. I am grateful for the consultation and assistance my laboratory members Dr. Angela Mariani, Dr. Andrew Yeatts and Mr. Josh Balsam provided, which contributed to some of the results featured in this work. I am happy and thankful to have such a good friend in Leah Buerman who reviewed my dissertation and provided comments. I thank my sister, Elena Spindel who has helped make me who I am today. I am grateful for my parents Steven and Helen Spindel and fiancé Justin Musaffi for their belief in me, words of encouragement, and for their never-ending support and love.

Table of Contents

List of Tables

List of Figures

Chapter 1: Motivation, Objectives, and Innovation

Technological advances in fields such as genomics, proteomics and metabolomics have advanced understanding of the underlying mechanisms of disease initiation, disease progression, and therapeutic response, and helped identify biomarkers useful in personalized medicine [1-3]. These biomarkers, such as proteins, can serve as diagnostic, prognostic, or therapeutic indicators and typically represent a surrogate endpoint used in addition to, or instead of, a clinical endpoint. Development of novel devices for biomarker measurement is important to the field of personalized medicine, a term which is defined in numerous ways. For the purpose of this work, personalized medicine is providing the best treatment specific to a patient's individual genetic, genomic, or proteomic profile to guide safer and more effective treatment [4-6]. Information about a patient's make-up on a cellular level can provide clues regarding the appropriate medication, pertinent drug dosage, disease state, or method for disease prevention [4]. The ultimate goal of personalized medicine is to achieve the 5 Rs: "the right patient, right diagnosis, right treatment, right drug/target, and right dose/time". Such a goal can only be realized through the combination of a clinical approach to medicine, completion of a comprehensive medical history, and utilization of data from appropriate testing such as *in vitro* diagnostic devices.

In Vitro Diagnostics (IVDs) are assays that probe samples taken from a patient (urine, blood, nasal swabs, etc.) for molecules in the genome, epigenome, or proteins and may be used for clinical diagnostics or prognostics or to aid in treatment selection [7]. Specific IVDs that are developed in parallel with a therapeutic agent, and are used in

conjunction with one another as specified on the labeling of the drug and device, are called companion diagnostics [6]. Specific analytes that IVDs probe are considered "biomarkers" if they can be objectively measured and evaluated and indicate normal or pathogenic biologic processes or pharmacologic responses to a particular therapeutic intervention [6, 8]. There are three major categories of biomarkers—biomarkers of exposure (e.g. diagnosis/identification of disease or to predict response to therapy), susceptibility (e.g. to distinguish patients with indolent or aggressive disease), and toxicity (e.g. to identify patients likely to develop adverse side effects) [9]. Ideally, the most useful IVDs should be high-throughput, rapid, and capable of real-time detection of many biomarkers. IVDs for personalized medicine should also be paired with a specific drug or drug combination that would be able to treat the patient safely and effectively with minimal adverse effects [10]. The scope of this work is to develop a new method capable of biomarker multiplexing (detecting multiple analytes simultaneously).

Significance of Multiplexed Protein Detection

Multiplexing is becoming increasingly important because disease and therapeutic response often involve the interplay between a variety of complex biological networks rather than single proteins [10]. DNA and proteomic microarrays have been crucial in identifying new biomarkers and will continue to play a significant role in their routine detection [4, 5, 11-15]. While many efforts have been made to understand the biological basis of diseases by studying gene expression, the relationship between an expression of a gene and the onset of disease remains

unclear, but the relationship between protein profiles and disease onset is becoming more understood [16]. As there are only around 25,000 genes in the human genome, but genes code for multiple variants of proteins, researchers often use proteomics, rather than genes, to provide insight into diseases [17] and new analytical tools can assist in this process [5, 6]. Multiplexing is important for immunoassays, a biochemical technique that uses antibodies for measuring the amount of a specific macromolecule present in a sample. Since antibodies are created due to the body's immune response against viruses, bacteria, and other hazards, using these biological molecules for detection purposes achieves superb specificity and sensitivity [17]. Concentrations as low as 10^{-21} moles/L have been detected using immunoassays [17]. Multiplexing can increase throughput and increase data generation while simplifying formats and decreasing the time and cost required to operate tests [18].

Device Attributes

Appropriately-designed IVDs can be particularly useful as point-of-care (POC) diagnostics, which may be used in a doctor's office or at home and can reduce the time, sample volume, and reagent volumes required as well as the overall cost of the test. Since many IVDs are homogeneous and simple to use (e.g., glucose test strips or home pregnancy tests), requiring only one mixing/sample addition step and one detection step, there is potential for these types of assays to become miniaturized and incorporated into high-throughput, POC devices [7, 19, 20]. As they are currently designed, standard techniques involving microtiter plates are not currently suited for a

POC environment because they are complicated and require trained personnel for operation.

A POC device must be cost-effective, highly accurate, low maintenance, easy to use, portable, robust, stable under harsh environmental conditions, have minimal user interface, have a rapid turnaround time, and be capable of high-throughput [21]. For home care or other "in the field" applications, the device must be relatively small in size (not much larger than a cellular phone), so the sample volume required to detect analytes should be $\leq 50\mu l$. Detection of analytes in low volumes is particularly relevant for situations in which certain sample types may be limited in volume, such as critically ill, neonatal, or pediatric patients. However, sample size is less of an issue for multiplex assays, which can be miniaturized. Efforts to miniaturize assays have involved microfluidics, lab-on-a-chip technologies, and improved excitation and detection methods [7, 19, 20, 22]. These advances are key for the integration of all aspects of an assay (sampling, testing, and detection) onto one hand-held platform to create a true biosensor [23]. A biosensor is defined by the International Union of Pure and Applied Chemists (IUPAC) as a self-contained device that provides quantitative analytical information using a biological recognition element such as an antibody or nucleic acid, which is in direct contact with a transduction element [10]. While the goal of this work was not to create a POC biosensing device, these device attributes were crucial in the design of the assay platform to allow for POC development in the future.

Real-World Applicability: Acute Kidney Injury Biomarkers

The main theme of this work was investigation of optical sensor platforms to study multiplexing capabilities using decreased sample volumes. Since the bulk of the work was on the evaluation of a new platform, relatively inexpensive proteins were used to characterize the platform and allow for comparison among platforms. However, to demonstrate the relevance to personalized medicine, we also investigated whether this platform could be used to measure renal injury biomarkers associated with Acute Kidney Injury (AKI), which is discussed in greater detail in Chapter 5. Measuring relatively new biomarkers such as Kidney Injury Marker-1 (KIM-1) and Neutrophil Gelatinase-Associated Lipocalin (NGAL) may improve personalized medicine by diagnosing patients correctly and quickly (earlier than existing methods allow) so that treatment can be administered based on the particular needs of the patient [24-26].

Current tests for diagnosing AKI involve measuring blood urea nitrogen and serum creatinine, but these biomarkers are typically not elevated until 50% of kidney function is gone, which is clearly not adequate for reducing or preventing AKI [27].

Diagnosing AKI at the POC using a small amount of sample is important in a number of clinically relevant situations. For example, a POC device could be used in the scenario of a biological attack where the lipopolysaccharide (LPS) of gram-negative bacteria could elicit an innate immune response [28, 29]. Exposure to LPS (endotoxin) can cause systemic vasodilation and decreased renal perfusion and

subsequent AKI [28]. Additionally, the resulting inflammation and cytokine release following exposure to the toxin will likely cause a nephrotoxic effect, leading to elevated levels of NGAL and KIM- 1, which could indicate early kidney damage [29]. In another example, a POC device is useful in the developing world, where AKI is a major medical complication particularly with regard to sepsis, diarrheal illnesses, and infectious diseases. In this environment, low-resource medical tests are needed. A third scenario where a POC device would be useful for AKI diagnosis is following crash injuries and natural disasters such as earthquakes, which could adversely affect kidneys. Lastly, rapid diagnosis of AKI is important because early diagnosis—leading to quickly-instituted treatment—results in more favorable outcomes for the patient. In these examples, testing and treating patients rapidly is of the utmost importance, and providing care to a large population using minimal resources can be facilitated by use of a POC device capable of multiplexing and using small samples.

Objectives

This work aims to address the concerns regarding current techniques for multiplexed biomarker detection using optical sensing platforms. *Specifically, the goal of this work is to evaluate technologies for multiplexing. This project investigated the multiplexing potential within a single well in a microtiter plate and the development of a novel multiplex immunoassay platform, planar surface fluorescent immunoassays, that can detect protein biomarkers in a manner that is amenable for further development into a POC device. The evaluated platforms were investigated with regard to limit of detection, specificity, and other performance parameters.*

LOD is defined as the concentration at which the signal is larger than the background signal plus three standard deviations. In these studies, the LOD was specified as the lowest concentration measured for which the intensity meets the requirements defined above rather than that extrapolated from a curve fit plot.

The primary objectives are:

1) Develop a new planar surface fluorescent immunoassay capable for protein multiplexing at low sample/reagent volumes. Multiplexed, low-volume planar surface fluorescent immunoassays were created with various surface modifications. In addition, several microfluidic designs and fluorescence detection mechanisms were tested and optimized.

2) Characterize the developed platform by using model protein analytes and evaluate its multiplexing capability. Direct and indirect sandwich assays were conducted to detect two common analytes. The planar surface fluorescent immunoassays performed similarly to fluorescent immunoassays conducted using microtiter plates. These results are particularly promising for biomarker detection for which larger volumes may not be obtainable.

3) Demonstrate the applicability of this developed platform for a real-world public health need to detect renal injury biomarkers. Current strategies for diagnosing and treating acute renal injury are flawed because they may only detect renal damage after 24 – 72 hours [24]. New biomarkers, Neutrophil Gelatinase-Associated LiPoCalin

(NGAL) and Kidney Injury Marker-1 (KIM-1) have been identified as having the potential to detect different aspects of renal damage after only two hours post injury [24, 25]. Detection of these proteins involved in AKI could allow for earlier intervention and better patient outcomes. The developed platform was tested using these biomarkers to investigate the feasibility and clinical utility of this technology. Application of this platform to renal injury biomarkers demonstrated that the system is capable of multiplexing, and can detect the analytes above baseline levels.

4) Evaluate multiplexing capability in standard fluorescent immunoassays utilizing microtiter plates in combination with unique Quantum Dot (QD) labels. In this phase of experiments, standard laboratory assays were performed involving microtiter plate fluorescent immunoassays using a variety of protein analytes. The multiplexing capability was investigated within a single well on the plate using QDs as unique labels to facilitate multiplex analysis. (QDs will be discussed in more detail in Chapter 6). Different detection labels were compared and LODs were established. Identifying the performance properties of plate immunoassays for multiplexing proteins using QDs allowed for the comparison of similar studies involving planar surface fluorescent immunoassays.

5) *Characterize the use of a unique evanescent wave detection platform to image QD-based planar surface fluorescent immunoassays*. In these experiments, we demonstrated that spatial and unique-label multiplexing on a glass slide can increase the potential number of analytes measured using this platform. We showed that the

filter and camera combination (detection system) can distinguish between two QDs bound within the same spot. Theoretically, this platform can be extended to detect multiple QDs within a single spot. This platform is amenable to a POC environment using an in-house developed evanescent waveguide detection system.

Innovation

Smaller Sample Volume

The planar surface fluorescent immunoassays developed here can be used for multiplexing and perform similarly to fluorescent immunoassays executed in a standard 96-well microtiter plate in terms of sensitivity and LOD. However, the planar surface immunoassays require distinctly less sample volume and reagents to perform experiments. A standard microtiter plate immunoassay requires 50 - 100 µL of sample or reagent per well [30]. Immunoassays have been conducted using microscope glass slides in many formats, including sandwich and reverse phase formats. Additionally, many different chemical modifications for immobilizing antibodies onto the surface have been used to conduct immunoassays. Despite their differences, most planar surface immunoassays require a sample volume in the high micro-to-milliliter range [31-34]. The use of vinyl/polycarbonate/acrylic templates developed in this work have the potential to detect analytes with much smaller volumes (e.g. 2µl). This is less than one-tenth of the volume that is needed for one well in a microtiter plate, and this volume can be used to quantify nine different spots for analysis using planar surface fluorescent immunoassays.

Small sample size confers an important advantage in that there may be less influence from matrix effects on the assay when experiments are conducted in biological fluids such as plasma and urine [17]. Different sample sizes, each containing the same amount of analyte may provide different results. However, in small samples, there is a lower proportion of the sample in the reaction, so the influence of matrix effects may be diminished and the accuracy improved. Consequently, an assay with a smaller sample size may be more sensitive and more robust.

The use of such small volumes is important for medical practice because large volumes of sample may not be obtainable from certain patients, such as infants or the critically ill [35-37] or from all sample types, such as tissue biopsy or cerebrospinal fluid [38-43]. Use of small sample volumes could enable the use of capillary blood taken from the finger of a patient rather than venous blood, requiring a phlebotomist's assistance. In this project, the focus is on the critical public health need to detect acute kidney injury earlier than current methods allow and with greater sensitivity. When a patient's kidneys are damaged, the production of urine may be inhibited, so performing a test on a small volume of fluid can be useful [29].

Smaller System

As opposed to the detection method for fluorescent immunoassays (e.g. use of microtiter plate reader), which typically requires large instruments coupled to a computer for quantitative output, the new platform that was investigated in this project may be more amenable to a POC environment. Although miniature ELISAs

and chip-based flow cytometry have been demonstrated as a proof-of-concept, no such devices have been commercialized, so the need to develop a POC biosensor is still paramount [44-46].

The planar surface fluorescent immunoassay platform is much smaller than a typical microtiter plate. The planar surface platform is only 75 mm (length) x 25 mm (width) x 1 mm (height), but the microtiter plate is 127.64 mm x 85.60 mm x 14.3 mm. Since the former has a smaller area, it can more easily fit into a hand-held device for on-the-spot analysis as opposed to the microtiter plate, which requires use of a plate reader such as the TECAN, which costs ~$65,000 dollars, weighs 29.5 kg and has dimensions as follows: width of 515 mm, height of 257.5 mm, and depth of 516.9 mm.

The detection method for analyzing the signal (mean fluorescence) of biomarkers for the planar surface fluorescent immunoassay platform could be coupled to a charge-coupled device (CCD) or complementary metal–oxide–semiconductor (CMOS) camera [47]. In this setup, either a light-emitting diode (LED) or a small laser diode could be used as the excitation source, but the LED may be more advantageous to cover the whole device, rather than a laser, which would have to move over a large distance in order to illuminate the entire surface, unless the laser causes total internal reflection fluorescence, which is described in more detail in Chapter 6. Using the platform to detect clinically-relevant biomarkers could potentially impact clinical practice because if the device is portable, disposable, cost-effective, requires minimal

user interaction, and meets a clinical need to obtain relevant information about analytes in small volumes [21], physicians could make diagnostic, prognostic, or therapeutic decisions more quickly than with existing technology [36].

Improvement upon Current Techniques

Currently, multiplexed optical biosensors are less robust than ELISA when probing for molecules within plasma or serum [10]. Furthermore, multiplexed immunoassays may exhibit cross-reactivity among capture antibodies, especially when target antigens may be present at varying concentration ranges. Lastly, immunoassays are prone to matrix effects, which can diminish sensitivity. While ELISA would also be prone to matrix effects, the enzyme amplification is generally more sensitive than fluorescent sandwich immunoassay that lacks the amplification step. This work sought to overcome these issues by testing an innovative optical sensor platform.

The approach for experimentation in this work is also novel in terms of testing the same samples across optical sensor platforms. Typically, studies conducted by one research group do not involve comparison of the same analytes among many platforms. Comparing optical sensor platforms while keeping the antibody and stock antigen sources, buffer solutions, and other reagents consistent across experiments enables comparison among the two main detection strategies: fluorescent immunoassays (performed in microtiter plates) and planar surface fluorescent immunoassays. Specific parameters that are of interest when comparing platforms include LOD, specificity, sensitivity, reproducibility, reliability, robustness, cost,

speed, and multiplexing capability. Conducting new experiments using all of these platforms is more advantageous than comparing experiments using the proposed platforms to existing studies published in the literature because among scientific research groups, there are variations in protocols and reagents, etc. However, we chose SEB for investigation so that we could also compare our results to those published in the literature. These studies will build upon the scientific community's growing interest in multiplexing, which has developed within the last decade [10]. This work adds to the scientific knowledge available regarding comparison of novel multiplexed arrays to existing sensing technologies, and may shift current research toward new platforms.

The multiplexing approach demonstrated here is novel in that both spatial and spectral multiplexing were achieved using QDs. This technique can increase the multiplexing capabilities for immunoassays because multiple QDs have broad absorption bandwidths and can be excited at one particular wavelength, yet they each have a narrow spectral bandwidth within the visible range. Therefore, the signal from each QD can be distinguished from one another. Studies involving detection of two analytes within a single spot were demonstrated using planar surface fluorescent immunoassays. Similarly, experiments using 96-well microtiter plates succeeded in deconvoluting signals from three different QDs corresponding to three different target analytes. These accomplishments indicate that, for example, a 96-well plate can yield more than 96 data points because more than one target analyte can be detected per well. The duplex using the planar surface fluorescent immunoassay can yield 216

data points, while the triplex using the 96-well plate can generate 288 data points. There is promise to extend these studies to distinguish between even more analytes by employing more than three QDs so long as their emission wavelengths are spectrally diverse.

The planar surface fluorescent immunoassays can be incorporated into a POC device and could impact science and engineering fields. Sensing multiple biological elements simultaneously using low sample volume and with increased sensitivity are desirable properties for many applications ranging from food safety and monitoring of agricultural products to military applications [48].

Chapter 2: Background

There are many different methods for quantifying protein analytes, such as the use of mechanical, electrical, or chemical sensors [49-53]. Current issues with these biosensing strategies include less than optimal limits of detection, low sensitivity and specificity, in addition to an inability to detect different analytes simultaneously (i.e. multiplexing) in an automated fashion [50]. Optical sensors are advantageous over many other detection strategies because they are immune to inferences from electrochemical and electromagnetic sources, are capable of real-time detection, and are amenable to lab-on-a-chip applications [54, 55].

This work focused on optical sensors that are capable of multiplexed protein detection. The gold standard for protein detection is Enzyme-Linked Immunosorbent Assay (ELISA), which can measure multiple targets using different wells (i.e. spatial separation) using colorimetric, fluorescent, or luminescent techniques [10]. This work focuses on the fluorescent assay. There are two main types of multiplexing strategies—spatial separation on a surface (i.e. different wells or spots) and the use of unique identifiers/labels (i.e. spectral separation due to different colored dyes or bead sizes/colors). Two commonly used fluorescent assays capable of multiplexed protein detection are standard microtiter plate fluorescent assays and the Luminex 100/200. Standard optical methods of multiplexed protein detection often require large instrumentation, highly-trained personnel, and must be performed in a typical laboratory setting [56, 57]. Point-of-Care (POC) devices, on the other hand, have many advantageous attributes as discussed in Chapter 1 such as their cost-

effectiveness, low maintenance, and portability. Various research groups have demonstrated viable POC devices capable of protein multiplexing, but few are available for commercial purchase [45, 46]. For example, some portable particle counters are on the market for very specific applications. More products are needed to detect other analytes.

Biosensors

A biosensor is defined by the International Union of Pure and Applied Chemists (IUPAC) as a "self-contained device that provides quantitative analytical information using a biological recognition element such as an antibody or nucleic acid, which is in direct contact with a transduction element" [10]. In other words, biosensors use a biological system to differentiate substances of interest from other components in a sample by employing a biological receptor to detect the analyte, a transducer to convert the recognition event to a signal, and a detection system that includes analysis and processing [17].

Antibodies are glycoproteins involved in host defense systems [17]. There are five human immunoglobulin classes: IgG, IgM, IgA, IgD, and IgE, but the first class of antibodies is used most often for biosensing needs because it is produced in the highest amounts following immunization, has a high affinity for the epitope, is stable during isolation, and has many functional sites that can be accessed for chemical coupling. Antibodies are composed of two identical heavy polypeptide chains that contain three constant domains and one variable domain. Each variable domain on

the heavy chain is linked to an identical light polypeptide chain, which contains a constant domain and a variable domain. The variable regions of antibodies are capable of binding to an antigen or immunogen at different sites called epitopes with great specificity.

There are a variety of biosensing platforms that have been developed to detect DNA or proteins through electrochemical, photometric, mechanical [49], piezoelectric [50], or optical methods of detection [10] such as the use of surface plasmon resonance [51] or with mass spectroscopy [58, 59]. Some biosensors are composed of nanomaterials [52], while others use microcantilevers [53], and other methods of detection that may involve label-based or label-free techniques [60]. Current issues with these biosensing strategies include less than optimal limits of detection, low sensitivity, and low specificity relative to the demands of specific applications. In addition, many biosensors are unable to detect different analytes simultaneously in an automated fashion [50]. Multiplexing is possible by employing a variety of different types of detection mechanisms. Optical sensors are advantageous over many other detection strategies because they are immune to interferences from electrochemical and electromagnetic sources, are capable of real-time detection [54], and are amenable to lab-on-a-chip formats [55].

Importance of Multiplexing for Clinical Use

Many scientific fields can benefit from the use of multiplexed optical sensors. For example, it is important for the food industry to test for various toxins that could be a

threat to public health. The U.S. Department of Defense may also be interested in these sensors for measuring biological threats in a field-deployable format [50]. The focus of this work is on the development of multiplexed biosensors for clinical use.

The need for the development of a multiplexed biosensor for use in clinical practice is paramount for therapeutic purposes and diagnostic purposes where both identification and quantification of biomarkers (analytes that indicate normal or pathogenic biologic processes) are important [35]. It is important to measure many different analytes simultaneously (multiplex) because one biomarker may be indicative of more than one disease, similar diseases can manifest with similar physical symptoms, and monitoring a disease requires the ability to detect subtle differences over time [36]. For example, due to the inter-relatedness of biomarkers, profiling as many as 70 genes or more than 100 antibodies may be required to predict a specific cancer patient's diagnosis or possible response to chemotherapy [10, 61].

Multiplexed sensors have the potential to revolutionize patient treatment by reducing exposure to potentially ineffective toxic drug treatments based on the assessment of many biomarkers [62]. Furthermore, multiplexed sensors can help prevent disease and prolong life if: a diagnosis is made early, patients are screened multiple times over a specific period, and only the best therapies are prescribed for patients.

Benefits of POC Biosensors in the Healthcare Field

The ideal POC device is small, portable, cost-effective, highly accurate, low maintenance, easy to use, robust, and stable under different environmental conditions [21]. The device should also require minimal user interface, have a rapid turnaround time, and be capable of high-throughput. A POC device is useful in the healthcare field because it can be used to confirm a patient's diagnosis while the patient is still present in the doctor's office, which can be particularly important if the patient is contagious or requires immediate treatment. A model POC device would require a single test sample, a single set of personnel to process and analyze the sample and a single point in time when the patient's blood or urine would need to be sampled. These benefits can help increase the likelihood of a patient to follow through for repeat care or to find out the outcome of a test, thereby improving the level of care provided.

In clinical practice, determining the presence of biomarkers typically requires a variety of laboratory tests and equipment that utilize several different types of technology. For a single diagnosis, many laboratories and various personnel can be involved in handling each test. The more laboratories and personnel needed to analyze samples for a single diagnosis, the greater the uncertainty associated with the results. Typical assays such as Enzyme Linked Immunosorbent Assays (ELISA) require each analyte to be detected individually, but multiplex POC devices can be used to probe for many biomarkers simultaneously using one uniform testing method, thereby allowing for greater consistency in the data for each analyte. Furthermore,

determining relationships between biomarkers is significantly easier and more reliable when using the same testing method as in a multiplexed POC device. Multiplex POC assays require less time, cost, and labor, and a small sample size; the sample size is often irrespective of the number of analytes tested and only dependent on the detection technique used [37].

Methods for Multiplexed Protein Detection

There are many scenarios where multiplexed sensors are applicable such as for patient diagnosis at a clinic or for monitoring a disease at home. A field-deployable multiplexed sensor is useful for detection of biological warfare agents or for detection of contaminated foods. Currently, there are many different methods for detecting proteins in a multiplexed fashion. The main techniques used for multiplexing biological molecules are described below.

Mass Spectrometry

Mass spectrometry is a technique that can be used to analyze protein mixtures and quantify thousands of proteins [63]. Measurements are conducted in the gas phase of ionized analytes. Mass spectrometers are composed of three components: an ion source to ionize analytes, a mass analyzer for measuring ionized analytes' mass-to-charge ratio (m/z), and a detector that counts the number of each m/z ion. The two most common techniques for volatizing and ionizing proteins are (1) electrospray ionization (ESI), which ionizes analytes from a liquid-based sample and (2) matrix-

assisted laser ionization (MALDI), which ionizes analytes from a dry matrix, with the former used more commonly for complex samples. This direct technique can achieve high specificity, but tends to have a lower sensitivity, and requires large laboratory equipment and is expensive to operate [17].

Surface Plasmon Resonance

There are many techniques that involve measuring molecular interactions using a label-free format including Quartz Crystal Microbalance, BioLayer Interferometry, and Resonant Waveguide Grating, but Surface Plasmon Resonance (SPR) is the leading technology [17]. SPR is a technique that measures specific molecular interactions such as the binding of proteins to antibodies where the analyte molecule in solution interacts with the molecules bound (e.g. via carbgoxmethylated dextran polymers) to the sensor surface, usually composed of a thin-gold film on a glass surface. The gold side of the sensor surface is in contact with a flow channel while the glass side of the sensor surface is positioned on a prism. Under total internal reflection, light transforms photons into surface plasmons contained in the gold layer. Light must hit the surface at a specific angle of incidence, which depends upon the refractive index in the proximity to the gold surface, in order to be reflected and reduced, generating a characteristic surface plasmon resonance (SP) band. When analytes bind to the surface, the change in mass concentration causes a shift in the refractive index, which in turn shifts the SP band and the amount of light absorbed by the detector. The angle of incidence is monitored so that detection of binding events occurs in real-time. While this technique has advantages of being label-free and

relatively sensitive, this technology typically requires laboratory-based equipment and highly-trained personnel, so it is not suitable for a POC environment.

Flow Cytometry

Flow cytometry is a technique that measures biological-labeled beads as they pass through a detector in a fluid stream, one at a time [64]. These beads are used for multiplexing by either changing the internal label used (different dyes) or the size of the beads. Flow cytometry allows fluorescent molecules associated with particles to be distinguished from free fluorescent molecules. This technique is employed in a variety of clinical applications ranging from measuring cellular DNA content to identifying disease-specific cell types for diagnostic and prognostic purposes [56, 65]. Flow cytometry is also used to perform immunoassays, such as to detect biomarkers involved in acute kidney injury [66-70]. There are many commercialized products capable of performing bead-based flow cytometry in a multiplexed fashion (e.g. Luminex products) by performing a sequential analysis on particles. Beads have been demonstrated as a means for sorting cells, proteins, or other particles of varying sizes [56]. Standard beads with a specific fluorescence intensity can be used for establishing quality control—data from samples taken over time and among different experiments can be normalized. Although flow cytometry can be used for diagnostic purposes, it is desirable to combine this technique with DNA analysis or other procedures to improve the value of flow cytometry [65]. Nevertheless, some advantages of this technique include its speed, accuracy, low background signal, reproducibility, rapidity, cost-effectiveness, and sensitivity [60].

ELISA

The most commonly used and best validated method to quantify biological molecules is Enzyme Linked Immunosorbent Assays (ELISAs), which are [10]. This method is capable of multiplexing by using spatially distinct wells that can probe for different proteins. The ELISA typically uses either a colorimetric or luminescent method for detection and causes a product of the colored reaction to absorb light in the visible range [71]. The optical density of the product is proportional to the amount of analyte measured. These assays are typically conducted using a 96-well microtiter plate. A similar method to the ELISA is the Meso Scale system, which uses an electrochemiluminescent method for multiplexing. The Meso Scale can probe for different analytes within one single well in addition to among several different wells on a single plate.

ELISAs, among many other biosensing platforms utilize the biotin-streptavidin interaction for numerous applications such as testing new materials and determining the interactions between proteins and ligands [72-75]. The biotin/avidin interaction is one of the strongest known noncovalent interactions (the association constant, $K_a \sim 10^{15}\,m^{-1}$) that occurs in nature. Biotin is an essential component of Vitamin B and its competitive binding to avidin is often utilized in assay formats [76-78]. Avidin is a protein that is commonly found in albumin, the white portion of eggs [79]. Some examples of how researchers use the avidin-biotin interaction are in conjunction with quantum dots (QDs) and gold nanoparticles [80-82].

An example of this method for conducting an ELISA is as follows (Figure 1):

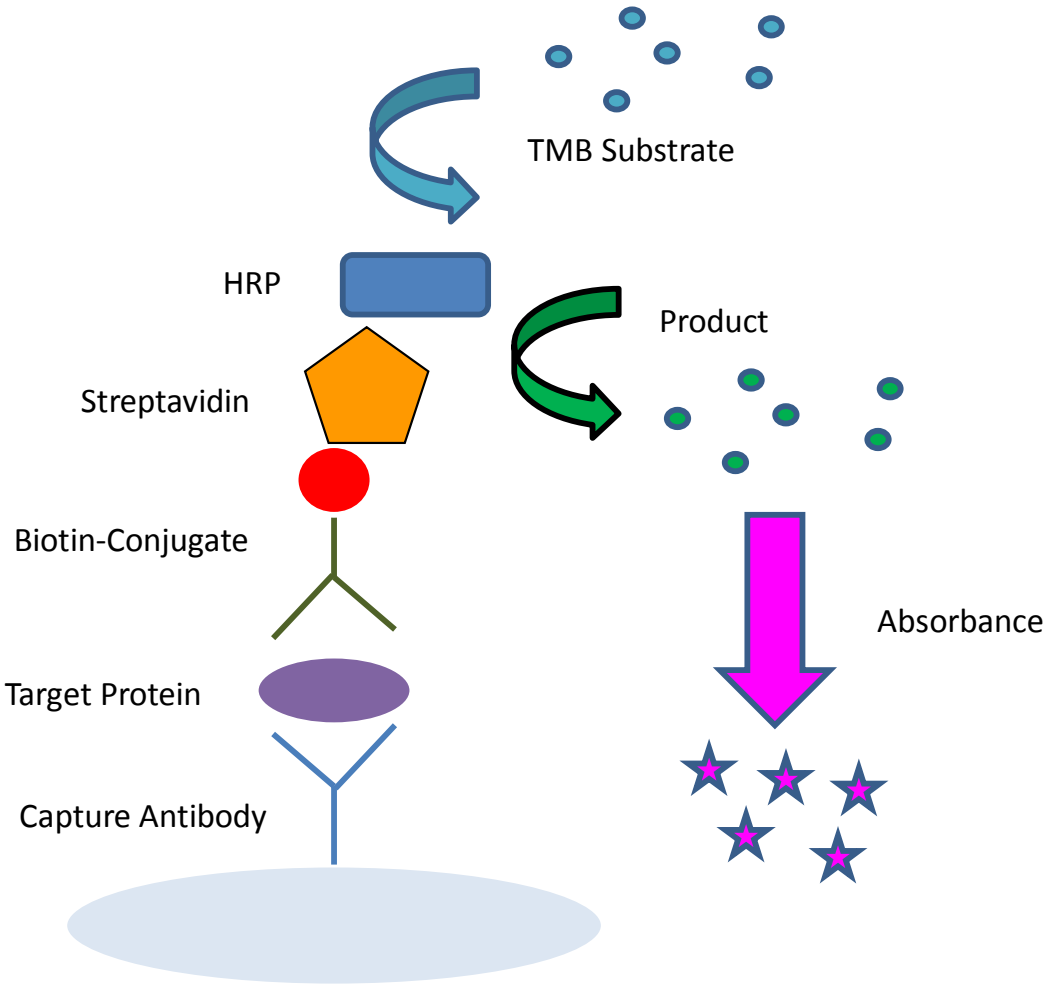

Figure 1. ELISA detection scheme using 96-well plate. The enzyme horseradish peroxidase (HRP) converts the substrate 3,3′,5,5′-tetramethylbenzidine (TMB) into a colored product measured by absorbance. .

1. Capture antibodies are immobilized onto the surface of the wells overnight, typically via non-specific interactions.
2. The next morning, the surface is blocked with a blocking buffer for 1-2 hours, depending upon the specific protocol to prevent non-specific binding to the surface. Common blocking buffers include milk or bovine serum albumin (BSA) in phosphate buffered saline (PBS), although there are a number of proprietary blocking buffers available commercially.
3. Wells are exposed to the sample containing the target protein for ~1 hr., followed by several washes to remove any non-specific binding.
4. A biotin-antibody conjugate is used to bind to the target protein and incubates for ~1 hr. Several washes are performed to remove non-specific binding between the target and the biotin-antibody conjugate to ensure that antibodies are only bound through specific biorecognition events.
5. A streptavidin-HRP (horseradish peroxidase) molecule is exposed to the wells and binds to biotin for ~20 min. Wash steps are conducted to remove any non-bound streptavidin-HRP.
6. A substrate, such as TMB (3,3′,5,5′-tetramethylbenzidine), or other chromogenic or luminescent substrate, is introduced to detect HRP. In the case of TMB, after incubation for ~20 min under low exposure to light yields a blue (Amax = 650 nm) color in the wells where the target is present.
7. Following incubation with TMB, a stop solution such as Sulfuric acid is used to stop the enzyme amplification process which turns the solution yellow (Amax = 450 nm).

8. For chromogenic-based ELISAs, the absorbance, which is an indication of the amount of sample present, is detected using a plate reader. The plate reader measures the absorbance in the 96-well plate at a specific wavelength (in the case of TMB, typically ~450 nm). For luminescent-based ELISAs, the luminescence from each well is measured by the plate reader. \

While Figure 1 shows the use of HRP as the enzyme label, there are many other labels that may be used [71]. Two others that are most commonly used are calf intestine alkaline phosphatase and *E.coli* β-D-galactosidase, but the latter is used less frequently than the first. HRP is the most popular choice as it is a relatively small protein and thus rarely causes steric hindrance and it is relatively inexpensive. However, HRP is incompatible with sodium azide and other preservatives. Alkaline phosphatase, on the other hand, is larger in size and therefore uses a lower enzyme to antibody conjugation ratio, resulting in lower activity for the number of bound enzymes. This enzyme may become inactive due to exposure to chelating agents, low pH, or inorganic phosphates. Keeping in mind the various advantages and disadvantages of each enzyme is important to ensuring that the assay performs adequately.

Just as selection of the right enzyme is important for preparing an ELISA, the correct substrate is also important. Since the two most commonly-used enzymes, peroxidase and alkaline phosphatase yield soluble reaction products, substrates that also create soluble products are appropriate [71]. Some substrates are very sensitive and have

fast reaction rates, whereas other substrates may take up to 30 minutes to product reaction products, but may be more amenable to assays where a large dynamic range is favorable. The common substrate for HRP is TMB, which is quite sensitive and produces a blue color that is measureable at 650 nm, which upon addition of the stop solution (sulfuric acid) turns yellow (measured at 450 nm).

ELISAs have limited applicability when it comes to POC requirements. Obtaining data from ELISAs typically require a dedicated laboratory and an expensive and bulky plate reader. However, Sapsford et al. demonstrated the miniaturization of colorimetric SEB ELISAs, reducing sample volume to <5 μL/well [44]. There are also some ways to decrease user interaction with experiments such as using a sequential injection analysis technique, which can automate the washing and addition of reagent solutions with the use of a syringe pump and switching valve [83]. Recently, a new technique called digital ELISA has been introduced where sub-femtomolar concentrations of proteins can be detected [17]. In this single-molecule immunoassay, a solution of enzymes are trapped in 50-femtoliter wells containing fluorogenic substrates, along with the sample, capture beads, and detection antibody, and sealed. Digital ELISA avoids reliance on diffusion, as in standard 96-well experiments requiring ~100 microliters of volume. While this technology is still in its infancy, digital ELISA is very promising for automated, high-throughput applications requiring single-molecule sensitivity.

Fluorescence Immunoassays

ELISAs are similar to fluorescent immunoassays in that they are typically conducted in sandwich formats (two antibodies specifically bind to different epitopes on a common target) [84]. However, ELISAs use an enzyme, such as horseradish peroxidase, coupled with a colorimetric or chemiluminescent substrate for signal generation, instead of a fluorescent label [85, 86]. In fluorescent immunoassays, the relative fluorescence units (number of photons emitted) are proportional to the amount of analyte present [71]. Fluorescent immunoassays do not necessarily require use of the biotin-streptavidin interaction, and may expose a dye-labeled antibody to the target protein for detection, decreasing the amount of time it takes to perform an assay. Additionally, fluorescent immunoassays are more sensitive and have a larger dynamic range compared to colorimetric assays.

Despite the difference in detection between ELISA and fluorescent immunoassays, limitations described in the literature involving ELISAs are relevant for fluorescent immunoassays. When Coenen et al. evaluated six different ELISAs for detection of the same target antibodies, the performance cutoff values, reproducibility, sensitivity, specificity, and accuracy for the detection of antibodies varied significantly, demonstrating the need for standardization among manufacturers' diagnostic tests [87]. Specifically, reagents, assays, data storage, and normalization techniques need to be standardized [37] due to the variability among similar assays.

In addition to standardization, fluorescent immunoassays are in need of other improvements. These techniques each require a variety of different laboratory equipment, dissimilar sample preparation and preservation techniques and other time-consuming procedures, as well as packaging needed to transport samples to laboratories for analysis. Microtiter well plate readers and flow cytometers are typically large laboratory instruments, and the latter requires expensive reagents and highly-trained technicians for operation [56, 57]. Although there has been scientific progress toward developing lab-on-a-chip flow cytometers, none are available for commercial purchase [45, 46].

Fluorescent Detection Labels

A variety of different fluorescent labels is available with their own specifications and may be employed in certain circumstances to maximize the LOD. Organic fluorophores (fluorescent compounds that may re-emit light following excitation) such as dimeric cyanine dyes, Cy3 and Cy5 are commonly used in the literature for quantifying proteins [88, 89]. Both dyes, are commonly used because of their brightness, because have low non-specific dye interactions, and because they are commercially available with a wide range of reactive chemistries that facilitate labeling, such as the ability to label protein lysine residues [60]. The emission and excitation wavelengths for Cy3 are 550 nm and 570 nm, respectively. The emission and excitation wavelengths for Cy5 are 650 nm and 670 nm, respectively. Although fluorescent dyes are frequently used, they have limitations such as low photostability and brightness, and intrinsic background fluorescence [90].

Quantum dots (QDs) used as fluorescent labels can be made from a variety of materials [91], but the most commonly used and best characterized QDs to date are composed of two layers—a semiconductor core (typically cadmium selenide) and shell (typically zinc sulfide) [60]. A variety of different quantum dots can be excited at the same excitation wavelength (QDs have broad excitation bandwidths), but they have narrow emission bandwidths, with the emission wavelengths very specific to the type and size of QD core material [92]. QDs are of particular interest because they possess a number of advantages compared to standard organic-based fluorescent dyes and can have increased sensitivity [33, 90]. The distinct, bright photoluminescence spectra (Figure 2) of quantum dots and their narrow emission bandwidths within the visible spectrum (Figure 2), along with other properties such as photochemical stability, high quantum yields, and large extinction coefficients, make quantum dots useful for multiplexing [33, 60, 90]. Quantum dots can be applied to both planar and suspension biochips, can be used to detect single molecules, and can be employed in fluorescence resonance energy transfer (FRET) for added specificity [90].

One drawback of QDs is their elevated cost in comparison to other fluorescent labels [93]. One way to avoid the expense associated with purchasing QDs is to synthesize them in-house [94]. Another drawback of QDs is that they are typically composed of heavy metals such as cadmium or lead, which are highly toxic materials and may pose concern when applied for *in vivo* applications [93, 95]. However, since we are concerned with their application *in vitro* and not *in vivo*, testing on living organisms is beyond the scope of this work and QD toxicity is not of a concern for our studies.

Lastly, QDs are typically larger in size than organic fluorophores, and this may disrupt the natural binding kinetics of proteins or aptamers that are involved in the biosensing platform. A comparison between the properties of QDs and organic dyes is shown in Table 1 [91].

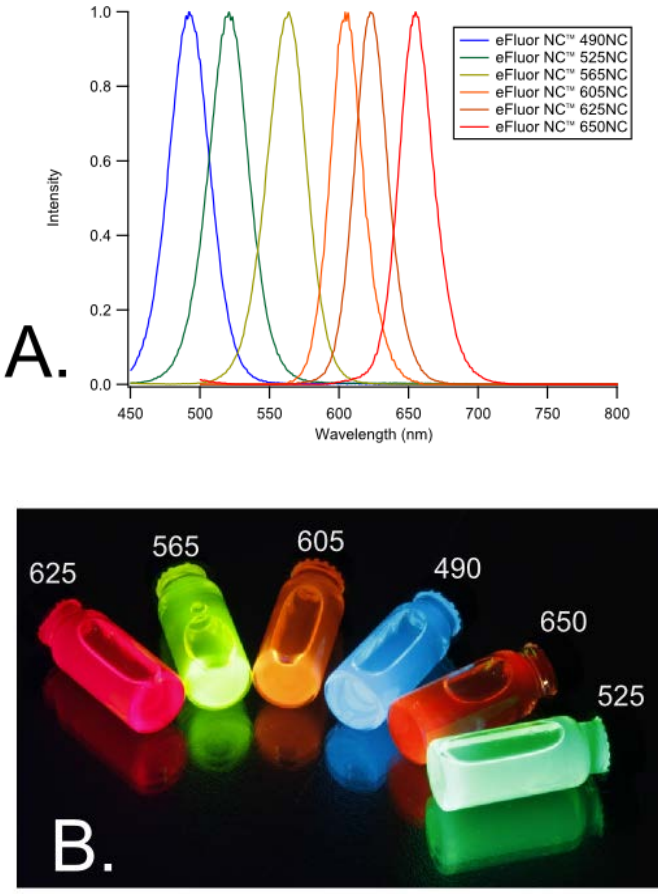

Figure 2. Properties of CdSe/ZnS quantum dots. (A) photoluminescence spectra, (B) quantum dots after UV excitation

Table 1. Properties of organic dyes and quantum dots [91]

Property	**Organic Dye**	**Quantum Dot**
Absorption spectra	Discrete bands	Steady increase toward UV wavelengths starting from absorption onset
Emission spectra	Asymmetric, often tailing to long-wavelength side	Symmetric, Gaussian profile
Stokes shift	Normally <50 nm, up to >150 nm	Typically <50 nm for visible wavelength-emitting QDs
Spectral multiplexing	Possible 3 colors (MegaStokes dyes), 4 colors (energy-transfer cassettes)	Ideal for multi-color experiments; up to 5 colors demonstrated
Quantum yield	0.5-1.0 (visible), 0.05-0.25 (NIR)	0.1-0.8 (visible), 0.2-0.7 (NIR)
Fluorescence lifetimes	1 – 10 ns, mono-exponential decay	10 – 100 ns; typically multi-exponential decay
Photochemical stability	Sufficient for many applications (visible wavelengths)	High (visible and NIR wavelengths); orders of magnitude higher than that of organic dyes
Toxicity	From very low to high; dependent on dye	Unknown
Size	~0.5 nm; molecule	6-60 nm (hydrodynamic diameter); colloid
Lifetime multiplexing	Possible	Lifetime discrimination between QDs not yet shown; possible between QDs and organic dyes
Signal Amplification	Established techniques	Unsuitable for many enzyme-based techniques, other techniques remain to be adapted and/or established

Commonly Used Analyte: Staphylococcal Enterotoxin B

Many biosensing platforms involve the use of a well-characterized target antigen, Staphylococcal enterotoxin B (SEB) [96-99]. SEB is one of many proteins produced by the bacterium Staphylococcus aureus, which when ingested may cause food poisoning in humans [100]. SEB is also a bioterrorism agent of concern and appears on the Centers for Disease Control and Prevention (CDC) list of agents in Category B because it can be disseminated easily and may cause moderate morbidity rates [101]. This toxin is often investigated to test sensing platforms as it serves as a basis to compare the LOD, sensitivity, etc. with other platforms published in the literature.

Miniaturized Assays

The standard techniques previously described are not currently suited for a POC environment. Ideally, a POC device must be cost-effective, highly accurate, low maintenance, portable, robust, stable under harsh environmental conditions, have minimal user interface, have a rapid turnaround time, and be capable of high-throughput [21]. For home care or military applications, the device must be relatively small in size (not much larger than a cellular phone), and have a sample volume required to detect analytes ≤ 50 μL. Detection of analytes in low volumes is particularly relevant for tissue biopsies for which volumes may be limited. In clinical laboratories, 0.5 mL of serum is required for antibody studies, and 0.15 mL is needed per assay. For some critically ill, neonatal, or pediatric patients, the amount of serum needed may be prohibitive for analysis. However, sample size is less of an issue for multiplex assays, which can be miniaturized.

Besides the clinical relevance of using small sample volumes, there are other advantages of using low volumes such as simplification of the platform format, an increase in sensitivity, and an increase in throughput and subsequent volume of data [18]. For example, some microfluidic heterogeneous immunoassays have been shown to detect bacterial toxins with a LOD in the femtomolar range [102]. The LOD of one miniaturized immunoassays reportedly attained 1/50th of the LODs of a classical ELISA and require 100-fold less volume [61]. This assay used a surface chemistry involving a maleic anhydride-alt-methyl vinyl ether (MAMVE) copolymer to immobilize histone proteins covalently onto the surface. The anhydride moieties on this copolymer react highly toward primary amino groups and were used to immobilize histone proteins, which then bound to autoantibodies implicated in autoimmune diseases. Other studies involving autoantibody arrays have shown four to eight times more sensitivity than ELISAs and were linear over a 1000-fold range [37]. These experiments spotted antigens onto the surface using a robotic arrayer and were probed with monoclonal antibodies or serum samples.

The use of protein array technologies for the analysis of diseases, while not a new concept, is emerging as a powerful technique for profiling protein levels and hence identifying biomarkers indicative of disease [5, 28-30]. Although many modified ELISAs exist as commercial antibody assays, the kits often require many washing steps, produce a lot of waste, are expensive, and involve lengthy processes [103]. Despite these challenges, there are also issues related to the use of microarrays such as technical problems related to printing and detection, normalization of data, lack of

reference samples between experiments and laboratories, as well as the ability to measure biomarkers that exist in samples at such varied concentrations [104].

Microscope glass slide arrays for multiplex detection of proteins have been developed previously, but the volumes needed to perform assays are still generally around 50 µL [105]. There are multiplexed platforms for proteins detection that have been developed by research groups and there are some commercially-available biosensors employing planar waveguide technology, but there is still potential for the reduction of volumes required to conduct these assays [106-113].

Protein Microarrays

Protein microarrays have many benefits over traditional ELISA and fluorescence immunoassays (performed in 96-well plates) because they are helpful for determining antibody reactivity to a large number of targets using a relatively small amount of sample and in some cases have been reported to achieve better sensitivity [114, 115]. They have been used for determining vaccination response, screening for disease-related biomarkers, and evaluating specificity of antibodies. Compared to DNA arrays, protein arrays are not as precise or reproducible [16]. Many research groups have used antibody microarrays for biomarker multiplexing and compared their results to standard ELISAs [93, 114]. While many journal articles address the potential of their platforms to be developed into POC systems, rarely are the reported systems actual stand-alone biosensors.

A variety of different types of technologies can be applied for protein microarrays. Figure 3 shows that there are multiple ways proteins can become attached to a surface such as via non-covalent or covalent attachment [116]. Different types of molecules can be immobilized onto the surface such as antibodies, peptides, or purified proteins. There are many technologies that can be used in conjunction with appropriate buffers to keep the immobilized proteins in their most active state. The figure also shows various methods for detection such as fluorescence, with some better than others for detection of low concentrations of proteins within small sample volumes. The detection method is important because there are no protein amplification procedures, unlike DNA. ELISAs can amplify the detection signal by employing an enzyme, but this does not amplify the protein itself. Based on the particular application and type of analysis desired, certain combinations of arraying technology, immobilization technique, capture molecules, and detection techniques (Figure 3) may be more suitable than others. With the right blend of microarray technologies, platforms can be designed to perform better than standard ELISA.

Protein microarrays are divided into two main groups: planar surface assays or bead/suspension assays [117]. The former can be conducted on glass, silicon, or nitrocellulose, and uses solid-phase kinetics. The latter uses micron-sized beads that may be distinguished by color code, shape, or size by using an instrument such as a Luminex. Bead assays use fluid-phase kinetics, which may allow for faster detection than using planar surface assays.

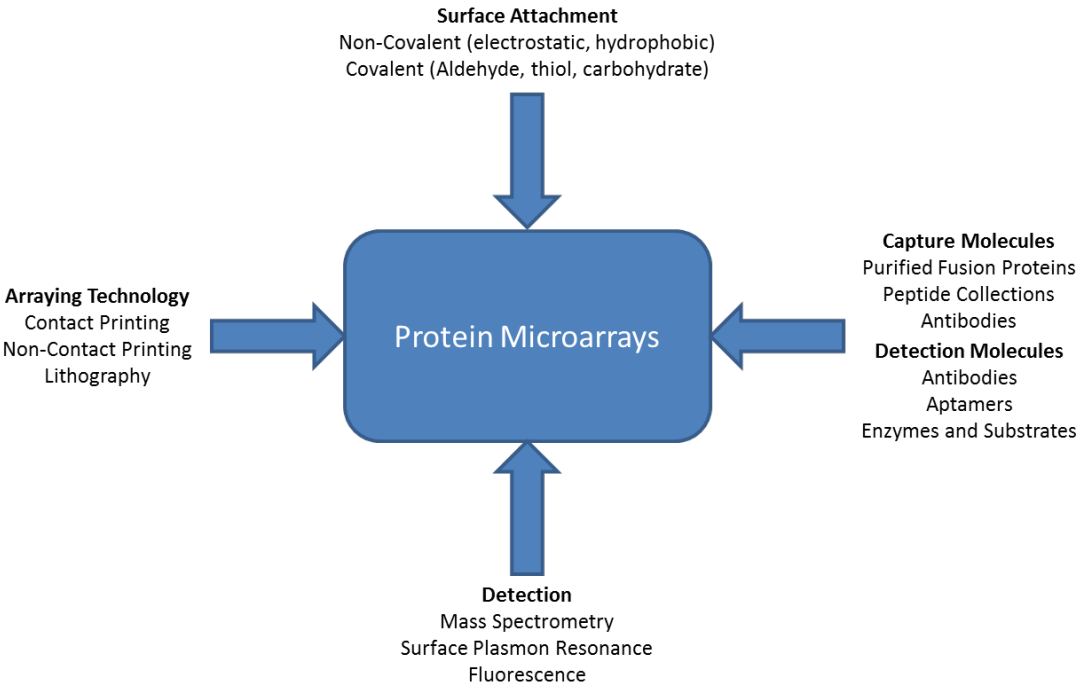

Figure 3. Different technologies for protein microarrays (adapted from Stoll, D., et al., *Protein microarray technology.* Front Biosci, 2002. 7: p. c13-32)

Within planar surface arrays, there are two main types of quantitative protein microarrays: forward and reverse arrays [16]. Forward protein arrays involve immobilizing antibodies onto a surface and assessing the protein levels in samples that bind to the immobilized antibodies. On the other hand, reverse phase protein arrays bypass the need for a capture antibody because extracts from clinical samples are printed onto the surface which is then probed with proteins or antibodies [118]. These types of assays are often used to assess phosphorylation status [16]. Reverse phase assays have relatively low sensitivity compared to forward phase assays because when a protein is present at a low concentration, less proteins of interest bind

to the surface compared to others, so primary antibodies have fewer binding sites available. However, reverse phase assays are only limited by the availability of high-affinity antibodies [118]. Since reverse phase formats rely on a single antibody, extensive validation is necessary for this type of assay. Reverse phase assays are common for autoantibody profiling [36].

Biological Molecule Immobilization

As mentioned, there are a variety of methods for immobilizing biological molecules onto different surfaces, using various buffers (Table 2). One common method for immobilization is via nonspecific physical absorption; this technique is not as effective and reproducible as employing covalent binding [16]. Covalent binding is advantageous because only certain reactive groups are involved in forming bonds. Primary amines on the amino acids lysine and arginine are frequently used as the reactive group for binding because these groups are present on essentially all proteins. The most commonly-used amine-reactive chemistry is N-hydroxysuccinimide (NHS) and 1-ehtyl-3-(3-dimethylaminopropoyl) carbodiimide (EDC) because EDC is reactive with the carboxyl group present on the surface. However, this method is prone to issues such as hydrolysis of EDC in aqueous environments, susceptibility to cross-linking, and the requirement for more than 1000-fold excess of reagent, which can cause mixed avidity and heterogeneous architecture [18].

Table 2. Biological molecule immobilization techniques

Reference	Buffer	Immobilized Molecule	Technique	Surface
[119]	PBST Blocking agent: PBST + 3% skim milk	Proteins; Peptides	FLEXYS Robotic Workstation	FAST (nitrocellulose polymer)
[120]	Sodium phosphate buffer with 40% glycerol	Antigens	Shanghai Precision Instrument	Epoxysilane-coated glass
[121]	Acrylamide/ bisacrylamide, Irgacure 2959, glycerol	Proteins	By hand (micropipette to create 1ul protein spots)	Acryl-functionalized glass slide.
[122]	Phosphate buffer	Ligands	Silicone gasket used to create 50 wells of 3 mm diameter and 1mm thickness to create 5-10 µl volume wells	Hydrogel-coated glass slides with NHS functional groups incubated with amine ligand
[123]		Carbohydrates		Nitrocellulose, SAM, thiol-functionalization
[124]	T-PER-SDS buffer	Cell lysates	Robotic Arrayer	FAST
[125]	Phosphate buffer (0.01 M, pH 7.2)	Antibodies	Soak in solution	Protein A+ Chromium and gold-coated glass slides
[126]	Acetate Buffer	Antibodies	Soak in solution	silicon wafer functionalized with 3-aminopropyltriethoxylsilane (APTES)

Sometimes, optimizing the surface chemistry is enough to yield reasonable results. However, other times, alternate materials such as plastics or silicon, as well as slides that are coated with nitrocellulose polymers, e.g. FAST slides are used. FAST slides have been demonstrated as good microarray surfaces because they have low coefficients of variation (CVs), low background (especially at blue excitation wavelengths), and high signal-to-noise ratios [35, 36, 61, 104]. Alternatively, silicon surfaces are promising because they exhibit low intrinsic auto-fluorescence [127], may have increased signals compared to microscope glass slides [128], and can be modified physicochemically to bind proteins with an affinity comparable to FAST slides [124]. In addition, there are a number of different commercial slide surfaces, designed specifically for use with robotic microarrayers, which can be evaluated in a similar fashion to studies described by Wilson, et al. [35].

Antibodies may be patterned onto the surface using PDMS flow cells, stencils such as those described in Chapter 3, or by printing with robotic machines [129]. Proteins may become immobilized in two main ways: by physical adsorption or via covalent bonds [130, 131]. Physical adsorption requires relatively easy experimental methods, but causes the antibodies to be randomly oriented on the surface in various conformations, and the antibodies are susceptible to changes in the ambient environment. Alternatively, covalent immobilization provides more control over the intermolecular interactions that ensue because there is more orderly orientation of antibodies compared to physical adsorption. Additionally, covalent bonds are relatively stable despite changing environmental conditions.

Some multiplex protein microarrays require quantification of the signal while for other applications, a qualitative response is sufficient. For example, Rowe-Taitt, et al. demonstrated the use of an assay to detect six different biohazardous agents using a format that requires fluorescent detection. Upon imaging, results can be interpreted by eye to determine whether or not an analyte is present (e.g. if the spot on the assay that probes for a specific analyte is bright or dull) [132]. In this case, simply knowing whether an agent is present is sufficient and the concentration of the agent is immaterial.

Some commercial protein microarrays have been developed such as the AtheNA Multi-Lyte test system and the BioPlex 2200 ANA screen, which both use Luminex's xMAP technology [117]. These immunoassays can screen for multiple autoantibodies that are involved in rheumatic diseases. The CombiChip Autoimmune is another commercially-available product that can be used to help identify autoimmune diseases; this product uses nitrocellulose-coated slides and requires manual imaging and analysis. The Meso Scale system uses an electrochemiluminescent method and can be used to quantify cytokines, chemokines, phosphoproteins, and toxicologic biomarkers, among many others.

Drawbacks of Microarrays

There are a number of areas of concern when developing multiplex platforms for biomarker screening, with reproducibility (inter- and intra-slide variation) and sample normalization being the major concerns. Balboni, Utz, and coworkers have attempted

to address some of the issues associated with protein arrays, in particular, antigen arrays for autoimmunity [34-36]. A variety of controls can be implemented to allow broad market application of microarrays such as replicate spots, negative control spots, marker spots for orientation, and spots to test cross-reactivity of capture and detection antibodies [117].

Other factors that can affect the utility of microarrays include the use of polyclonal or monoclonal antibodies. Choosing the most appropriate antibody for experiments is important as the affinity and specificity can be affected. In addition, the conditions under which patterning of antibodies takes place such as the temperature and humidity must be tightly controlled. Lastly, blocking the surface with a blocking buffer/agent such as PBS + 1% Bovine Serum Albumin (BSA) following patterning is critical to prevent non-specific adsorption of proteins.

In addition to assay variability, some microarrays exhibit less-than-optimal linear dynamic range [114]. Current methods for analyzing data typically rely upon the direct comparison of signal intensities, which limits quantification between antibodies and the fluorescent signal. Microarrays do not have a common standard for detecting antibodies that bind to different targets, as opposed to ELISA, which can utilize an independent standard curve. Since the affinity of antibodies for their targets can vary in biological matrices, a method is needed to quantify independent antibody concentrations in microarrays. Yu, et al. created a nonlinear calibration to quantify the amount of antibody binding to the surface using a microarray nonlinear

calibration (MiNC) method. This method adds a series of known amounts of antibodies (from the same species) onto an array. Immunoglobulin G (IgG) is used to create a nonlinear standard curve, which is used to interpolate the amount of antibody that specifically binds to the epitope of each protein.

In addition to the drawbacks inherently associated with conducting protein microarrays, there are drawbacks with commonly used microarray scanners that are used to quantify results. Using the GenePix for analysis is problematic because the lasers used for excitation are confined to either the green or red range (532 nm and 635 nm) and the blue range is preferred for analyzing microarrays that use QDs. Another drawback is that the filter emission cannot be configured with each type of label used. Rather, the GenePix is optimized for Cy3 and Cy5. The GenePix 4000B Microarray Scanner, like the TECAN plate reader is not optimized for POC use. The GenePix has dimensions of 13.5" x 8" x 17.5" and a weight of 25 lbs. and costs >$50,000. The laser power settings are limited to only 100%, 33%, or 10%. As a result, development of data detection platforms that are designed specifically for use with a certain fluorescent label are becoming more popular. In-house developed platforms can be configured to employ the proper lasers and filters to administer the most appropriate excitation wavelength and to capture the best range of emission wavelengths.

Lab-on-a-Chip Devices

Lab-on-a-chip devices integrate processing steps such as sampling, sample pre-treatment, separation, detection, and data analysis into one small machine. Ideally, a Lab-on-a-Chip device should meet several specifications. First, the optic, electronic and fluidic components of the device must be incorporated in separate compartments so that the function of the optics and electronics is not impaired by exposure to fluid [48]. Second, the optics components should be incorporated into the device in a manner that makes replacing parts easy. Third, the reservoirs for fluid should be amenable for injection molding, as required for mass production. Fourth, the reservoirs for the sample and tracer molecules must be compartmentalized so that they do not mix.

Microfluidic systems are capillary networks (10 – 50 μm deep and 10 – 400 μm wide) fabricated on materials such as silicon, glass, or polymeric substrates [133]. Flow of fluid is usually controlled by electroosmotic effects such as application of an electric field or vacuum. Microfluidics can allow for parallelization and integration of sample processing steps onto one small device [134]. Other benefits include miniaturization, automation, disposable units for single-use devices. Microfluidic systems have been demonstrated for use in protein separation, kinase reactions, and immunoassays [133]. Sandwich assay formats, which require addition of the analyte, followed by a labeled antibody, have been demonstrated in microfluidic systems using glass or polystyrene beads that are immobilized and entrapped with samples containing the analyte of interest. In one example, when a syringe pump was used to

control the flow, the reaction time was 30 min for four reaction chambers contained on a 50 mm x 70 mm space. In another example, Weishan, et al. developed a "SlipChip" for conducting immunoassays using magnetic beads [135]. This approach involved two microfabricated glass slides with various inlets, outlets, and wells where the sample was exposed to the reagents required.

Microfluidic systems have rarely matured from the proofs of concept in the academic world to commercialized products [134]. However there are some label-free microfluidic systems commercially available such as the Triage system and the VIDAS platform, which use fluorescence for multiplex detection of proteins related to cardiac diseases [117].

Fiber Optic Methods

Many research groups have developed fiber optic methods for biological sensing [106-113]. For example, Wang et al. developed a portable fiberoptic fluorescence analyzer for determination of glomerular filtration rate of the kidney in animals [136]. King, et al., have developed a device called the RAPTOR, a portable optical fluorimeter, that uses multiple single fiber optic probes to detect multiple analytes (one probe for each target) in a rapid and automated manner [50]. The RAPTOR has been shown to fluorescently detect spores and ovalbumin, among other bacterial, viral, and protein analytes, in 10 minutes, without any false positives, and without any sample processing (samples are added manually or via a computer-controlled air sampler) [48]. The authors also demonstrated the ability of the device to be reused

with the same efficacy after undergoing several cycles of washing. This device improves upon previous optical biosensors such as the Analyte 2000, which connects single fiber optic probes in series to perform a multiplexed immunoassay [103] and the MANTIS, the precursor to the RAPTOR [50]. The RAPTOR can perform four sandwich immunoassays on the surface of waveguides in a field-deployable format where all processes, including data analysis, are automated [48, 50].

Despite its benefits, there are some disadvantages of the RAPTOR, such as its size (18.6 cm x 27.4 cm x 17.3 cm) and weight (2 lbs.), both of which are larger than the ideal specifications for a portable POC device [50]. Additionally, the RAPTOR utilizes a separate fiber optic waveguide to detect each analyte, so each sample must be analyzed one at a time, and a total of only four analytes can be detected using its four different channels [48]. The next generation RAPTOR, the BioHawk, both sold by Research International, can detect up to eight analytes simultaneously, but each sample must be assayed individually [137]. The BioHawk design can potentially discern between up to eight analytes and assess various samples simultaneously [50].

Summary

Various types of sensing methods from ELISA and fluorescent immunoassays to protein microarrays and hand-held field-deployable POC platforms have a variety of applications. These analytical tools may be used for detecting protein analytes that are critical for diagnosing specific diseases such as AKI, which is discussed in Chapter 5. Although the scope of this work relates to diagnosing biomarkers related to a specific type of renal disease, the tools described in this chapter can be used for other purposes such as detecting contaminants in food, maintaining and monitoring a safe water supply, and for detecting proteins that could be involved in a chemical or biological attack [83, 138, 139].

Chapter 3: Development and Characterization of Planar Surface Fluorescent Immunoassays

Abstract

One new optical detection method for proteins involves the use of planar surface fluorescent immunoassays using in-house microfluidic templates for design production that help minimize sample volume and maximize multiplexing capacity. The templates were designed in CorelDRAW X4 and micromachined using a computer controlled Epilog Legend CO_2 65 W laser cutter. The dimensions of each of the details on the various templates were adjusted in order to minimize the volume required for each step of the assay. Minimizing volume is an important feature for clinical test methods as the bodily matrix being tested may be scarce. Once the design templates were optimized, the parameters for performing the immunoassay were adjusted by testing various surface modifications and concentrations of the immobilized capture antibodies. Two proteins, Chicken IgG and Staphylococcal Enterotoxin B (SEB), were used to characterize and optimize the platform. These two proteins were characterized using standard microtiter plate fluorescent immunoassays and demonstrated similar LODs as compared to the planar surface fluorescent immunoassays. While the background fluorescence of the slides have some variation, the targeted regions of the slide (functionalized with capture antibodies) demonstrated proportional increases in signal as the concentration of the target analyte increased and variation among spots did not seem affected by spatial position.

Background

An optical sensor platform involving microscope glass slides was named a planar surface fluorescent immunoassay. The goal of this new multiplexed platform is to reduce the volume needed to perform an assay several-fold, making incorporation of the miniaturized assay into a POC device possible. This platform builds upon the work by Bernard, et al., who developed micromosaic immunoassays to test samples against an array of antigens by delivering solutions across a surface using a microfluidic network, and Murphy, et al., who applied the immunoassay to a sandwich format [30, 140, 141]. Rather than employing silicon wafers fabricated using reactive ion etching as the surface, which is a complex technique involving production that can cause non-uniformity, roughness, varying aspect ratio (depth/width), and damage to the surface, in our work, we use more a cost-effective surface, standard microscope glass slides [142]. Instead of using PDMS stencils to deliver samples and reagents across the surface, which is hydrophobic and may cause proteins adsorption, and requires hours for production, we use a combination of vinyl, polycarbonate, and acrylic materials to create the flow channels [143]. The performance of this newly-developed platform was assessed in relation to standard microtiter plate fluorescence immunoassays.

As mentioned in Chapter 2, antibody microarrays offer many advantages over standard techniques, namely the possibility of integration with microfluidics and development of a stand-alone biosensor for POC use. Morales-Narvaez, et al. demonstrated the use of an antibody microarray for detection of Alzheimer's Disease

biomarkers using a common method employed by various research groups [93]. In this method, microarrays are fabricated by spotting antibodies onto the surface of an epoxysilane glass slide using a Microgrid II, a machine that automates the spotting. Each spot was kept separate using a microarray cassette and the same general method of blocking and performing a sandwich assay was applied involving detection of an analyte that relies upon two different antibodies (Figure 4). The studies presented in this chapter improve upon typical antibody microarrays because the surface functionalization method applied uses a covalent bond (the strongest intermolecular interaction), lowering potential for variation in the surface over time and making the assay more amenable to a POC environment.

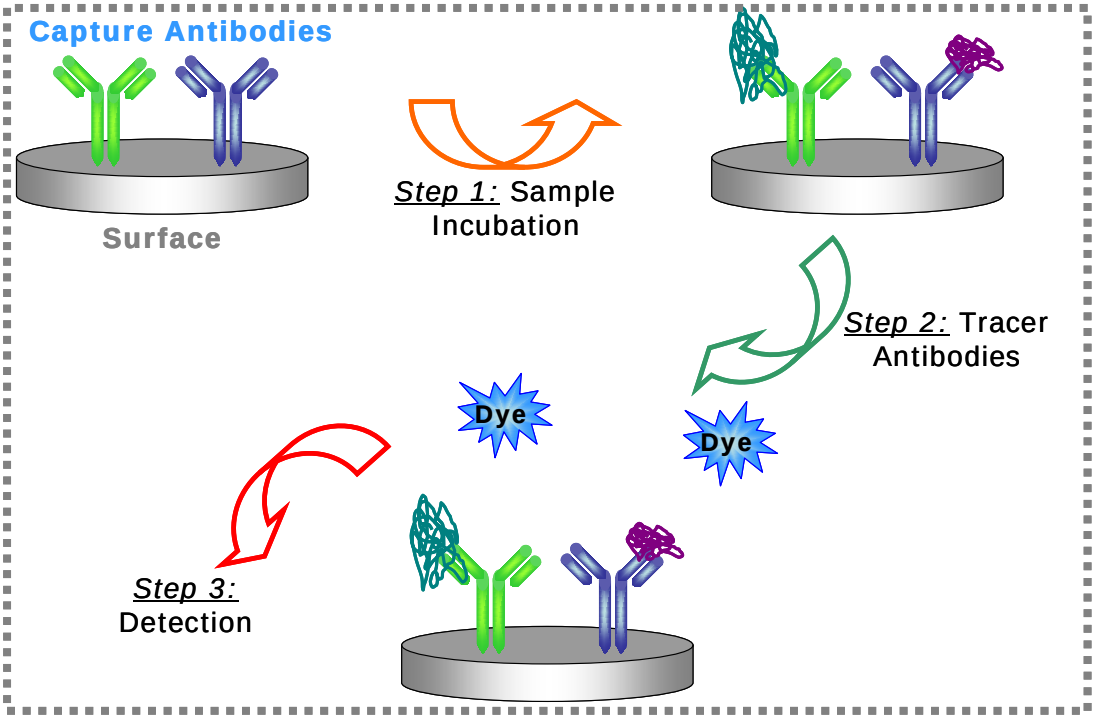

Figure 4. Sandwich assay format experimental methods involving dyes as tracer molecules [144]

In order to perform assays on glass surfaces, the surface must be modified with functional groups that allow for either covalent or non-covalent biological attachment. Different surface chemistries can be employed for patterning antibodies onto the surface of the slide as discussed in Chapter 2. Some reagents that were used to modify the glass surface include epoxy silane, hydrophobic C18 silane, amino-silane, thiol silane, and thiol silane with an N-gamma-maleimidobutyryl-oxysuccinimide ester (GMBS) hetero-bifunctional crosslinker. The GMBS crosslinker is composed of anime and thiol reactive chemistries. These surface chemistries cause either covalent interactions or weaker non-covalent interactions (Van der Waal's, electrostatic, or hydrophobic) with the antibodies, resulting in surface immobilization.

Our studies have shown the utility of the thiol silane/GMBS crosslinker surface for covalent immobilization of antibodies. The protocol for creating the thiol silane/GMBS crosslinker surface is shown in Figure 5 where the glass slide is immersed in 10% potassium hydroxide in methanol, followed by exposure to 2% thiol-silane in toluene, and addition of GMBS in ethanol. The GMBS creates an amine reactive surface, which is used to covalently attach antibodies. A conventional cross-linker for biosensing applications is glutaraldehyde [145]. Glutaraldehyde was not investigated because it is toxic, very messy to handle, can cross-react, can adversely affect the physicochemical properties of the surface, and unlike the GMBS chemistry described above, has the potential for form multiple layers.

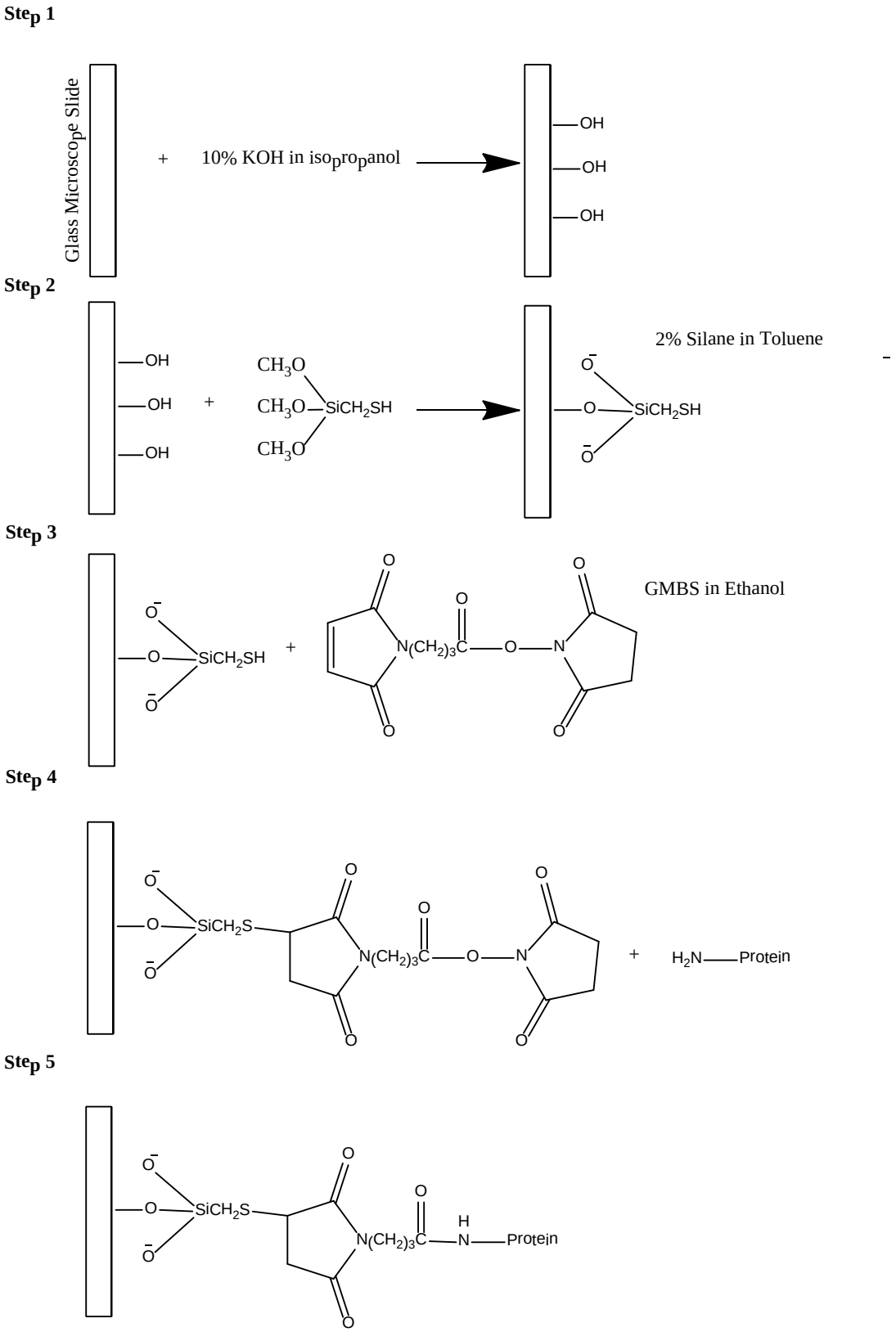

Figure 5. Thiol silane/GMBS crosslinker surface functionalization procedure. GMBS stands for 4-maleimidobutyric acid N-hydroxysuccinimide ester

Another popular immobilization strategy that has been employed to create protein arrays involves functionalizing the glass surface with a biotin-binding protein such as NeutrAvidin or streptavidin. In this case, antibodies to be immobilized onto the surface must be biotinylated, forming a strong non-covalent bond between the biotin-antibody and the immobilized avidin-protein. While the biotin/avidin chemistry is non-covalent in nature, it represents one of the strongest non-covalent interactions known, with a dissociation constant of ~10^{-15} M and may improve the sensitivity of the system by immobilizing the capture antibody with greater strength than many of the other chemistries involving hydrophobic or electrostatic interactions [146, 147]. Although there are many other immobilization chemistries that exist [34, 61], the chemistries listed above have demonstrated success for protein immobilization [92].

The volume needed to perform a standard 96-well microtiter plate (50-100 μL of volume/well) assay is comparable to previous studies involving the use of planar surface fluorescent immunoassays [32]. However, the goal of this study is to minimize the volume required to perform the assay to below 20–80 μL of volume, which is what 384-well plates require per well.

Methods

Materials

Staphylococcal enterotoxin B (SEB) and affinity purified rabbit anti-SEB were purchased from Toxin Technology Inc. (Sarasota, FL). Rabbit anti-Chicken IgG (IgY) and Chicken IgG were purchased from Jackson ImmunoResearch Laboratories

Inc (West Grove, PA). Phosphate buffered saline (PBS), Phosphate buffered saline with Tween (PBST), and bovine serum albumin (BSA), methanol, potassium hydroxide, toluene, ethanol, dimethyl sulfoxide, (3-mercaptopropyl)triethoxysilane, 3-glycidyloxypropyl)trimethoxysilane, trichloro(octadecyl)silane, (3-aminopropyl)trimethoxysilane, 4-meleimidobutyric acid N-hydroxysuccinimide ester, and J. Melvin Freed Brand Microscope Slides, Plain were obtained from Sigma-Aldrich (St. Louis, MO). Doubly distilled water (ddW) was used throughout the experiments and was prepared in house using a Nanopure Diamond™ water purification system (Barnstead, Dubuque, IA). Clear acrylic was obtained from Piedmont Plastics (Elkridge, MD). Impact-Resistant Polycarbonate was obtained from McMaster-Carr (Robbinsville, NJ). Fluid handling chips were designed in CorelDraw X4 (Corel Corp. Ontario, Canada) and micromachined using a computer controlled Epilog Legend CO2 65 W laser cutter (Epilog, Golden, CO). 3M 9770 adhesive transfer tape was used to hold together the layers of the planar surface fluorescent immunoassay. A REGLO Digital pump and tubing were obtained from Ismatec (Wertheim, Germany). Appropriate connectors for the tubing were obtained from Cole Parmer (Vermon Hills, IL). Data was analyzed using Microsoft Excel (Microsoft, Redmond, WA) and GraphPad Prism (GraphPad Software, La Jolla, CA).

Epilog Printer Templates

In this study, novel stencils were created to allow for patterning of capture antibodies onto the surface and performing sandwich assays. A multi-layer system used for patterning and performing assays for protein arrays was designed in CorelDRAW 11

(Corel Corp., Ontario, Canada) and then micro-machined in various materials, including vinyl, polycarbonate (McMaster), and acrylic (Piedmont Plastics) using a computer-controlled laser cutter Epilog Legend CO2 65W (Epilog, Golden, CO). The channels made of vinyl (0.25 mm) that were used for patterning and conducting the assay had dimensions of 50 mm x 0.4 mm and 18 mm x 0.4 mm, respectively (Figure 6). Double-sided tape was placed on one side of the vinyl and acrylic templates to allow for manual application onto microscope glass slides (25 mm x 75 mm x 1 mm). Templates were wiped using Kimwipes® disposable wipers (Sigma) and ddW to remove debris prior to application.

Surface Functionalization

Plain microscope glass slides were scored using a diamond-tip tool to create a label on the edge of the slide to allow for subsequent identification. The slides were wiped using Kimwipes® disposable wipers (Sigma) and ddW. Slides were placed in a slide holder and immersed in a 10% KOH in methanol solution (5 g KOH in 50 mL methanol, which was mixed using a magnetic stirrer). Following incubation at RT for 30 min, slides were rinsed in DI water and ddW water, dried, and placed in a new slide holder. A variety of different silane-based surface modifications (3-mercaptopropyl) trimethoxysilane, 3-aminopropyl)trimethoxysilane, trichloro(octadecyl)silane ≥90%, (3-glycidyloxypropyl)trimethoxysilane - ≥98) (Sigma) were tested using the procedure demonstrated in Figure 5, but GMBS (step 3) was only applied for the thiol-silane chemistry. Slides were placed in a 2% silane solution prepared in toluene (1 mL silane in 50 mL toluene) and allowed to incubate

for 1 hr. at RT. Slides were rinsed with toluene using a glass pipette. If the 4-maleimidobutyric acid N-hydroxysuccinimide ester (GMBS) cross-linker was used, a 2mM solution was prepared (12.5 mg were placed in 250 µL dimethyl sulfoxide (DMSO)) and vortexed and mixed in 50 mL ethanol. Slides were immersed in this solution for 30 min at RT. A contact angle goniometer developed in-house was used to measure the contact angle when one drop of ddW was placed onto the slide. The patterning template must be attached to the slide surface and exposed to the patterning antibody relatively quickly (within ~2 hrs. at a maximum) in order to ensure that the chemistry remains active for covalent binding. In order to manually force out air bubbles between the slide and the vinyl patterning template, a piece of polycarbonate was placed on top of the template and a plastic tool was used to apply pressure on the surface in a sliding motion. The next template layer (polycarbonate) was assembled and air bubbles were removed using this same method. Manual pressure was applied to the final layer (acrylic) to ensure a good seal with the polycarbonate layer.

Capture Antibody Patterning

Antibodies were then patterned onto the surface functionalized glass slides. Anti-chicken IgG or anti-SEB antibodies (10 µg/mL) in phosphate buffered saline (PBS) were patterned onto the slide in channels oriented in the horizontal direction (Figure 6) using a REGLO Digital pump. Experimentally, the antibodies were flowed through the device with the use of tubing, appropriate connectors, and a peristaltic pump (REGLO Digital; Ismatec, IDEX Health & Science).

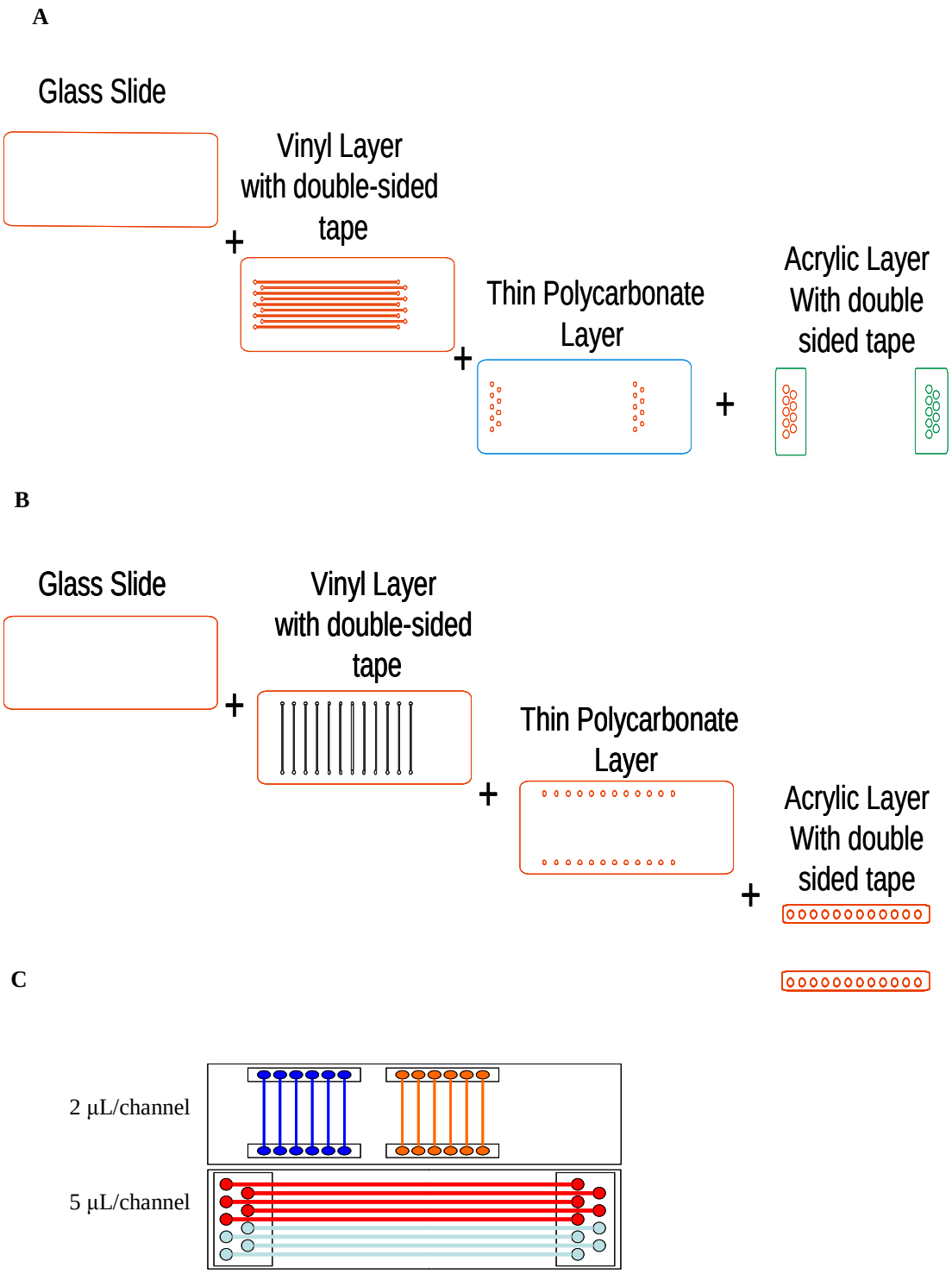

Figure 6. Epilog printer templates. (A) patterning design, (B) assay design, (C) assembled devices

Slides were placed in a petri dish containing wet paper towels to create a humid environment. The channels were covered with parafilm to further prevent evaporation. Following incubation at 4^{o}C overnight, the fluid was withdrawn and the patterning template was removed from the slide and the slide was rinsed with ddW.

Planar Surface Fluorescent Immunoassays

Capture antibody modified slides were blocked for 1 hr. at RT in 1% BSA+PBS and rinsed with ddW. Slides that were not used immediately were stored in PBS for up to four weeks. Slides were dried with air and assay templates were applied by hand, as described above for the patterning template. The slide was then exposed to different concentrations of chicken IgG and SEB (0 to 800 ng/mL in 0.1% BSA+PBST (PBS with 0.05% Tween)), which were loaded onto the slide via channels oriented perpendicular to the rows of patterned capture antibodies (i.e. in the vertical direction, (Figure 6) using a REGLO digital pump. Inlets and outlets were covered in parafilm to prevent evaporation and placed in a humid chamber for 1 hr. at RT. Fluid was removed and washed with PBST 3X. Following washing, Cy5-labeled tracer antibodies (Rb anti-Chicken or Rb anti-SEB) in 0.1% BSA+PBST were exposed to the slide via vertical channels. Again slides were covered with parafilm and placed in a humid environment for 1 hr. at RT. Aluminum foil was used to cover the humid chamber. Slides were washed with PBST 3X and the templates were disassembled. Slides were washed with ddW and dried with air.

In order to test the auto-fluorescence of the glass slide upon functionalization, slides were imaged at various power and gain settings using a GenePix 4000B Array Scanner (Molecular Devices; California, USA) and compared to the images taken at the same settings after conducting the assay. Investigating auto-fluorescence allows for normalization of the fluorescence data (e.g. fluorescence values can be reduced or divided by the value of the background fluorescence).

Analysis of the mean fluorescence was conducted by imaging the slide with a GenePix 4000B Array Scanner (Axon Instruments, Inc., Union City, CA). The GenePix Array Scanner has two laser light sources—one at 532 nm, and another at 635 nm. The 635 nm light source was used to image slides exposed to Cy5. The glass slides were quantified using software associated with the GenePix instrument by measuring the mean intensity of each spot minus the background signal adjacent to the spot and intensities were normalized. The quantitative values of the mean fluorescence and standard deviation between spots were analyzed using Microsoft Excel. The LOD was determined as the lowest concentration assayed for which the signal was larger than 3-sigma of the background measurement. The background measurement was determined by averaging the signal from all of the spots within the assay only exposed to buffer rather than a concentration of the analyte.

Results

Surface Functionalization

Different patterning techniques were investigated in order to optimize the procedure for immobilizing multiple proteins onto the surface of the slides. The five different chemistries investigated were CH_3-Silane, SH-Silane without GMBS, SH-Silane with GMBS, NH_2-Silane, and Epoxy-Silane. These five chemistries were selected because of their success in previous investigations [148]. Furthermore, GMBS surfaces were selected because they have the least amount of nonspecific binding and the highest amount of immobilized antibody compared to aminosilane and adsorption alone [149]. The different surface chemistries that were tested had contact angles ranging from 42.1^0 to 87.68^0; hydrophobicity was the parameter measured here because of the common association with binding antibodies through non-covalent interactions. The measured contact angles are shown in Table 3. While CH_3-Silane was the most hydrophobic chemistry tested, the more hydrophobic surface does not necessarily indicate the most reactive with antibodies. The results presented in this work ultimately used the covalent chemistry SH-Silane with GMBS, which targets the lysine groups on the surface of the antibodies, because this surface chemistry proved to be the most reliable in terms of producing consistent results when repeat assays were performed.

Table 3. Immobilization chemistries and associated measured contact angles

Immobilization Chemistry	Contact Angle
CH_3-Silane	$87.68^0 \pm 4.46^0$
SH-Silane without GMBS	$71.94^0 \pm 1.23^0$
SH-Silane with GMBS	$68.54^0 \pm 1.7^0$
NH_2-Silane	$49.75^0 \pm 0.86^0$
Epoxy-Silane	42.10 ± 0.220

Epilog Printer Template Design

Several design iterations of the vinyl/polycarbonate/acrylic templates were tested and used for patterning capture antibodies and performing planar surface fluorescent immunoassays. The vinyl template was chosen to be in intimate contact with the glass slide because upon removal, it does not leave a sticky residue on the slide surface unlike double-sided tape, which is used to attach the polycarbonate and vinyl layers of the structure. These templates were used in a sandwich format (Figure 4). The microfluidic platform was designed to perform all of the assay steps including: passing the sample over the protein array surface, performing subsequent washings steps, and exposing the array to "tracer" antibodies, which enables detection of the target protein. Figure 6 depicts illustrations of the two microfluidic platform designs used during patterning and performing the assay. These templates build upon designs developed by the Ligler group which used PDMS flow cells requiring much larger volumes, typically 50 to 100 μL [30]. These templates use only 2 μL/channel for performing the assay and only 5μL/channel for patterning the capture antibodies.

Each of the channels is 1 mm in width. In this design, alternating colors of food dye were added to the channels to illustrate that no leaking is apparent amongst the channels in either the horizontal or vertical directions (Figure 7). These results demonstrate a noticeable reduction in the sample/reagent volumes required and this feature makes this device desirable for a POC environment.

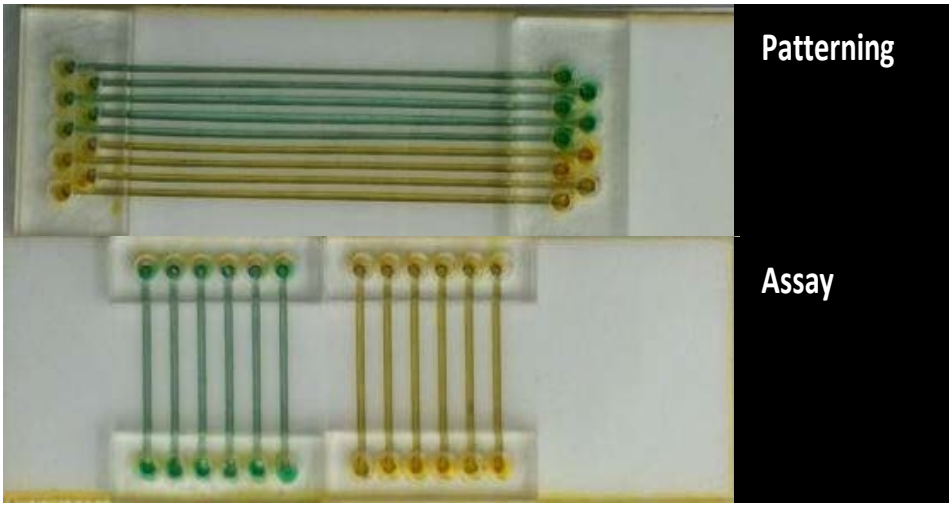

Figure 7. Assembled planar surface fluorescent immunoassay devices containing food dye

Background Fluorescence Post-Patterning

An experiment was conducted to show that when the patterning antibody is patterned onto the surface and washed three times with buffer, the mean fluorescence (aka background fluorescence) was consistent. The graph and slide image show that the surface does not display an abnormal fluorescence after patterning (Figure 8).

A

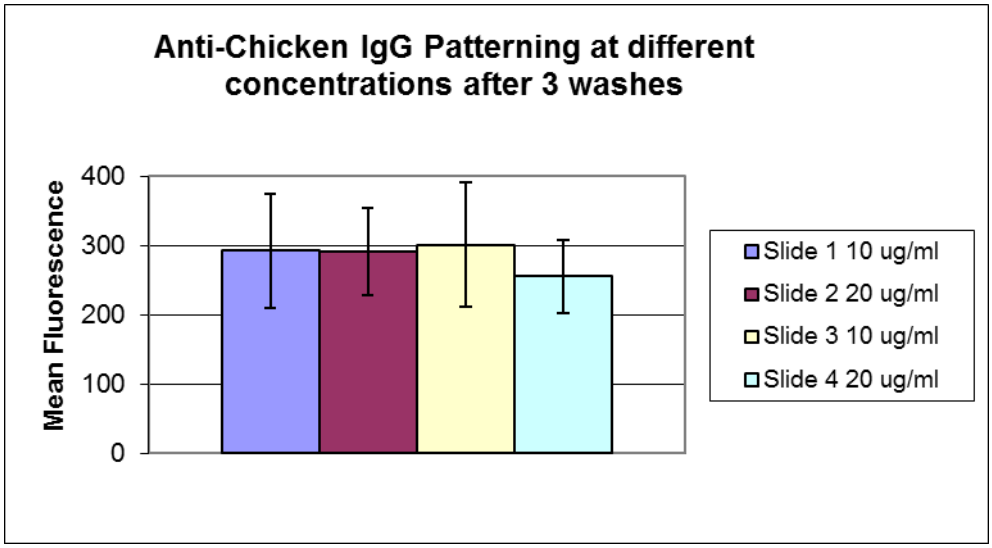

B

Figure 8. Background fluorescence post-patterning of (A) Rb-anti-chicken IgG at 10 and 20 µg/mL and (B) corresponding image at 10 µg/mL.

Optimal Capture Antibody Concentration

Experiments were conducted to determine the optimal patterning concentration when using three washes in the protocol. The capture antibody, anti-chicken IgG, was prepared at 1, 10, 20, and 50 µg/ml and sandwich assays were conducted by exposing the surface to chicken IgG, followed by the tracer antibody, Cy5-anti-chicken IgG. Experiments using a patterning concentration of 10 µg/ml gave a similar assay dose

response as higher patterning concentrations (Figure 9). As a result, 10 µg/ml was selected for use in subsequent studies because of its cost-effectiveness. Using a concentration of 10 µg/ml for patterning allowed for use of fewer reagents without compromising assay sensitivity.

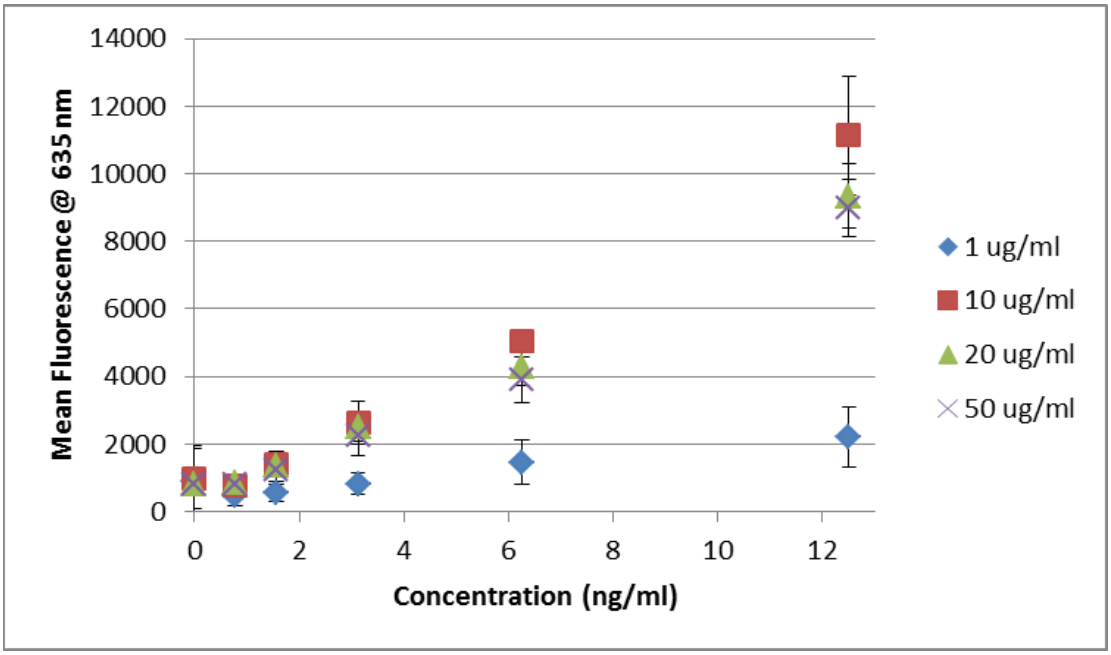

Figure 9. Determination for optimal antibody patterning concentration using thiol-silane with GMBS chemistry for immobilization. Sandwich assay experiments were conducted keeping all parameters the same, except with varied capture concentrations of anti-chicken IgG. 10 µg/ml Cy5 tracer was used.

In another set of experiments, the effect of flow of PBST over the different surfaces patterned at different concentrations (1, 10, 20, and 50 µg/ml) was characterized. In these studies, the surface was patterned with the fluorescently-labeled antibody to chicken IgG and a "simulated assay" was conducted where instead of exposing the surface to the analyte and the labeled antibodies, PBST was used. These experiments

bolstered the selection of 10 μg/ml as the patterning concentration because the lower concentration (1 μg/ml) did not allow for even coverage of the surface (i.e. surface was not evenly saturated). After 0, 3, and 6 washes with PBST, the fluorescence intensity when using 10 μg/ml was consistently the highest with the least variation, making this concentration most desirable (Figure 10). The 10, 20, and 50 μg/ml patterning concentrations demonstrated similar results after washes with PBST. After three washes, non-specifically bound antibodies were removed from the surface, yielding lower fluorescence intensities and this difference was most notable in the least hydrophobic surfaces (NH_2- and Epoxy-Silane). However, after six washes, the intensity decreased only slightly, suggesting that additional washes did not remove bound antibodies.

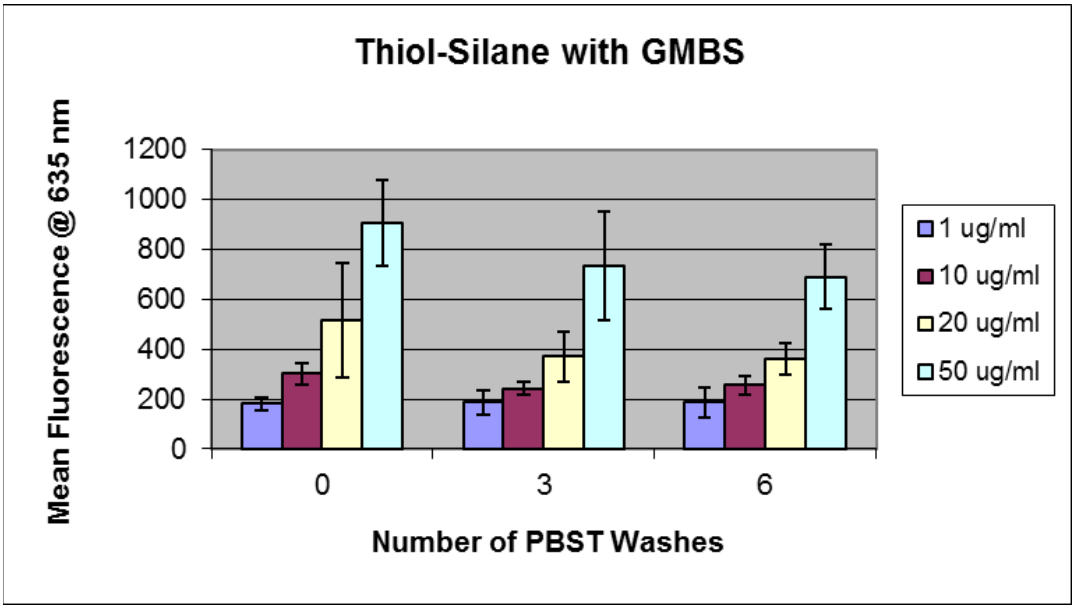

Figure 10. Effect of number of PBST washes on patterning concentration. Fluorescently-labeled anti-chicken IgG was patterned onto the surface and a "simulated assay" was conducted where PBST was used for all steps instead of exposing the surface to the analyte and the labeled antibodies.

In a third set of experiments to determine the optimal capture antibody concentration, experiments were conducted using 20 μg/mL or 10 μg/ml as a patterning concentration for both anti-SEB and anti-chicken IgG. As demonstrated, the LOD for detecting SEB is halved when the patterning concentration is doubled (Table 4). While the prospect of halving the LOD sounds appealing, doubling the patterning concentration for SEB is not warranted because of the cost of using more anti-SEB reagents. Furthermore, the signal for SEB is not as consistent compared to the chicken IgG assays, so the reliability of obtaining this lower LOD does not justify the added expense of using a higher patterning concentration.

Table 4. LOD for chicken IgG and SEB sandwich assays conducted using either 10 μg/ml or 20 μg/ml as the antibody patterning concentration and 10 μg/ml for the Cy5 tracer-antibody conjugates

Analyte	Patterning Concentration	Tracer	Limit of Detection
Chicken IgG	10 μg/ml	Cy5-Rb-Anti-Ch	0.4 ng/ml
	20 μg/ml		0.4 ng/ml
SEB	10 μg/ml	Cy5-Rb-Anti-SEB	0.3 ng/ml
	20 μg/ml		0.16 ng/ml

Consistency of Capture Antibody without Fluid Flow

To demonstrate that the capture antibody is patterned evenly onto the surface, the surface was patterned with the fluorescently-labeled antibody in certain regions and the unlabeled antibody in other regions of the same slide. In these experiments, surface was not exposed to the flow of any fluid (Figure 11). The fluorescence intensity was consistent across each of the spots where the surface was exposed to the

fluorescently-labeled antibody. As expected, the areas exposed to the unlabeled antibody had very low intensities. These image shows that the capture antibody is patterned evenly onto the surface and no leaking between the channels occurred in the fluorescently-labeled antibody exposed regions.

A

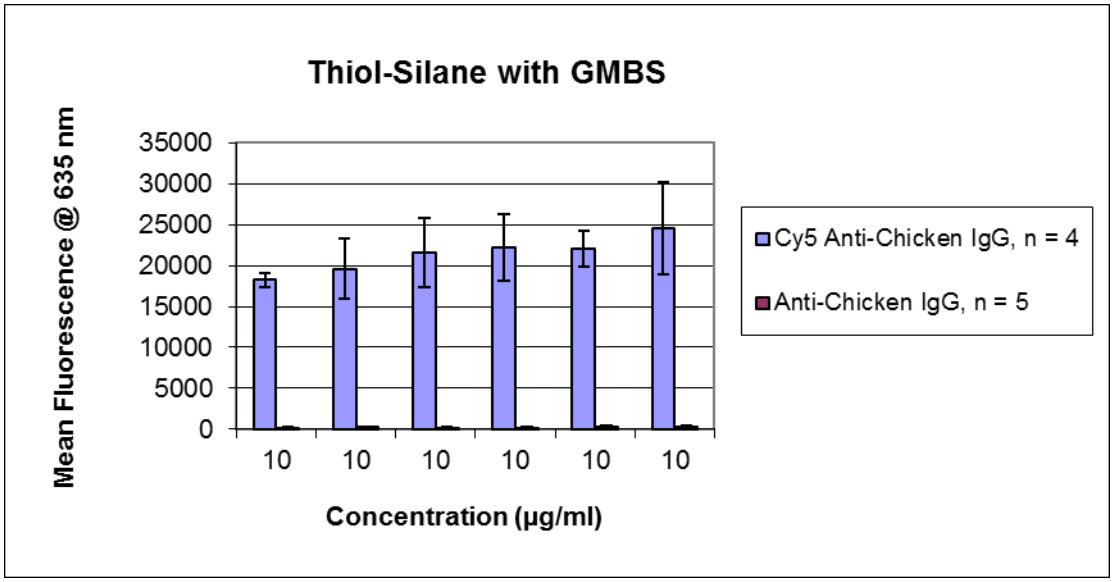

B

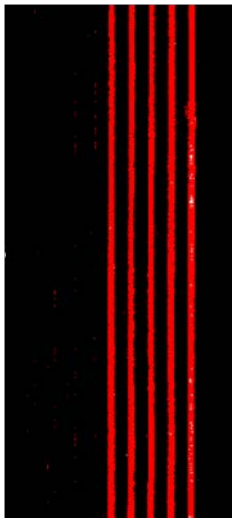

Figure 11. Consistency of capture antibody when (A) patterned onto the surface using thiol-silane with GMBS cross-linker as the immobilization chemistry and (B) corresponding image

Consistency of Capture Antibody with Fluid Flow

The consistency of the capture antibody across the surface when exposed to the flow of fluid was also assessed. The surface was patterned with the unlabeled capture and a sandwich assay was performed by exposing the surface to chicken IgG, followed by the tracer antibody. The signal was assessed in the patterning channel in three locations: above, in, and below the assay channel (Figure 12). The results demonstrated that there is no leaking of the assay channels because the intensity in the channel where the capture antibody is immobilized is significantly higher than above or below the channels. These experiments show that the capture antibody is consistently immobilized onto the surface during a sandwich immunoassay.

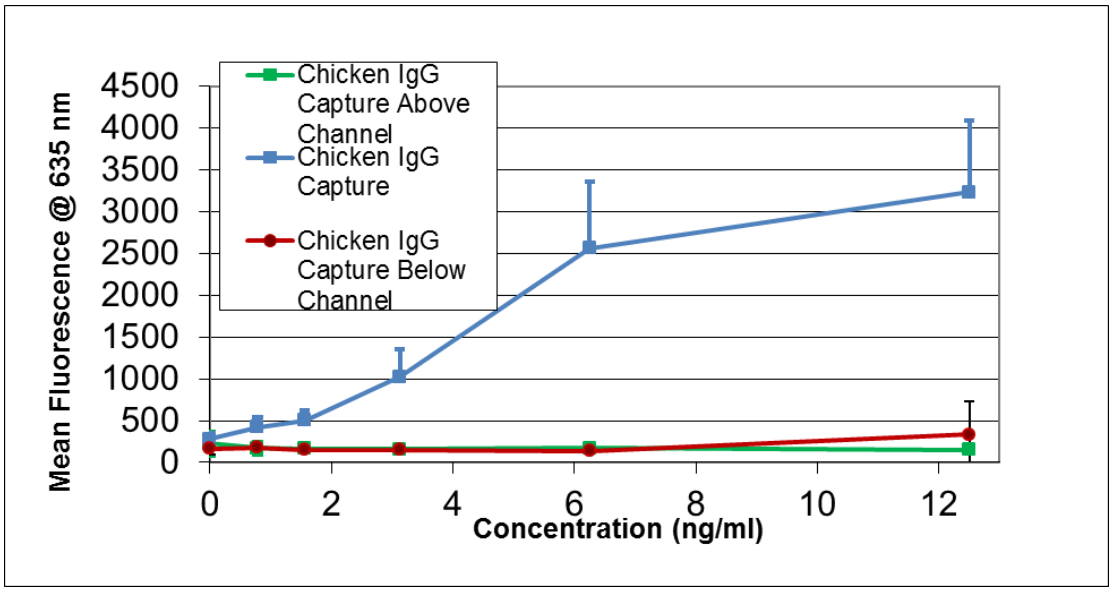

Figure 12. Consistency of capture antibody with fluid flow. Chicken IgG antibodies were patterned onto the surface and exposed to chicken IgG, followed by Cy5 tracer antibodies. Data was taken in the patterning channels, within the assay channel and on both sides of the assay channel (i.e. above and below).

Effect of Fluid Flow on Fluorescence Intensity

The effects of fluid flow on the surface when performing a sandwich assay were analyzed using each of the immobilization chemistries and data using the thiol/GMBS surface are shown in Figure 13. The same intensity pattern was discovered when immobilizing either the capture antibody or the fluorescently-labeled antibody and exposing the surface to chicken IgG and the tracer antibody. The difference between the fluorescence results of either capture antibody at each concentration showed a smooth dose response curve. The intensity of the labeled capture antibody was consistently higher than that of the unlabeled capture antibody. These data demonstrate the consistency with which the assay is performed (Table 5). While the CH_3-silane surface shows favorable coefficients of variation for both intra- and inter-slide variation, the relative intensities were lower than those achieved with the SH-Silane + GMBS cross-linker. Since the SH-Silane chemistry with or without the cross-linker showed similar CVs, a cross-linker was used in further studies because of the advantages of employing a covalent bond for protein immobilization.

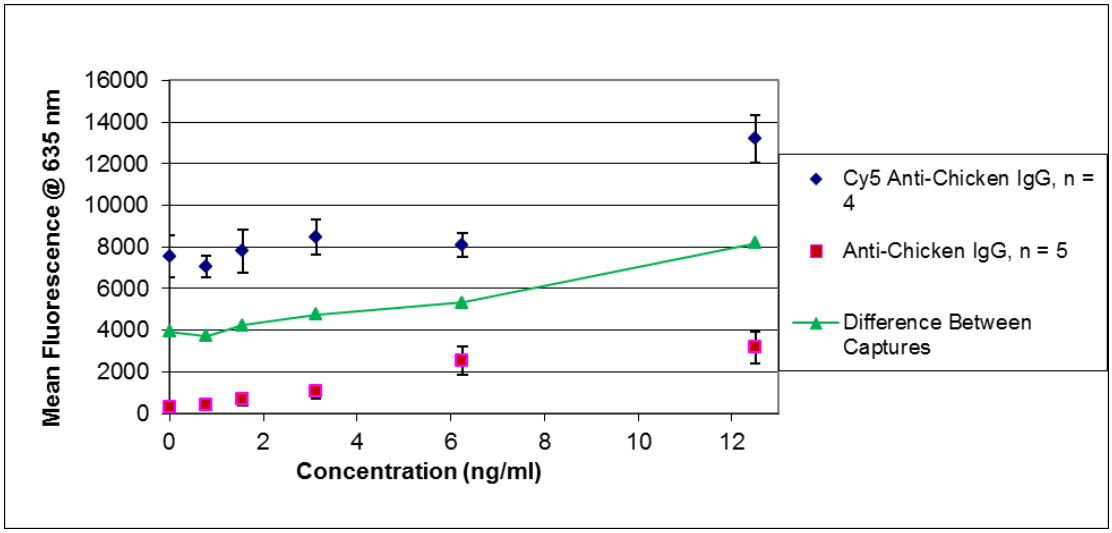

Figure 13. Effect of flow on fluorescence intensity when a chicken IgG sandwich assay was performed. Either Cy5-anti-chicken IgG or anti-chicken IgG was used as capture antibody and Cy5-anti-chicken IgG was used as the tracer molecule.

Table 5. Intra-slide and inter-slide variation among immobilization chemistries when patterned with either anti-chicken IgG or the Cy5-anti-chicken IgG and exposed to chicken IgG, followed by Cy5-anti-chicken IgG

Immobilization Chemistry	**Intra-Slide Variation (CV)**		**Inter-Slide Variation (CV)**	
	Cy5-Anti-Chicken IgG	Anti-Chicken IgG	Cy5-Anti-Chicken IgG	Anti-Chicken IgG
CH_3-Silane	0.19	0.20	0.19	0.20
SH-Silane without GMBS	0.10	0.21	0.26	0.27
SH-Silane with GMBS	0.13	0.28	0.14	0.29
NH_2-Silane	0.17	0.35	0.18	0.34
Epoxy-Silane	0.43	0.37	0.28	0.27

Spatial Analysis

The variation of chicken IgG and SEB using a Cy5 fluorescent tracer followed a similar pattern when comparing a high and low concentration of analyte. In other words, a slide that had a relatively higher fluorescence at the low concentration, in comparison with the other slides, also had a relatively higher fluorescence at the high concentration when compared with other slides (Figure 14). Data for other labels such as Cy5-Streptavidin and Cy5-NeutrAvidin that are discussed in Chapter 4 are in Appendix A.

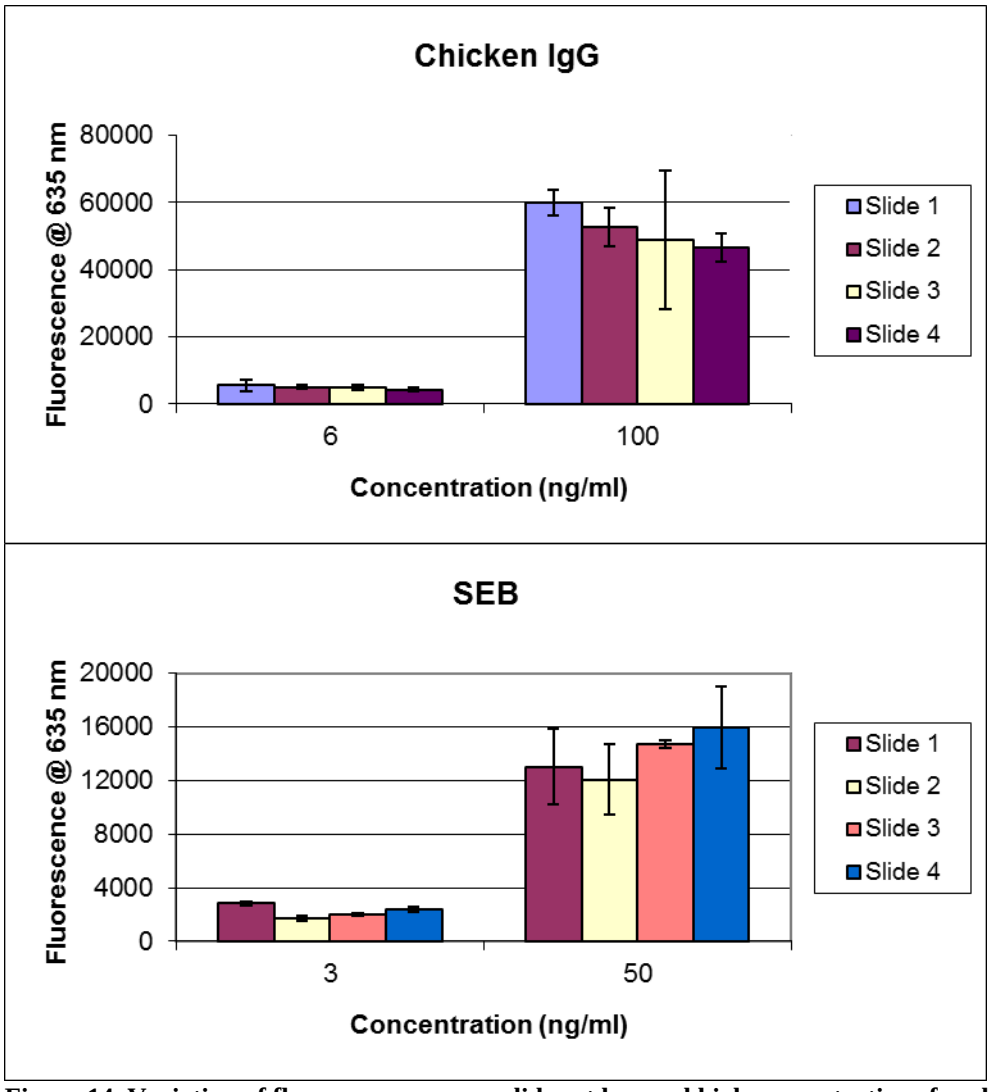

Figure 14. Variation of fluorescence among slides at low and high concentrations for chicken IgG or SEB sandwich assays using Cy5 tracer

Comparison of Five Immobilization Chemistries

Figure 15 shows each of the five immobilization chemistries used for detection of chicken IgG or SEB. The figures show that when SH-Silane is used with or without the GMBS cross-linker, the signal increases in greater proportion with each increase in concentration of the analyte as compared to the other chemistries. The inter-slide variability for each chemistry is reasonable for a biological assay where ~15% is expected. The differences in the signal between the surface chemistries became more apparent as the concentration of the analyte increased, with epoxy-silane and NH-silane performing the worst due to the lower increase in signal compared to the other chemistries. A summary of the characteristics of these surfaces is shown in Table 6, which indicates that SH-Silane with GMBS is the most ideal immobilization chemistry. An analysis of these surfaces will follow in the Discussion.

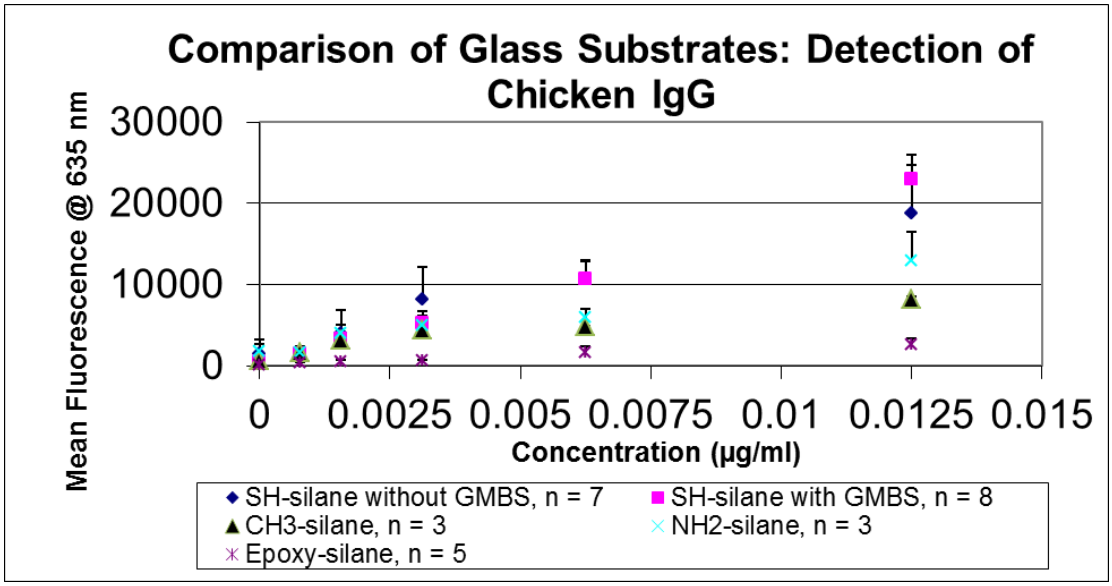

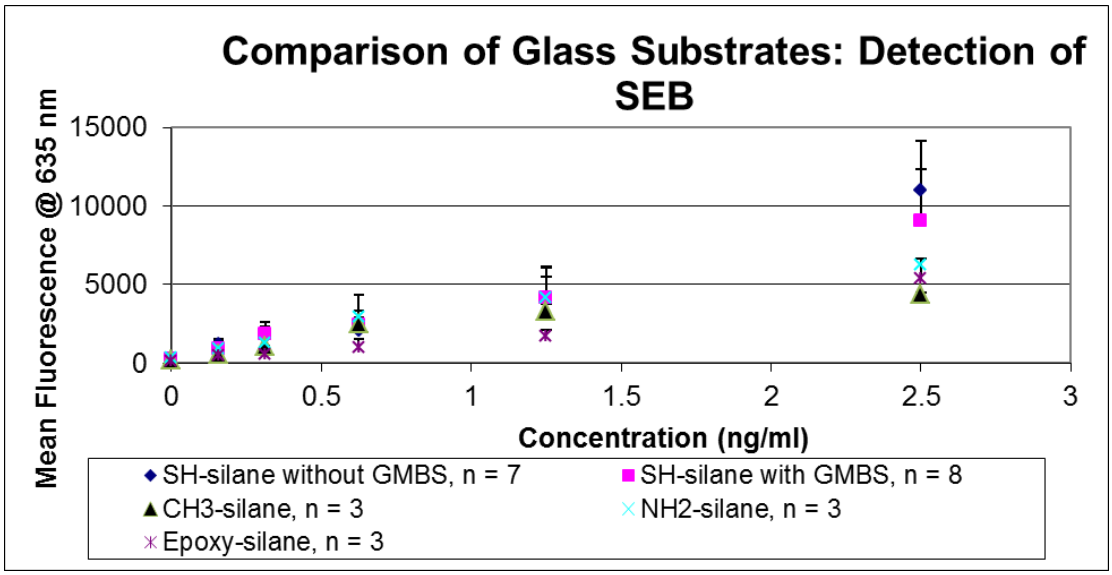

Figure 15. Comparison of immobilization chemistries for chicken IgG and SEB detection using a sandwich assay format

Table 6. Summary of immobilization chemistry characteristics

Immobilization Chemistry	Force	Contact Angle	Ease of Procedure	Consistency of Capture Antibody	LOD Chicken IgG (µg/ml) SEB (ng/ml)	Normalized Intensity	Overall Reproducibility
CH_3-Silane	Covalent	$87.68^0 \pm 4.46^0$	No	Yes	0.78 0.16	Low	OK
SH-Silane without GMBS	Hydro-phobic	$71.94^0 \pm 1.23^0$	Yes	Yes	3.1 0.16	High	Good
SH-Silane with GMBS	Covalent	$68.54^0 \pm 1.7^0$	Yes	Yes	0.78 0.16	High	Good
NH_2-Silane	Non-Covalent	$49.75^0 \pm 0.86^0$	Yes	Yes	3.1 0.16	Low	OK
Epoxy-Silane	Non-Covalent	42.10 ± 0.220	Yes	No	0.78 0.16	Low	OK

Comparison to Microtiter Plate Fluorescent Immunoassays

Experiments were conducted using fluorescent microtiter plate immunoassays to compare the LODs using planar surface fluorescent immunoassays. Experiments using Cy5-antibody conjugates as well as biotin-antibody combined with streptavidin-Cy5 conjugates were compared (Figure 16). The LODs for both chicken IgG and SEB detection were on the same order of magnitude. The LODs for chicken IgG detection were 0.4 ng/mL and 0.3 ng/mL for the planar surface and microtiter plate fluorescent immunoassays, respectively. Use of the Cy5-antibody conjugates as well as biotin-antibody combined with streptavidin-Cy5 conjugates yielded the same LOD for chicken IgG detection. The LODs for SEB detection were 0.3 ng/mL and 0.1 ng/mL for the planar and microtiter plate fluorescent immunoassays, respectively. Use of the Cy5-antibody conjugates as well as biotin-antibody combined with streptavidin-Cy5 conjugates yielded the same LOD for SEB detection. These results demonstrate that the planar surface fluorescent immunoassays perform on par with the fluorescent microtiter plate experiments. However, planar surface fluorescent immunoassays are advantageous over 96-well/384-well plate experiments because of their greater potential to be developed into a POC device due to smaller reagent volume requirements and the ability to automate the fluidic components.

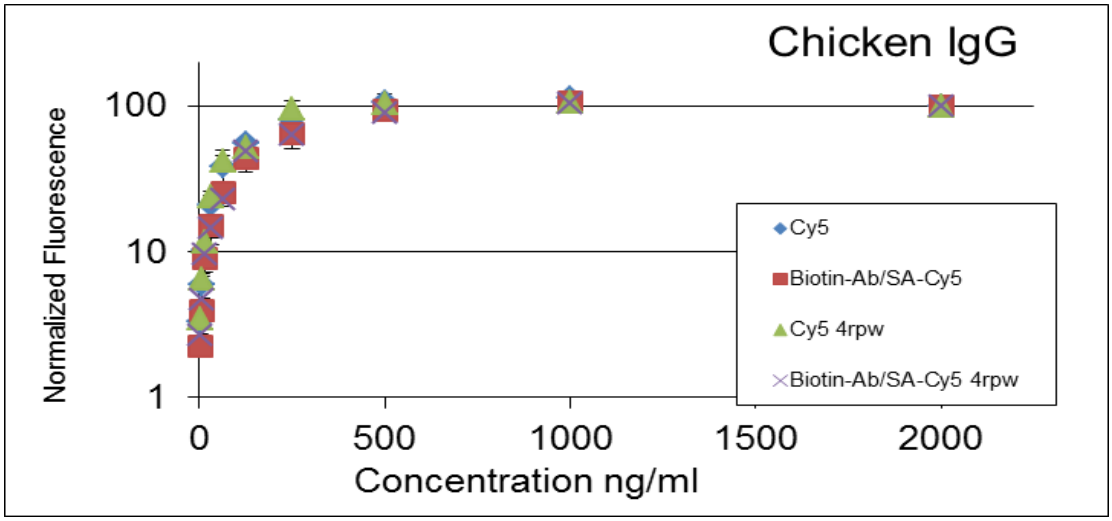

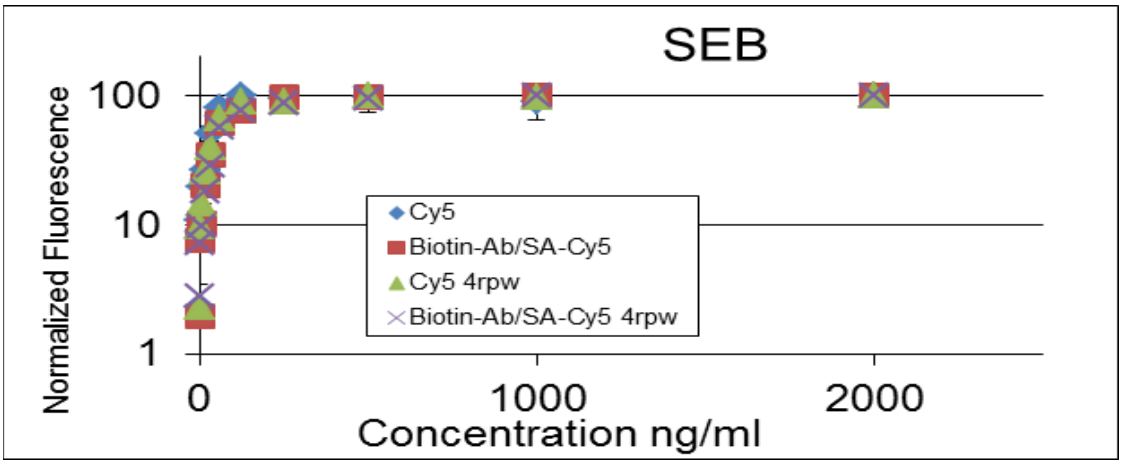

Figure 16. 96-well microtiter plate fluorescent immunoassay characterization of chicken IgG and SEB. Cy5 and biotin-antibody/streptavidin-Cy5 methods are shown as well as data using 1 read per well (rpw) and 4 reads per well.

Luminex

In addition to exploring fluorescent immunoassays to detect biological molecules, bead-based assays using the Luminex 100/200 is a common technique for multiplexing that is done in solution rather than using a surface as with the planar surface fluorescent immunoassays. However, like the planar surface technique, but unlike ELISA, the Luminex does not use amplification. The Luminex allows for

multiplexing with the use of different "colored" beads that are coated with a capture antibody [10]. Measurements regarding proteins, DNA, RNA, and other molecules can be made with the use of beads [64]. The Luminex offers up to 500 internally color-coded unique beads using various dye combinations and could therefore potentially detect up to 500 different proteins simultaneously. Using this method, beads coated with different capture antibodies can be used to detect various analytes.

SEB singleplex detection on the Luminex has an initial jump in intensity above background that gives an LOD of approximately 1.9×10^{-6} ng/mL. However, this initial jump remains fairly flat until the dynamic range of the curve which spans a region of 0.24 ng/mL to 500 ng/mL. When testing SEB in a multiplex format with three other toxins (Anthrax Lethal Factor, Ricin, and *Yersinia enterocolitica*), the LOD was 0.015 ng/mL. Reported LODs for SEB detection via similar immunoassay techniques are typically between 0.003-0.1 ng/mL [150-156]. However, many of these reported values are for multiplexed detection or detection in a realistic buffer, which raises the background. The LOD for chicken IgG detection on the Luminex was 0.0005 ng/mL with an average dynamic range of 0.3052 to 1250 ng/mL. The Luminex is a promising method for detecting multiple analytes at the same time, and there have been some efforts to miniaturize the technology[45, 151].

Discussion

The objective of this chapter was to develop a planar surface fluorescent immunoassay for detection of multiplexed protein analytes using low sample and reagent volumes. Various microfluidic designs and materials were tested in order to create the new detection platform. Once the final design was created, in order to characterize the immunoassay, a variety of studies were conducted to compare and contrast the features of several immobilization chemistries, to optimize the antibody patterning concentration and its consistency, to assess the effects of washing the surface and fluid flow, and to determine the signal variation both within and between slides. These assessments demonstrated the ability of the planar surface fluorescent immunoassay for use in detecting protein analytes.

Template Designs

In order to demonstrate the advantage of using this new platform over standard techniques, the goal was to keep the sample volume below 20 μL, which is the lowest working volume recommended to perform a fluorescent immunoassay in a standard 384-well plate. Several iterations of various channel dimensions and microfluidic designs were investigated to optimize the assay for the needs of multiplexing and using low reagent/sample volumes. Although the design was set at 108 spots with 9 patterning channels and 12 assay channels, the template could be amended for future needs if more or less spots are desirable.

Surface Functionalization

In addition to adjusting the template designs, the surface functionalization chemistry could be changed to suit particular needs. Five different chemistries were tested for potential antibody immobilization and thiol silane with a GMBS crosslinker was used for the majority of subsequent tests. Despite the many advantages of using this immobilization chemistry for the biosensing needs in this work, different applications may make alternate chemistries (e.g., more hydrophobic) more appropriate. The templates used in this work could be applied for performing immunoassays using other surface immobilization chemistries. Not only can the different surface chemistries be adjusted based on needs, but different types of assays such as reverse phase assays and competitive assays may be possible using planar surface fluorescent immunoassays.

Several immobilization chemistries were tested for use with the planar surface fluorescent immunoassay. Taking the standard deviation into account (Figure 15), the thiol silane with or without GMBS performed similarly, but due to the LOD, the consistency of patterning antibodies onto the surface, and due to other factors discussed above, thiol silane with the cross-linker was chosen for further studies. A summary of the parameters that were taken into account when selecting the "best" immobilization chemistry are shown in Table 6. The surfaces with the larger contact angles employing covalent or hydrophobic interactions (CH_3-Silane and SH-Silane with/without GMBS) theoretically should theoretically have yielded the best results. However, CH_3-silane had a lower level of reproducibility as compared to the SH-

silane surface. The LOD for CH_3-silane and SH-silane with GMBS were the same for both chicken IgG and SEB detection, but the LODs for SH-silane without GMBS were not as good as with GMBS for chicken IgG detection. The fluorescence intensity increased more with each doubling of the analyte for SH-silane with/without GMBS as opposed to CH_3-Silane. The procedure for thiol/GMBS is easy to conduct, results in a covalent bond to consistently immobilize proteins onto the surface, is the most reproducible chemistry of five tested, and demonstrates low LODs and large increases in signal as the analyte concentration increases. All of these characteristics taken together indicated that SH-silane with GMBS was the most suitable immobilization chemistry to use for subsequent experiments.

Patterning Technique: Gridder Accent (Digilab)

In addition to the vinyl/polycarbonate/acrylic templates that were employed for immobilization of antibodies onto functionalized microscope glass surfaces, a Gridder Accent (Digilab) was also investigated for depositing antibodies onto glass surfaces. The Gridder Accent is a type of contact arrayer, which is a mechanical instrument that can be programmed to put antibodies onto a surface in a prescribed pattern for creating microarrays. The instrument can handle up to three reagent plates and can pattern up to 50 slides in an environment of variable humidity. The instrument utilizes High-Efficiency Particulate Air (HEPA) filters to operate in a dust-free environment and the pins used for printing can be cleaned with the built-in sonication system. Like the manual patterning technique previously described, the microscope glass slide must first be primed with a specific type of chemistry. Various surface

modifications such as the thiol silane/GMBS (Figure 5) were investigated to determine the optimal one for use with the Gridder Accent. To perform the assay on patterned slides, alternate flow cells were created using Epilog Printer templates. The new flow cells required optimization to reduce sample volume. Different surface chemistries and machine parameters such as humidity were investigated when patterning with the Gridder Accent to determine the best conditions for printing on various modified surfaces.

Ultimately, use of the Gridder Accent was nixed for future experiments because the instrument is large, expensive, requires maintenance and highly-trained personnel for operation. Moreover, microarray printers have already been demonstrated in the literature for various uses such as identification of antigens, screening of small molecule ligands, and comparison of genotypes [157-159]. Some disadvantages of using microarray printers have been noted such as production of spots containing higher densities of proteins, which can be problematic when assessing analyte signal, and the evaporation of solutions, which are exposed to the environment [160].

On the other hand, the template designs micromachined on the Epilog Printer, combined with the method for performing an assay, create a smaller and cheaper platform that can be more readily transitioned to a POC device. Additionally, this system is easy to create and customize to particular sensing needs, it is less likely to suffer from evaporation of reagents or samples because of the closed channels, and

reactions can take place quicker than other techniques because of the microscale volumes used [160].

Immunoassay LOD

Compared to results published in the literature, our platform's performance is on par with other platforms. For example, the LOD for SEB in milk was 0.5ng/mL when using a PDMS microfluidic device [161]. Other LODs reported for SEB in-house developed immunoassays using chemiluminescent methods ranged from 0.01 ng/mL to 0.1 ng/mL [162-164]. Despite similar LODs between the planar surface fluorescent immunoassay and those reported in the literature, our device is more readily amenable to a POC device.

Immobilized Protein Orientation

There are many methods for immobilizing and orienting proteins onto a surface and a review of the published literature describes mixed results regarding the usefulness of orientation control. Consequently, protein orientation procedures were not investigated in the experiments described in this work. Instead, a procedure that uses covalent binding for protein immobilization was used because of the non-controversial benefits of using this type of format.

Immobilization of proteins, either physically or chemically, onto a surface is common for numerous biosensing applications [130]. However, immobilization procedures can cause proteins to undergo slight, moderate, or even total loss of conformational

activity due changes in the structure of the protein. When proteins are immobilized, their conformation changes to enable interaction with the immobilization construct, particularly with hydrophobic surfaces. For example, adding carbonyl groups increases the hydrophilicity of a surface leading to an increase in the total number of proteins adsorbed, but the proteins often have distorted structures [165]. Due to the various molecular interactions involved with the immobilization technique, proteins are randomly oriented on the surface, and some proteins may no longer be able to recognize the intended target because the epitope (F_{ab}) is hindered by immobilization [130, 131].

Covalent immobilization restricts the number of ways proteins can become immobilized to specific reactive groups, creating more predictable protein orientation [131]. When covalent immobilization is used, enough antibodies randomly orient themselves appropriately to undergo the desired biological interactions without decreasing sensitivity. Common residues used for covalent protein immobilization are lysine and cysteine because the former is typically present on a protein's exterior (especially antibodies) and the latter can form disulfide bonds via the thiol group [130]. One drawback of using lysine residues is that multiple bonds between a single antibody and the surface often form, which can reduce binding ability and cause multiple orientations of proteins on the surface.

When using noncovalent adsorption, proteins can attach to the surface in numerous ways, so orientation of the protein is varied and control is limited. To allow for more

control over the orientation of proteins on a surface, researchers have developed alternatives to noncovalent adsorption which position proteins in a manner that ensures single point attachment and availability of specific binding sites for further interactions [130]. However, it is challenging to orient all antibodies in one direction, even using complex procedures. Studies have indicated improved outcomes by controlling the immobilization process in a reproducible manner, such as engaging/introducing unique amino acid residues less likely to affect the target binding ability of the antibody, using Protein G or Protein A which target the F_c portion of antibodies, or using biotin, which is introduced to unique sites on the antibody [130, 166-173]. Protein A can be used to orient proteins on a surface, but it is not ideal for sandwich formats because it can non-specifically interact with tracer antibodies, causing a high background. Some studies have demonstrated improved assay performance by as much as 10-fold when single point protein immobilization strategies were used [165]. Other studies have shown that controlling the orientation of proteins can be highly reproducible, yet in some cases only 70% of antibodies are in the desired orientation [130, 165].

Despite some of the advantages described, there are various drawbacks with orienting proteins onto a surface. For example, when proteins were covalently linked to the surface, researchers did not find dramatic differences in epitope binding between oriented and randomly immobilized proteins [130]. In addition, thiol group immobilization techniques do not create stable bonds under reducing conditions (i.e. the bond to the solid support can become reduced) [130]. Furthermore, researchers

found that site-directed immobilization does not necessarily provide advantages. When four methods of immobilization (biotin-avidin, thiol/disulfide exchange, aldehyde coupling, and carbodiimide coupling) were investigated, each demonstrated comparable binding capabilities. Lastly, coupling via carbohydrate moieties is flawed because both the F_{ab} and F_c regions on an antibody may be involved in the immobilization process, reducing the ability of the epitopes to bind to the intended target.

The results of orientation controls in published literature are contradictory. Some studies demonstrate benefits, while others state there is limited to no improvement. Due to these challenges and limited benefits regarding orientation of proteins discussed above, the type of immobilization technique employed (covalent bond) in our studies, and the success of our experiments, protein orientation procedures were not investigated.

Conclusion

Planar surface fluorescent immunoassays were developed using stencils designed and created to minimize the amount of sample and reagents needed. These templates were constructed of vinyl, polycarbonate, and acrylic components and only required 2 µL per channel for patterning antibodies onto the surface and 5 µL per channel for performing an assay. A variety of different surface functionalization chemistries were investigated and the best-performing was thiol-silane with a GMBS cross-linker, which covalently bonds proteins by their amine groups. Experiments demonstrated low background fluorescence after patterning antibodies onto the surface. Experiments were conducted to determine the optimal patterning concentration of antibodies (10 µg/mL) as well as the consistency of patterning both with and without flow of fluid over the surface. Planar surface fluorescent immunoassays demonstrated higher fluorescence when higher concentrations of analytes were present and the proportional increase from one concentration to another was consistent among slides. Comparison of planar surface fluorescent immunoassays to standard microtiter plate fluorescent immunoassays and those reported in the literature was favorable as the LODs were on the same order of magnitude.

Novelty of work

There have been no peer-reviewed publications featuring a similar design as the low-volume planar surface fluorescent immunoassays featured in this work. This design is novel in that only 2 µL is needed per horizontal channel and only 5 µL is needed

per vertical channel. This design is unique in that the assay can be customized to the needs of the particular application. For example, multiplexing is possible in either the horizontal direction or vertical direction, enabling either 9 or 12 different samples or capture antibodies to be used.

The materials used to create templates for patterning and performing the assay (vinyl, polycarbonate, and vinyl) are cheap to purchase and fabricate, making them attractive for use. Assembling the templates in a multi-layer fashion is easy to accomplish, but could be made even easier with the use of automated machinery. The assay itself is relatively cheap to conduct because all of the components and reagents needed are required in smaller amounts than traditional standard detection systems.

The application of the methods employed for surface functionalization in conjunction with the designed templates is new and has not yet been published. Characterization of the assay using two commonly-used analytes demonstrates comparable performance compared to standard microtiter plate fluorescent immunoassays. However, use of microtiter plates is not amenable to a POC environment. On the other hand, this newly-developed platform is small enough to be incorporated into a hand-held device and uses volumes low enough to make it suitable for future development into a POC device.

Chapter 4: Spatial Multiplexed Detection of Planar Surface Fluorescent Immunoassays

Abstract

Planar surface fluorescent immunoassays were evaluated for multiplexing of two proteins, chicken IgG and SEB. Assessments demonstrated that there is no cross-reactivity of the antibody or reagent contamination between the channels when patterning antibodies onto the surface or when performing the assay. Results show the specificity of capture and detection antibodies. Planar surface fluorescent immunoassays performed similarly to standard microtiter fluorescent immunoassays using a variety of different Cy5-labels.

Background

This chapter builds upon the work of Chapter 3. Following characterization of this newly developed platform, planar surface fluorescent immunoassays were tested using the thiol-silane and GMBS crosslinker chemistry. Full dose responses and LODs were determined for the analytes (chicken IgG and SEB) individually as well as in a multiplexed format. SEB was chosen for investigation because this toxin is often involved in testing sensing platforms and usually serves as a basis to compare the LOD with other platforms published in the literature.

Methods

Materials

Staphylococcal enterotoxin B (SEB) and affinity purified rabbit anti-SEB were purchased from Toxin Technology Inc. (Sarasota, FL). Rabbit anti-Chicken IgG (IgY) and Chicken IgG were purchased from Jackson ImmunoResearch Laboratories Inc (West Grove, PA). Phosphate buffered saline (PBS), Phosphate buffered saline with Tween (PBST), and bovine serum albumin (BSA), methanol, potassium hydroxide, toluene, ethanol, dimethyl sulfoxide, (3-mercaptopropyl)triethoxysilane, 4-maleimidobutyric acid N-hydroxysuccinimide ester, and J. Melvin Freed Brand Microscope Slides, Plain were obtained from Sigma-Aldrich (St. Louis, MO). Doubly distilled water (ddW) was used throughout the experiments and was prepared in house using a Nanopure Diamond™ water purification system (Barnstead, Dubuque, IA). Clear acrylic was obtained from Piedmont Plastics (Elkridge, MD). Impact-Resistant Polycarbonate was obtained from McMaster-Carr (Robbinsville, NJ). Fluid handling chips were designed in CorelDraw X4 (Corel Corp. Ontario, Canada) and micromachined using a computer controlled Epilog Legend CO2 65 W laser cutter (Epilog, Golden, CO). 3M 9770 adhesive transfer tape was used to hold together the layers of the planar surface fluorescent immunoassay. A REGLO Digital pump, appropriate connectors, and tubing were obtained from Ismatec (Wertheim, Germany). Appropriate connectors for the tubing were obtained from Cole Parmer (Vermon Hills, IL). Data was analyzed using Microsoft Excel (Microsoft, Redmond, WA) and GraphPad Prism (GraphPad Software, La Jolla, CA).

The same methods as in Chapter 3 were used in these studies regarding surface functionalization, epilog printer templates, and capture antibody patterning for the planar surface fluorescent immunoassays, using the optimized SH-silane/GMBS chemistry.

Planar Surface Fluorescent Immunoassay

All of the steps for fabrication, assembly, and experimentation are the same as in Chapter 3. However, if biotin-streptavidin interaction was utilized (Figure 17), after exposure of the sample, a detection antibody conjugated to biotin was exposed to the surface for 1 hr. at RT in a humid chamber, covered with aluminum foil. Following 3X PBST washes, Jackson ImmunoResearch Cy5-Streptavidin (JISA), Thermo Scientific Cy5-Streptavidin (TSSA), or Cy5-NeutrAvidin (TSNA) was applied and incubated for 1 hr. at RT. Following exposure to the tracer antibody, 3 washes with PBST were conducted. A GenePix 4000B slide scanner was used to quantify the Cy5 fluorescence.

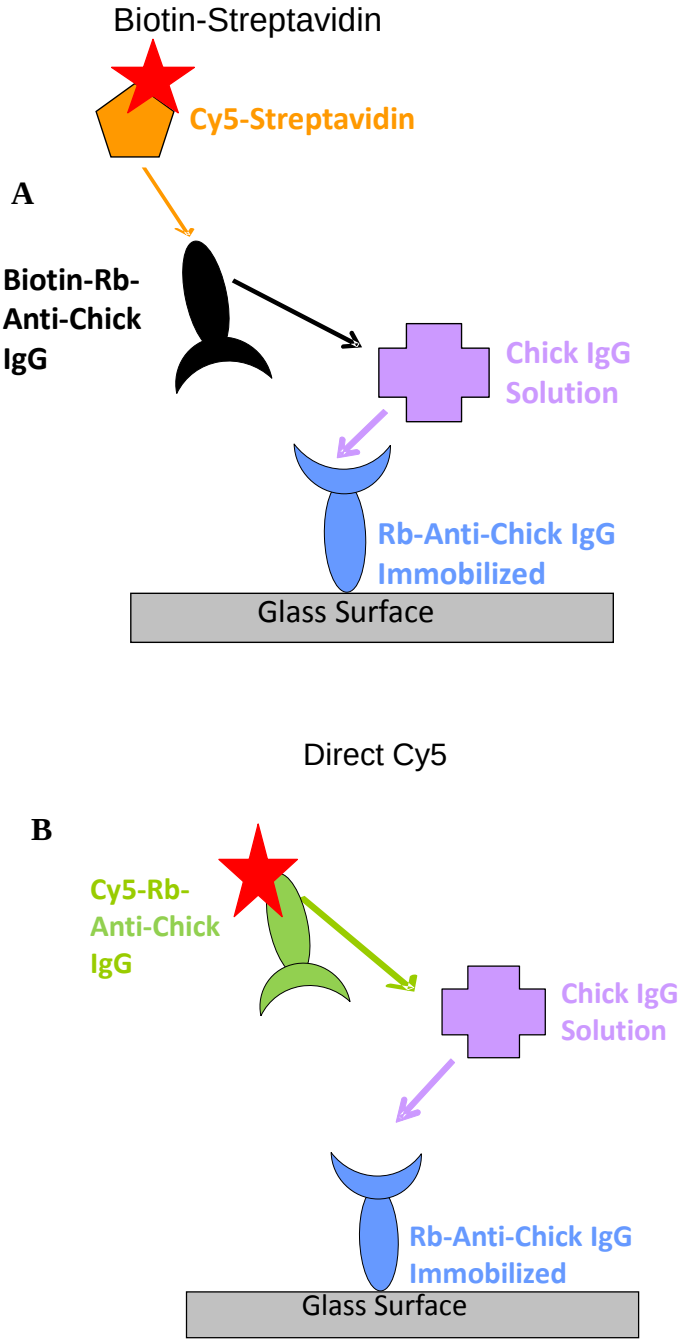

Figure 17. Comparison of (A) biotin-streptavidin and (B) direct Cy5 detection schemes using a sandwich assay format

Results

Planar Surface Fluorescent Immunoassay – Various Detection Labels

Experiments were conducted to demonstrate the versatility of the platform for use in typical sandwich assays using Cy5-labeled antibodies as well as assays utilizing biotin (Bt)-streptavidin (SA) interactions. In these assays, the analyte is first bound by the capture antibody immobilized on the surface before being exposed to either Biotin-anti-chicken IgG (Bt-αCh) or Biotin-anti-SEB (Bt-αSEB), followed by fluorescently labeled (Cy5) SA (Figure 17). Three different Cy5-SA conjugates were compared: ThermoScientific Streptavidin (TSSA), ThermoScientific NeutrAvidin (TSNA), and JacksonImmuno Streptavidin (JISA). Optimization experiments demonstrated that the optimal concentrations of biotin and tracer were 10 μg/mL and 7.5 μg/mL, respectively. JISA, TSNA, and TSSA performed similarly, so JISA was chosen for future experiments due to its cost-effectiveness.

A singleplex image of a sandwich assay involving biotin-NeutrAvidin detection for SEB is shown in Figure 18. This image shows how each spot exposed to a specific concentration of chicken IgG is distinct and of a consistent intensity. To demonstrate the full dose response of the assay, experiments were conducted at higher concentrations to show saturation of the signal. For chicken IgG, saturation is evident at 200 ng/mL for Cy5-JISA and 400 ng/mL for Cy5-Rb-αcChicken and Cy5-NeutrAvidin (Figure 19). For SEB, saturation is evident at 400 ng/mL for all tracers (Figure 19). All experiments were conducted at a gain of 700 to allow for analysis among slides. In this mode, the highest mean fluorescence obtained is 65,000 units.

Patterning
Anti-SEB
10 µg/ml

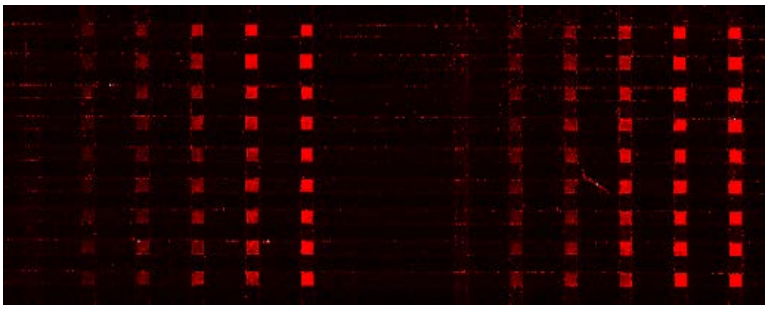

1 2 3 4 5 7 8 9 10 11 12
6

SEB Assay:
Rows 1, 7 – 0 ng/ml
Rows 2, 8 – 1.25 ng/ml
Rows 3, 9 – 2.5 ng/ml
Rows 4, 10 – 5 ng/ml
Rows 5, 11 – 10 ng/ml
Rows 6, 12 – 20 ng/ml
Tracer Antibody:
Step 1: Rows 1-6 – 10 ug/ml Cy5 Rb-anti-SEB
Rows 7-12 – 10 ug/ml Bt Rb-anti-SEB
Step 2: Rows 1-6 – PBST
Rows 7-12 – 7.5 ug/ml Cy5-NA

Figure 18. Image of planar surface fluorescent immunoassay: Detection of SEB using either direct detection (Cy5-Rb-anti-SEB for rows 1-6) or NeutrAvidin (NA)-Cy5 plus Biotin-Rb-anti-SEB (rows 7-12) as detection label

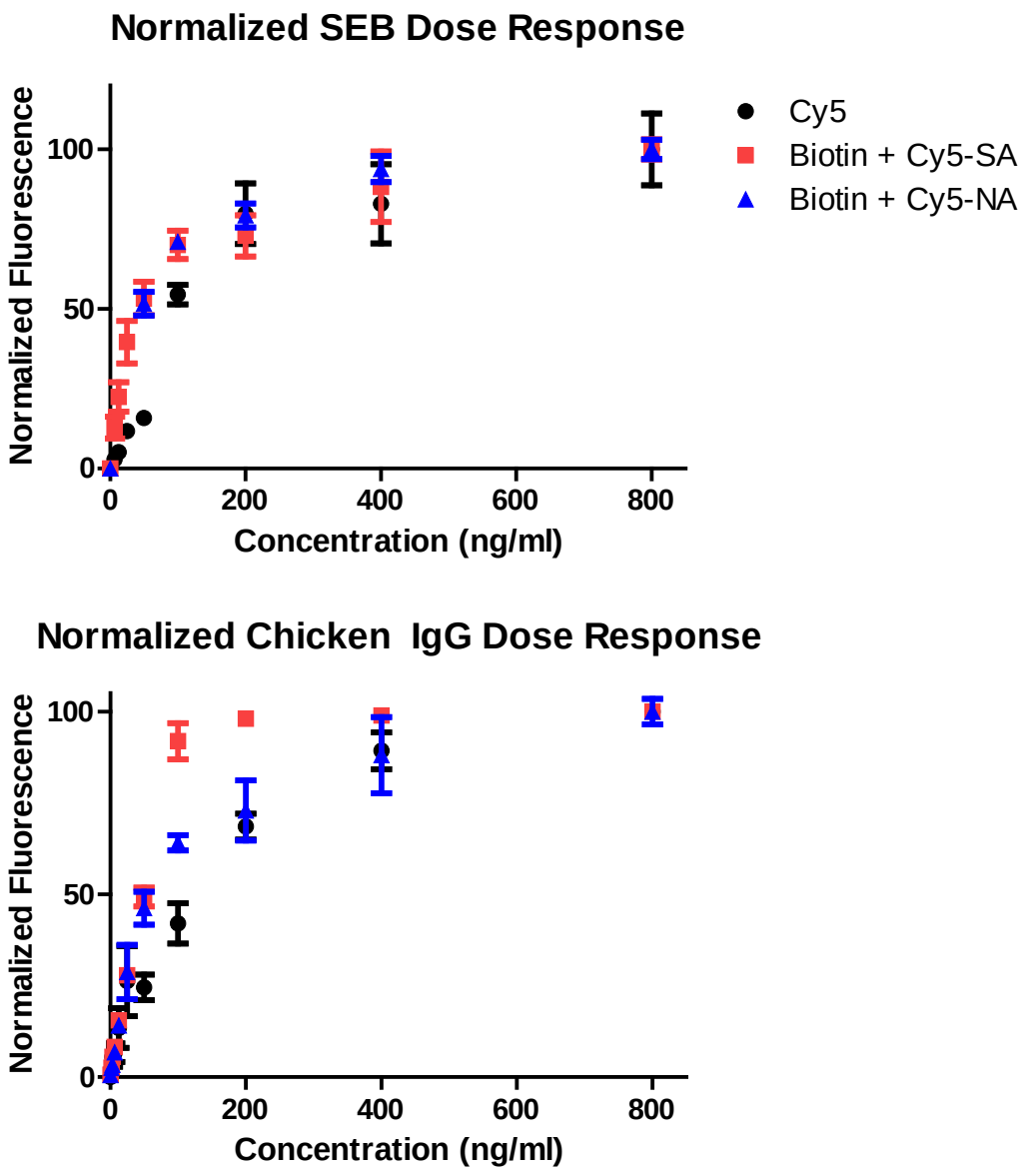

Figure 19. Platform characterization: dose response for SEB and chicken IgG using different fluorescent labels: Cy5, biotinylated antibody + Cy5-streptavidin, and biotinylated antibody + Cy5-NeutraAvidin

Following characterization of the platform for each analyte using direct and indirect detection methods, multiplexed experiments involving detection of both analytes were conducted. Figure 20 shows an image of a multiplexed assay using a JISA-Cy5 detection label. Simple interrogation by eye shows the specificity for each antibody for the respective target protein. The Cy5-SA tracer or Cy5-SA + Bt-antibody demonstrated a much higher signal in the region where anti-chicken capture antibodies were patterned and exposed to chicken IgG than in the region where anti-SEB capture antibodies were patterned (and also exposed to chicken IgG). For example, the upper left quadrant represents the region where Rb-anti-chicken IgG capture antibody was patterned on the surface and where chicken IgG was exposed to the surface in increasing concentrations from left to right. The intensity of the red spots becomes increasingly brighter as the concentration increases. There are no bright spots in the left-most lane where only buffer was exposed during the assay. Additionally, in the bottom left quadrant, where the Rb-anti-SEB capture antibody was patterned, there are no bright spots.

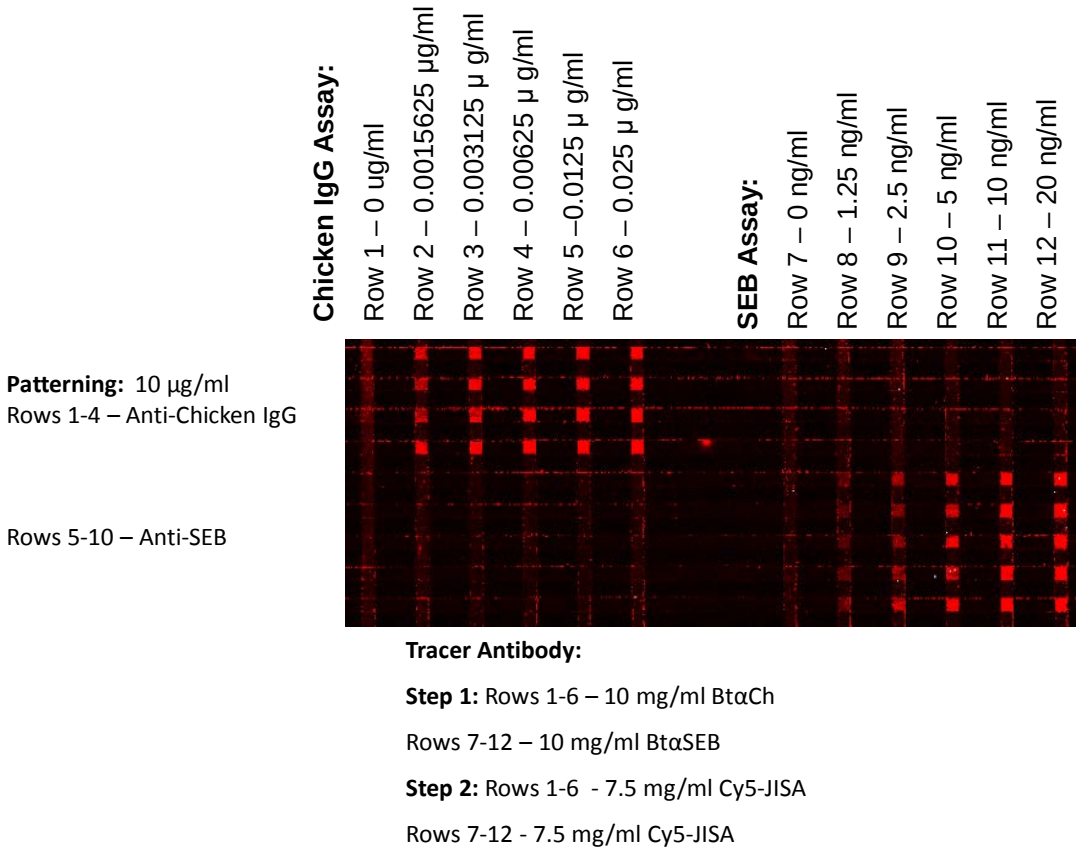

Figure 20. Image of planar surface fluorescent immunoassay: multiplexed detection of chicken IgG and SEB using JacksonImmuno streptavidin-Cy5 as detection label

Likewise, the Cy5-SA tracer or Cy5-SA + Bt-antibody demonstrated a much higher signal in the region where anti-SEB capture antibodies were patterned and exposed to SEB versus the region where anti-chicken IgG capture antibodies were patterned (and also exposed to SEB). The upper right quadrant shows low levels of intensity where the SEB assay was performed on the part of the surface where Rb-anti-chicken IgG antibodies were patterned. As predicted, the lower right quadrant, the region where Rb-anti-SEB capture antibodies were patterned on the surface, shows increasing levels of intensity from left to right as the concentration of SEB increases. These

results demonstrate the specificity of the anti-chicken antibodies for chicken IgG, and anti-SEB antibodies for the SEB. The image also shows the success of this design in that a decrease in fluorescence was associated with a lower amount of the target present (the brightness of the red spots decreased). This data elucidates the success of meeting one benchmark—the assessment of any cross-reactivity of the antibody or reagent contamination (due to leaking or pipetting error) between channels that could occur when patterning or when performing the assay. Furthermore, no contamination occurs because the fluorescence of spots expected to be bright are bright, and vice versa.

The results visually shown in Figure 20 regarding the specificity of the capture and detection antibodies in a multiplexed format are graphically represented in Figure 21. This figure shows that dose response curves for chicken IgG were obtained from regions of the glass slide patterned with chicken capture antibodies, but no signal was observed in the SEB capture regions of the slide. Likewise, the second graph in Figure 21 shows that dose response curves for SEB were obtained from regions of the glass slide patterned with SEB capture antibodies, but not in the chicken capture regions. These results demonstrate the functionality of the multiplex assay.

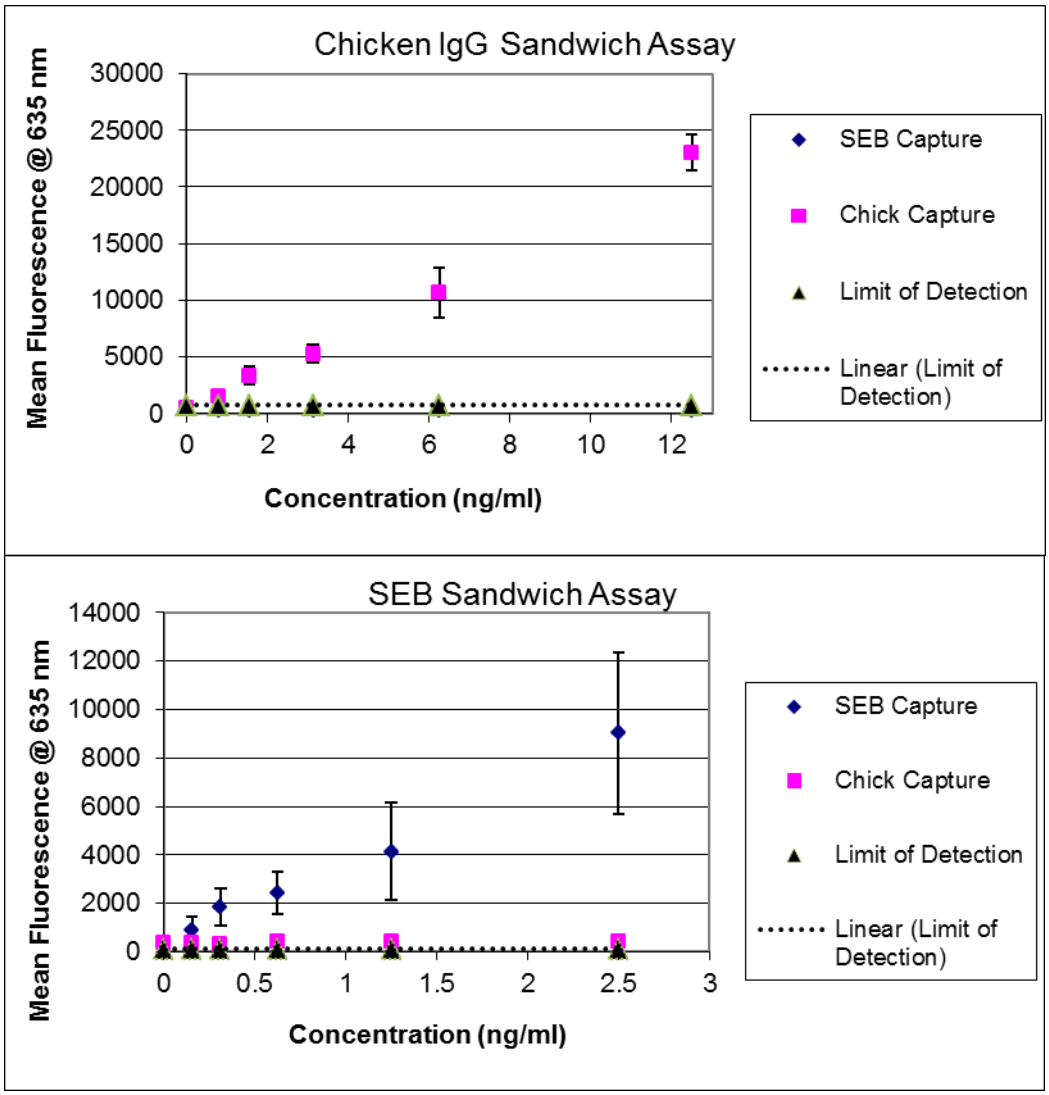

Figure 21. Mean fluorescence vs. concentration for multiplexed detection of chicken IgG or SEB in a sandwich assay format.

The limit of detection was at or below the background signal obtained on a capture region immobilized with chicken IgG when an SEB assay was performed. Likewise, the LOD was at or below the background signal obtained on a capture region immobilized with SEB when a chicken IgG assay was conducted. Here, as the concentration of the analyte increased, the fluorescence increased proportionately, but the fluorescence of the opposite capture antibody region remained low across the slide. Increasing the concentration of SEB in the assay channel did not increase the background signal on the Rb-anti-chicken IgG capture antibody region of the slide. These results demonstrate the specificity of the antibodies for their target proteins and the ability of the developed platform to clearly separate one channel from another. Due to the success of using chicken IgG antibodies and SEB, we expected to be able to distinguish other proteins using a similar experimental design.

Comparison to Microtiter Plate Fluorescent Immunoassays

Table 7 shows the LOD for detection of SEB and chicken IgG using the newly developed planar surface fluorescent immunoassay and standard microtiter plate fluorescent immunoassays (using the 1 read per well setting) for a variety of different detection labels. These results demonstrate that the planar surface platform performs on par with the standard platform (LODs are on the same order of magnitude) with respect to direct (Cy5) and indirect (Bt-SA) detection methods. While TSSA yields the lowest LOD for detection of either analyte, JISA was used for subsequent experiments due to its cost-effectiveness.

Table 7. LOD comparison of 96-well microtiter plate and planar surface fluorescent immunoassay platforms. TSNA = ThermoScientific NeutrAvidin, JISA = JacksonImmuno Streptavidin, TSSA = ThermoScientific Streptavidin.

		Limit of Detection	
Analyte	**Tracer**	**Planar Surface**	**96-well Plate**
Chicken IgG	Cy5-Rb-Anti-Ch	0.4 ng/ml	0.3 ng/ml
	TSNA	0.4 ng/ml	
	JISA	0.4 ng/ml	0.3 ng/ml
	TSSA	0.1 ng/ml	
SEB	Cy5-Rb-Anti-SEB	0.3 ng/ml	0.1 ng/ml
	TSNA	0.3 ng/ml	
	JISA	0.3 ng/ml	0.1 ng/ml
	TSSA	0.08 ng/ml	

Discussion

The objective of this chapter was to demonstrate the multiplexing capability of the planar surface fluorescent immunoassay. The studies presented here investigated detection of two proteins, chicken IgG and SEB. Different tracers involving Cy5 dye were used to characterize the multiplex sandwich assays in either a direct (antibody conjugated to Cy5) or indirect (using biotinylated antibody and streptavidin-Cy5) method. The LOD and specificity of each label was demonstrated and compared to results using standard 96-well plate experiments. Results showed that the planar surface fluorescent immunoassays are capable of multiplexing and perform with similar LODs as microtiter plates, but require much less sample and reagent volumes. These results are promising for potential clinical use of planar surface fluorescent immunoassays for detection of proteins in biological matrices for which large volumes may not be obtainable.

Spatial Multiplexing

While studies have only been done on two analytes and a limited number of detection labels, the applications of these methods are much broader because of the ability to modify the spatial multiplexing ability for specific sensing needs. The experiments conducted in these studies used the 9 horizontal channels for patterning antibodies onto the glass surface and the 12 vertical channels for performing assays. However, if desired, 12 different antibodies could be patterned onto the surface and 9 different samples could be tested instead. Additionally, the template designs could be re-drawn using CorelDRAW X4 to increase the number of channels in either direction to

maximize multiplexing for the desired needs. While some settings (e.g., power and speed) for printing on the Epilog Legend laser cutter may need to be adjusted to accommodate different designs and materials, the flexibility exists to create new biosensing strategies.

Changing the design and/or materials for conducting immunoassays to cater to biosensing needs is not the only way to increase multiplexing potential. While only organic fluorescent labels such as Cy5 were investigated in this study, other labels with emission spectrums that span the visible and IR range such as QDs could be tested in addition to newer products such as Kodax X-sight nanospheres [174].

Conclusion

This chapter established that two different types of analytes can be detected simultaneously, at very low volumes, using Epilog printer templates to perform planar surface fluorescent immunoassays. These results are encouraging for detection of biomarkers for which larger volumes may not be obtainable. The data suggest that this type of immunoassay may be capable of detecting more analytes simultaneously than currently demonstrated here. This new platform is promising because planar surface fluorescent immunoassays performed similarly to microtiter plate fluorescent immunoassays using a variety of different organic labels, employing either a direct or indirect (biotin/avidin) detection method. While microtiter plates are limited in their use as laboratory-only experimental assays, planar surface fluorescent immunoassays can be leveraged for use in a POC environment.

Novelty of Work

This work represents the first instance of low-volume planar surface fluorescent immunoassays for spatial protein multiplexing. The immunoassay is cheap to perform because the required reagents and other components are not needed in large quantities. Since the planar surface fluorescent immunoassays performed as well as microtiter plate fluorescent immunoassays using a variety of different tracer molecules, the former could be conducted in place of a traditional assay, especially in the case where sample volume is limited.

Chapter 5: Multiplexed Detection of Renal Biomarkers

Abstract

The developed planar surface fluorescent immunoassay was evaluated using clinically-relevant biomarkers to provide some insight with regard to the potential utility of this technology for applications such as detecting acute kidney injury biomarkers. Specifically, Neutrophil Gelatinase-Associated LiPoCalin (NGAL) and Kidney Injury Marker-1 (KIM-1) were evaluated because these biomarkers reflect different aspects of renal injury. These markers may provide earlier clues regarding injury (~2 hours post insult) as opposed to standard biomarkers such as serum creatinine (SCr) and blood urea nitrogen (BUN), which only indicate damage after 24-72 hours when the kidney may already be significantly damaged [24-26]. Colorimetric assays using microtiter plates were used to evaluate these biomarkers and compared to planar surface fluorescent immunoassays. Assays were conducted in buffer as well as in spiked control urine and plasma from Sprague-Dawley rats. Assays were also conducted using urine and plasma obtained from rats treated with gentamicin (a known nephrotoxicant). While the planar surface fluorescent assays did not perform as well as the colorimetric ELISA-based microtiter plate experiments due to weaker signals overall (the colorimetric assay has an amplified signal), the LODs were still within the clinically-relevant range when spiked into PBS (KIM-1:401 pg/mL, NGAL:6.3 ng/mL).

Background

Once the optical sensor platforms were thoroughly evaluated, the planar surface fluorescent immunoassays were used in further studies for multiplexed detection of clinically-relevant renal injury biomarkers. The previous chapters demonstrated the proof-of-concept of the new optical sensor platform, while the focus of this chapter is to demonstrate the real-world relevance of this technology. The planar surface fluorescent immunoassays were applied to detection of Acute Kidney Injury (AKI) biomarkers.

The kidney filters 350 – 400 mL/100 g of tissue per minute and generates 150 – 180 L/day of ultrafiltrate, 99% of which is readsorbed, while the remaining 1% is excreted as urine [175]. The kidney operates under three basic processes: filtration, readsorption, and secretion. There are many types of diseases that can afflict the kidney such as glomerular diseases, urinary tract obstructions, nephrolithiasis, and vascular injury, to name a few, and there are a variety of causes for kidney illness, but the most common are ischemia, sepsis, and nephrotoxins (endogenous or exogenous), with sepsis being the primary cause in the developing world [29]. Ischemia can be caused post-operatively from cardiac surgery with cardiopulmonary bypass or result from complications due to burns, among other causes and diseases. Nephrotoxins such as contact agents used for imaging, antibiotics or other drugs (e.g. chemotherapeutic agents), endogenous toxins (e.g. myoglobin), and exogenous toxins (e.g. automobile antifreeze, compounds released from medical device materials) can also cause kidney disease because of the extremely high blood perfusion of the

kidney and high concentration of substances where water is readsorbed [29, 176]. All of these causes of kidney injury can lead to a diagnosis of Acute Kidney Injury (AKI).

The focus of this chapter is on detection of biomarkers associated with AKI. AKI is characterized by a sudden onset of impaired kidney function, causing retention of waste products that are normally cleared by the kidneys [29]. AKI is not a single disease, but a group of conditions that cause an increase in blood urea nitrogen (BUN) and/or an increase in the plasma or serum creatinine (SCr) and often a decrease in urine output. AKI is diagnosed as an elevation in SCr concentration of at least 0.3 mg/dL or 50% higher than baseline within a period of 24-48 hours or a reduction in urine output to 0.5 mL/kg per hour for greater than 6 hours. AKI is a major public health concern because it is associated with a high mortality rate of up to 80% [3]. BUN and SCr are not ideal biomarkers because they are up-regulated when 2/3 of the nephron's function has already been diminished.

Diagnosis of AKI using more sensitive and specific biomarkers has many applications. For example, novel biomarkers could be tested in preclinical evaluations to improve identification of nephrotoxic compounds [176]. These novel biomarkers could also be used during clinical trials for evaluating new drugs and medical devices as exposures to residues and contaminants can cause renal pathogenesis. Testing kidney biomarkers could also be useful for identifying exposure to toxic compounds that may be occupational concerns. For example,

workers in the heavy metal industries are routinely monitored for renal risk and would benefit by being tested by more sensitive and specific biomarkers [177]. Another area where early markers of nephrotoxicity may be beneficial is to test recipients of metal-on-metal implants, which may release cobalt and chromium, molecules that are correlated with renal failure [177].

It may be particularly important to diagnose AKI using a small POC device in the case of a biological attack on a large population where rapid diagnosis using small samples is critical. For example, exposure to lipopolysaccharide (LPS) from Gram-negative bacteria can cause systemic vasodilation and decreased renal perfusion and subsequent AKI [28]. Additionally, exposure to LPS causes an innate immune response and cytokine release, which may cause a nephrotoxic effect, leading to AKI [29]. Use of a small diagnostic device is also useful for operation in a low-resource setting such as in the developing world where AKI is a major medical complication resulting from infectious disease or diarrheal illnesses. A POC device would also be useful following a crash injury or natural disaster such as an earthquake where kidneys could be adversely affected. Lastly, rapid diagnosis using a small POC device is critical because subsequent early treatment is often more successful.

There are various limitations of the RIFLE (acronym for Risk, Injury, and Failure; and Loss, and End-stage kidney disease) criteria for diagnosis of AKI [178]. For example, the criteria rely upon changes in serum or plasma creatinine, which often unreliably responds to changes in glomerular filtration rate (GFR). Although

normalization of new kidney biomarker levels to serum creatinine (SCr) is controversial, a recent study states normalization is not beneficial since patients are not in a steady state of creatinine turnover [179]. Since SCr is a relatively small molecule (113 Da), it can pass through the glomerular filter while larger molecules such as NGAL cannot. Furthermore, RIFLE depends upon baseline creatinine levels, which may not be easily obtainable for many patients who have already started to exhibit renal complications. Moreover, SCr relies upon an assumed level of lean muscle mass, which may not represent the individual patient accurately. SCr has been known to rise and fall depending upon the cause of AKI, so repeated measurements are needed to assist in determining the appropriate therapeutic intervention.

Another biomarker that is often used to assess kidney function is blood urea nitrogen (BUN), but this marker, along with SCr, is insensitive for early and subtle renal insult as the kidney compensates for renal mass loss [180]. Due to the many issues associated with the RIFLE criteria and measuring BUN, there is a need for more sophisticated biomarkers that can be quantified to assess kidney function and assist in AKI diagnosis. SCr and BUN are functional biomarkers that measure GFR and are slow to rise following injury. If urine output drops to the level of the current diagnostic measure of AKI, additional novel biomarkers could be used to test urine output. This could help to determine the root cause of AKI and personalize subsequent treatment. In addition to the need for more specific biomarkers,

assessment of multiple biomarkers using the appropriate biological matrix is helpful to compensate for the relative weaknesses of some individual markers.

Understanding the compositions of the plasma and urine proteomes provides insight to the input and output of the kidney, respectively. To fully investigate kidney function, measuring biomarkers in these two matrices is important, but testing in urine is useful from a practical perspective due to its noninvasive nature [180]. Jia, et al. analyzed the proteomes of human plasma and urine and discovered that there are distinct plasma-only proteins, urine-only proteins, and select proteins found in both matrices [175]. While many proteins found in urine are due to kidney filtration and secretion, some are derived from shedding of glands in the urine tract, and a subset of these proteins may interfere with kidney output, which can impact interpretation of kidney biomarkers. One difference between the proteins in urine and those in plasma is that those in urine have a molecular mass lower than ~45 kDa because all proteins larger than this mass cannot be filtered via the kidney [181]. A recent study by Jia, et al. determined that there are 2611 proteins in plasma and 1522 proteins in urine when secreted proteins from the kidney were removed from analysis [175]. These proteins are involved in many biological processes such as response to wounding, response to stress, cell adhesion, among others. Based on these findings, it is important to investigate the presence of biomarkers in both plasma and urine to fully appreciate a patient's kidney status. Plasma is particularly important for evaluation because it represents the most comprehensive version of the human proteome [181].

The biomarkers NGAL and KIM-1 were investigated in plasma and urine because they show better sensitivity and specificity than BUN and SCr [180]. These biomarkers have high stability in urine and have no interference with pathologies unrelated to the kidney [3]. KIM-1 is one of the best-described biomarkers for renal damage and it is qualified preclinically as an accepted biomarker by the US Food and Drug Administration and the European Medicines Agency, and Pharmaceuticals and Medical Devices Agency [180]. This biomarker adds information to SCr and BUN and outperforms them. KIM-1 can indicate damage in the proximal tubule and is a transmembrane protein expressed by the tubule epithelial cells following injury [26]. KIM-1 is also a receptor for phosophatidylserine and enables the phagocytic capacity to remove cell debris following injury. KIM-1 plays a critical role in renal regeneration and has been shown to be elevated in response to nephrotoxic agents such as gentamicin, mercury, cadmium and chromium [25, 176, 180]. Studies have shown that urinary KIM-1 is as predictive of the severity of kidney injury as renal histopathology and can be detected at lower doses of nephrotoxicant as compared to BUN and SCr [176]. In one study, KIM-1 was elevated after exposure to three different nephrotoxicants (gentamicin, chromium, and mercury) after 72 hours while BUN and SCr were no different from controls. KIM-1 is increased in patients diagnosed with AKI of various causes, particularly in patients who obtained renal transplants or had tubular dysfunctions [25, 180]. KIM-1 may be elevated less than 12 hours following renal insult and can discriminate between causes of renal failure when other biomarkers cannot [182]. These studies demonstrate the sensitivity and specificity associated with KIM-1, which may be able to improve detection of AKI.

However, since KIM-1 is such a new clinical biomarker, there are no known fully-established and accepted reference intervals or values above which damage is indicated.

NGAL, also known as Lipolaclin-2 is indicative of tubule damage (not specific to proximal or distal portions). NGAL can show one of the earliest responses to renal damage, but may increase with several kidney injuries and can be released from a number of tissues following acute distress [176, 180]. NGAL is found in activated neutrophils and epithelial cells and is considered an acute-phase protein. NGAL participates in glomerular filtration and readsorption by proximal tubule cells as well as innate immune response [25]. NGAL is low in healthy kidneys, has been shown to have an elevated response to gentamicin, and is increased in patients with AKI of various causes [25, 180]. An emerging body of literature suggests that measuring NGAL in either urine or plasma can be useful for detection of inflammation and following exposure to endotoxin as well as detection of AKI [28, 176, 183]. In one study, NGAL has the most consistent predictive performance of AKI, up to 24 hours prior to clinical presentation of the disease, when compared with KIM-1, α-glutathione-S-transferase, and π-glutathione-S-transferase [179]. Since NGAL is not as specific as other biomarkers, it is important to multiplex additional biomarkers. Vashist, et al. claims that the healthy ranges of NGAL in urine and plasma are 110 – 40,000 ng/mL and 25 – 3491 ng/mL, respectively, but that in acute renal failure, these values can rise above 350 ng/mL and 400 ng/mL for urine and plasma, respectively [184]. However, the Mayo Clinic states that the cut-off value for NGAL in urine,

above which AKI is apparent, is 65 ng/mL [185]. Other studies have cited the cut-off value of NGAL as 150 ng/mL [186, 187]. Similar to KIM-1, more research may be needed to define the most informative reference interval for NGAL, if any [24]. However, unlike KIM-1, NGAL is not yet clinically-approved for diagnostic purposes.

Nevertheless, companies are developing technology to detect NGAL. For example, the diagnostics company Alere is developing a POC test to detect NGAL for use as a predictive biomarker of AKI following cardiopulmonary bypass surgery [17]. While prevention of false positives and false negatives are both important for development of a diagnostic test for AKI, much more care should be taken to avoid false negatives. The consequences of not detecting AKI early enough could result in the patient developing irreversible kidney damage, leading the patient to need dialysis or a kidney transplant. On the other hand, the consequences of treating a patient suspected of having AKI with fluids or administering drugs to correct the problem in the case of a false positive are not as dire because treatments are less likely to cause irreversible damage and the patient would probably be in a monitored setting in the hospital.

Table 8 shows various concentrations of KIM-1 and NGAL that have been reported in rats or humans. The data illustrates that the kidney may respond differently to these various insults, which contributes to the diversity in the reported values.

Table 8. Concentrations of reported Acute Kidney Injury biomarkers in healthy or diseased subjects

Reference	*Species*	*Nephrotoxic Agent*	*Biological Matrix*	*KIM-1*	*NGAL*
[25]	Sprague Dawley Rats	Cisplatin	Urine	48.26 pg/mg creatinine	2911.8 pg/mg creatinine
[26]	Wistar rats (male)	Gentamicin: 60 mg/kg bw; 120 mg/kg bw	Urine	80 µg/24 hr. at day 7; 120 µg/24 hr. at day 7	100 µg/24 hr. at day 7; 80 µg/24 hr. at day 7
[26]	Wistar rats (male)	BI-3: 100 mg/kg bw; 1000 mg/kg bw	Urine	10 µg/16 hr. at day 12; 150 µg/16 hr. at day 12	30 µg/16 hr. at day 12; 500 µg/16 hr. at day 12
[26]	F344/N rats (male)	Ochratoxin A: 21 µg/kg bw 70 µg/kg bw 210 µg/kg bw	Urine	0 ng/20 hr. at day 90; 75 ng/20 hr. at day 90; 75 ng/20 hr. at day 90	1800 ng/20 hr. at day 90; 1900 ng/20 hr. at day 90; 1700 ng/20 hr. at day 90
[188]	Wistar rats (male)	IMM125: 30 mg/kg bw 100 mg/kg bw	Urine	0.4 ng/mg creatinine at day 12; 2 ng/mg creatinine at day 12	N/A
[189]	Humans (Caucasian)	Healthy; Altered glucose tolerance	Serum	N/A	60 ng/ml; 50 – 150 ng/ml
[178]	Humans (Swedish)	ICU patients with septic shock with and without AKI	Plasma; Urine	N/A	Plasma: 134 ng/ml w/o AKI; 216 with AKI Urine: 63.5 ng/mg creatinine w/o AKI; 319 with AKI
[182]	Humans	Healthy	Urine	500-1000 pg/ml	N/A
[186]	Humans	Healthy	Plasma	N/A	Cut-off value 150 ng/ml after 2 hours post insult
[187]	Humans	Healthy	Urine and Plasma	N/A	Cut-off value of 150 ng/ml after 2 hours post insult

These numbers highlight the challenge when comparing results from various research groups because of the multiple variables that are not constant from one study to another: the time point at which measurements are taken, the agent and dose used to cause nephrotoxicity, the reported units of each biomarker, the species of rat, duration of study, etc. Natural variation exists between individuals, so analyte levels are expected to increase or decrease based on physiological states, as well as age and sex [17]. In addition, people's ethnicity can influence the risk of developing AKI (e.g. Malays have an increased risk compared to Chinese), which could suggest that baseline levels of biomarkers may be naturally elevated in certain populations and that the clinical presentation of the disease could vary based on the person's heritage [190].

Even if differing reference intervals were developed based on a personalized assessment of factors including ethnicity, standardization and development of a cut-off point or reference interval is complicated by the fact that different standards are generated by various organizations [17]. Some organizations develop standards based on bioassay units, others based on mass or mass concentration units. Even International Standards can have different cut-off points regarding whether the test is an immunoassay or other type of assay. For example, human chorionic gonadotropin (hCG), which is detected in POC pregnancy tests, has a standard of 75/589 for all tests except immunoassays, where the standard is 99/688. In some cases, it is better for each laboratory to determine its own cut-off level based on a normal population rather than relying on one reference interval.

Just as the stated values of KIM-1 and NGAL vary from one research group to another, under different conditions for healthy and unhealthy subjects, there is also variability among the LODs reported for these biomarkers. Vashist, et al. developed an ELISA for NGAL detection that utilizes a chemical crosslinking mechanism as opposed to traditional passive adsorption [184]. They reported an LOD of 3 pg/mL and a dynamic range of 2.5 – 5120 pg/mL, which improves upon conventional ELISA (LOD of 44 pg/mL and detection range of 40 – 5120 pg/mL). A comparison of the reported LODs for various commercially-available sandwich ELISA kits for NGAL detection are shown in Table 9.

Table 9. Comparative analysis of commercially-available sandwich ELISA kits for NGAL detection [184]

Manufacturer	**LOD**
R&D Systems, Inc.	78 pg/ml
Boster Biological Technology Co., Ltd.	10 pg/ml
Antibody Immunoassay Services	0.4 ng/ml
BioPorto Diagnostics	0.2 ng/ml
CycLex Co., Ltd	26.7 pg/ml
BioVendor	20 pg/ml
Argutus Medical	0.4 ng/ml

The studies in this chapter aimed to ascertain whether planar surface fluorescent immunoassays can simultaneously detect and quantify certain clinically-relevant AKI biomarkers, namely KIM-1 and NGAL, and how its performance compares to standard techniques.

Methods

Materials

Rabbit anti-Chicken IgG (IgY) and Chicken IgG were purchased from Jackson ImmunoResearch Laboratories Inc (West Grove, PA). Phosphate buffered saline (PBS), Phosphate buffered saline with Tween (PBST), methanol, potassium hydroxide, toluene, ethanol, dimethyl sulfoxide, (3-mercaptopropyl)triethoxysilane, 4-meleimidobutyric acid N-hydroxysuccinimide ester, J. Melvin Freed Brand Microscope Slides, Plain, Corning Costar® flat bottom high binding clear 96-well assay plates, Thermal Seal® sealing film for 96-well plates, sulfuric acid, tetramethylbenzidine liquid substrate, and bovine serum albumin (BSA) were obtained from Sigma-Aldrich (St. Louis, MO). Sureblue TMB Microwell peroxidase substrate was obtained from KPL (Gaithersburg, MD). Doubly distilled water (ddW) was used throughout the experiments and was prepared in house using a Nanopure Diamond™ water purification system (Barnstead, Dubuque, IA). Commercially-available colorimetric kits were evaluated using 96 well plates (colorimetric detection) and planar surface fluorescent immunoassays. R&D System Cat# DY3689 was supplied with a monoclonal capture antibody and a polyclonal detection antibody for KIM-1 detection. R&D Systems Cat# DY3508 was supplied with polyclonal capture and detection antibodies for NGAL detection. Clear acrylic was obtained from Piedmont Plastics (Elkridge, MD). Impact-Resistant Polycarbonate was obtained from McMaster-Carr (Robbinsville, NJ). Fluid handling chips were designed in CorelDraw X4 (Corel Corp. Ontario, Canada) and micromachined using a computer controlled Epilog Legend CO2 65 W laser cutter (Epilog, Golden, CO).

3M 9770 adhesive transfer tape was used to hold together the layers of the planar surface fluorescent immunoassay. A REGLO Digital pump, appropriate connectors, and tubing were obtained from Ismatec (Wertheim, Germany). Appropriate connectors for the tubing were obtained from Cole Parmer (Vermon Hills, IL). Data was analyzed using Microsoft Excel (Microsoft, Redmond, WA) and GraphPad Prism (GraphPad Software, La Jolla, CA).

96-Well Plate ELISA Studies using Standards

The microtiter plate ELISAs were conducted in a sandwich format (Figure 4). In this format, capture antibodies were immobilized onto the surface of the wells. Only a single capture antibody species was immobilized onto the surface (using 50 µL per well). In these experiments, either 2 µg/mL of Anti-KIM-1 or 0.8 µg/mL of Anti-NGAL in PBS were immobilized in each well. To allow ample time for the capture antibodies to adsorb to the plate, the plate was sealed with Thermal Seal® sealing film and incubated for overnight at RT.

The 96-well plates used in this study were clear Corning Costar flat bottom high-binding polystyrene plates that have an ionic/hydrophobic chemistry that enables them to bind to the capture antibodies. No preparation was required to prepare the surface of each well to ensure binding to the capture antibodies. The antibodies randomly oriented themselves and attached to the surface.

The following day, the wells were emptied and washed three times with 200 µL/well Wash Buffer (0.05% Tween® 20 in PBS). The surface was blocked with 300 µL per well of a blocking buffer (1% BSA and PBS) to prevent non-specific binding to the surface. The plate was placed on a rocker for ~1 hr. at RT during blocking (The Belly Dancer, Stovall LifeScience, Inc, Greensboro, NC, USA), followed by three washes with the Wash Buffer.

The next step of the immunoassay was to expose the wells to the target antigen (50 µL/well) for 2 hrs. on a rocker, followed by three washes with the Wash Buffer to remove any non-specific binding (4 x 200 µL/well). The singleplex immunoassays were exposed to samples of either KIM-1 (0–500 pg/mL) or NGAL (0-5000 pg/mL) in 1% BSA + PBS. The wells were exposed to either the KIM-1 (200 ng/mL) or NGAL (150 ng/mL) biotin-labeled detection antibody and placed on a rocker for 2 hrs. followed by three washes to remove any non-specific binding (3 x 200 µL/well). Each well was exposed to 100 µL of 1:200 Streptavidin-HRP (in 1% BSA + PBS) for 20 min on the rocker and covered with aluminum foil to prevent direct exposure to light. Following, three washes with the Wash Buffer, the wells were exposed to 100 µL of the Substrate Solution (Tetramethylbenzidine (TMB)), covered with foil, and placed on the rocker for 20 min. The Stop Solution (1 M Sulfuric Acid) was applied to each well (100 µL) and the plate was tapped to ensure thorough mixing. The optical density of each well was determined using a plate reader (Tecan Infinite M1000 Dual Monochromator Multifunctional Plate Reader (Tecan, Research

Triangle Park, NC)) set to measure absorbance at 450 nm. Data was analyzed and interpreted using Microsoft Excel.

Negative controls were always present for each assay to determine whether the assay was performing appropriately. For example, a negative control involved exposing some wells of the 96-well plate solely to buffer instead of samples. In this case, the capture antibodies were exposed to buffer only and therefore were not exposed to the analyte, but were exposed to the detection antibody, Streptavidin-HRP, Substrate Solution, and Stop Solution.

Planar Surface Fluorescent Immunoassays using Standards

The same methods described previously were used in these studies regarding surface functionalization, epilog printer templates, and capture antibody patterning, except the antibodies, standards, and detection antibodies were those involving KIM-1 and NGAL. Note that the assays conducted here used the Biotin-antibody conjugate + Streptavidin-Cy5.

Capture antibody modified slides were blocked for 1 hr. at RT in 1% BSA+PBS and rinsed with ddW. Slides that were not used immediately were stored in PBS for up to four weeks. Slides were dried with air and assay templates were applied by hand. The slide was then exposed to different concentrations of KIM-1 and NGAL in 1% BSA+PBS, which were loaded onto the slide via channels oriented perpendicular to the rows of patterned capture antibodies (i.e. in the vertical direction, Figure 6) using

a REGLO digital pump. Inlets and outlets were covered in parafilm to prevent evaporation and placed in a humid chamber for 1 hr. at RT. Fluid was removed and washed with PBST 3X. After exposure of the sample, a detection antibody (either anti-KIM-1 or anti-NGAL) conjugated to biotin (in 1% BSA+PBS) was exposed to the surface for 1 hr. at RT. Following 3X PBST washes, Jackson ImmunoResearch Cy5-Streptavidin (JISA) (in 1% BSA+PBS), was applied and incubated for 1 hr. at RT in a humid chamber, covered with aluminum foil. Following exposure to the tracer antibody, 3 washes with PBST were conducted and the templates were disassembled. Slides were washed with ddW and dried with air. A GenePix 4000B slide scanner was used to quantify the Cy5 fluorescence.

Each biomarker was characterized individually and assays were optimized first in a buffer matrix, using purified target biomarkers, and then in spiked plasma or urine to fully characterize the LOD of the assay under different conditions. LOD is defined as the concentration at which the signal is greater than the background signal plus three standard deviations. In these studies, the LOD was specified as the lowest concentration measured for which the intensity meets the requirements defined above rather than that extrapolated from a curve fit plot. Once each biomarker was characterized and optimized individually, the assays were analyzed in a multiplexed format.

In order to address the many issues associated with protein arrays, duplicate spots and controls were included in our experimental design, such as those outlined below:

(a) Incorporate a minimum of three repeat capture regions for each biomarker on the array surface, which can be used to account for inter- and intra-slide variation.
(b) Spike a non-related positive control, chicken IgG, into the sample (at a fixed concentration) prior to analysis, with the appropriate capture antibody immobilized onto the array [25].
(c) Expose the surface to PBS without containing any biomarker for use as a negative control.

Commercial Urine & Plasma from Rats

Non-filtered urine and plasma (with sodium heparin) was obtained from mixed gender Sprague Dawley rats (Bioreclammation, NY). These samples were used to conduct ELISAs using 96-well plates and planar surface fluorescent immunoassays using the same procedures as above, except instead of using buffer as the matrix, urine or plasma was used as the matrix. An "in house" biomarker-positive matrix was generated (containing spiked NGAL or KIM-1) and biomarker-negative matrix (i.e. not spiked with target and therefore contains just a baseline/inherent level of the target of interest) and exposed to the platform. The matrix (e.g. urine) was prepared at the LOD as well as at concentrations within the clinically-relevant range for each analyte to establish the sensitivity of the assay. Normal background levels of KIM-1 and NGAL are around 500 – 1000 pg/mL and 150 ng/mL, respectively [182, 187]. In order to encompass the relevant ranges, 50% serial dilutions were conducted from 500 ng/mL for NGAL and 50% serial dilutions were conducted from 8 ng/mL for KIM-1.

Sprague-Dawley Urine Samples

Urine from Sprague-Dawley rats was obtained as a gift from FDA collaborators for use in planar surface fluorescent immunoassays. These animals had been exposed to gentamicin at 50, 100, 200, and 300 mg/kg and urine was collected after 24 hours. Our collaborators also shared data for NGAL and KIM-1 in these samples as obtained by using Meso Scale technology, which employs a chemiluminescent method for detection.

Results

96-Well Plate ELISA Studies using Standards

One benchmark for success when evaluating the performance of the new platform in its ability to detect clinically-relevant biomarkers is to compare the performance with the gold standard for protein detection, ELISA. Therefore, the biomarkers KIM-1 and NGAL were characterized using standard instrumentation and methods. A colorimetric kit purchased from R&D Systems was used to perform ELISAs to detect KIM-1 and NGAL. The assay was conducted on 96-well microtiter plates using horseradish peroxidase (HRP) as the colorimetric tag and performed better than the kit anticipated, with a LOD of 19.5 pg/ml for KIM-1 and 78 pg/ml for NGAL (Figure 22).

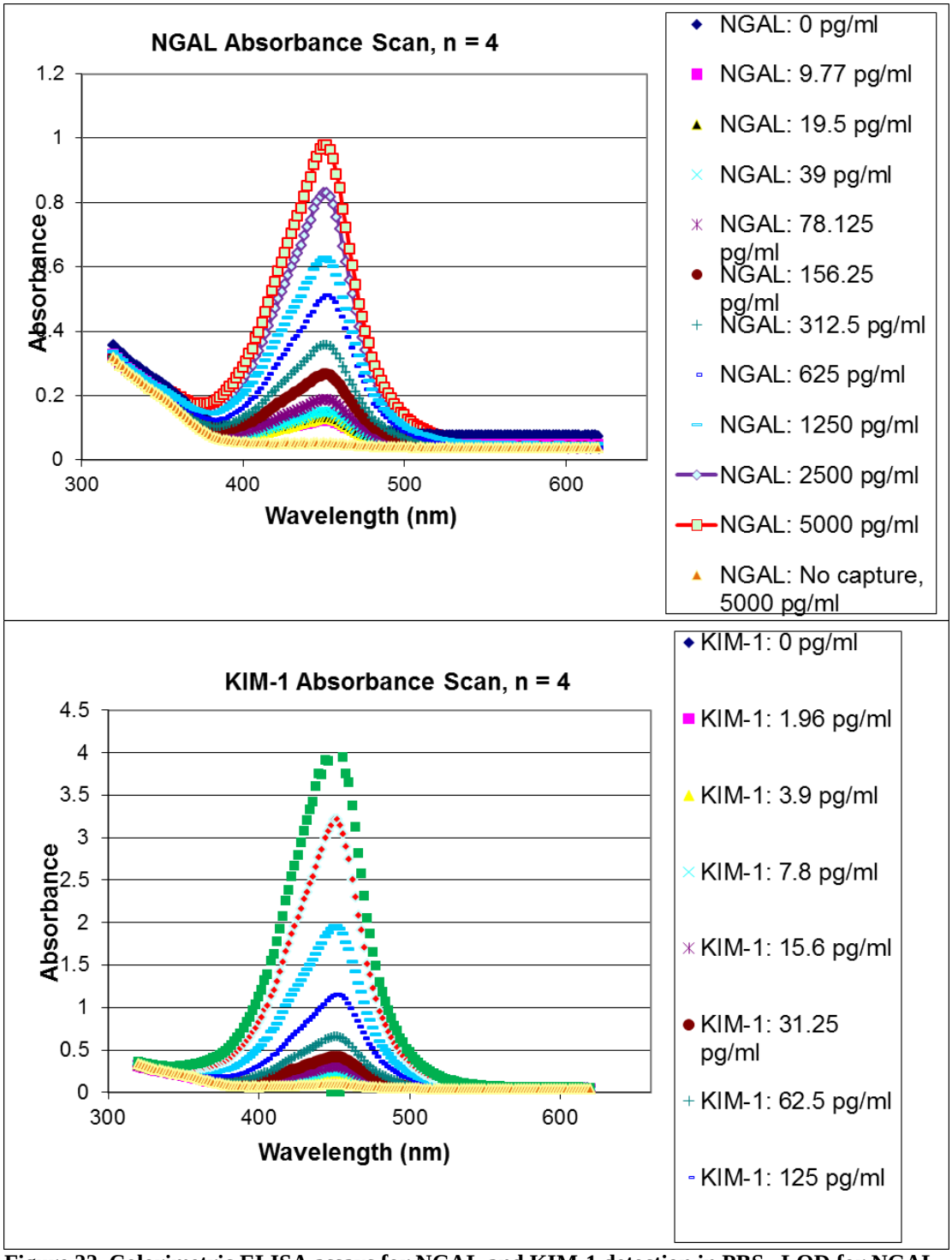

Figure 22. Colorimetric ELISA assays for NGAL and KIM-1 detection in PBS. LOD for NGAL is 78 pg/mL and LOD for KIM-1 is 195.5 pg/mL.

Planar Surface Fluorescent Immunoassays using Standards

Different surface chemistries were tested as described in previous chapters. Despite attempts of using different immobilization chemistries such as CH_3-Silane, the measurements were still best using the thiol-silane and GMBS chemistry, mainly because of issues with reproducibility using the CH_3-Silane. All results present here represent those obtained using thiol-silane with the GMBS crosslinker.

Experiments were conducted using AKI biomarkers by spiking the standards into PBS. A dose response was conducted for KIM-1 with a LOD of 401 pg/mL (Figure 23). This LOD is one order of magnitude lower than the LOD for KIM-1 using the 96-well plate colorimetric ELISA detection method (fluorescent immunoassay method was unavailable). This difference in the LODs between the planar surface fluorescent immunoassay and the colorimetric ELISA 96-well plate assay is lower than expected based on previous studies comparing the two detection methods. Our studies demonstrated a 2-3 order of magnitude difference between fluorescence and colorimetric detection, with both methods using 96 well microtiter plates. By comparison, the planar surface method performed better than anticipated. Detection of KIM-1 has a dynamic range from 401 pg/mL to 260 ng/mL, as evidenced by both the graph and image in Figure 24. The LOD for NGAL is 6.3 ng/mL, which is two orders of magnitude higher than detecting NGAL with the colorimetric assay (Figure 23). The maximum concentration detected was 260 ng/mL (Figure 24). Compared to clinically-reported levels of KIM-1 and NGAL (discussed in the Background section

of this chapter), the LODs for these AKI biomarkers are below the level that is known to indicate disease (KIM-1:500-1000 pg/mL, NGAL:150 ng/mL) [182, 187].

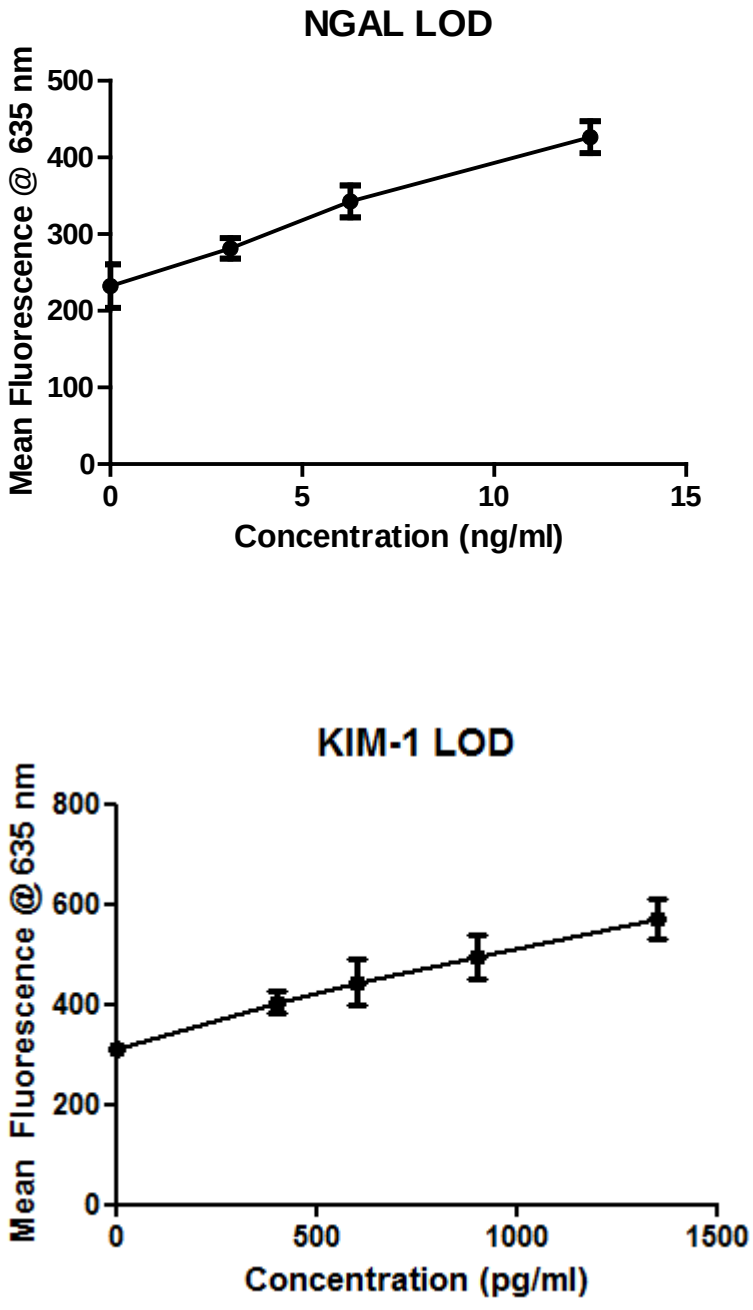

Figure 23. LOD for KIM-1 (401 pg/mL) and NGAL (6.3 ng/mL) in buffer using planar surface fluorescent immunoassay

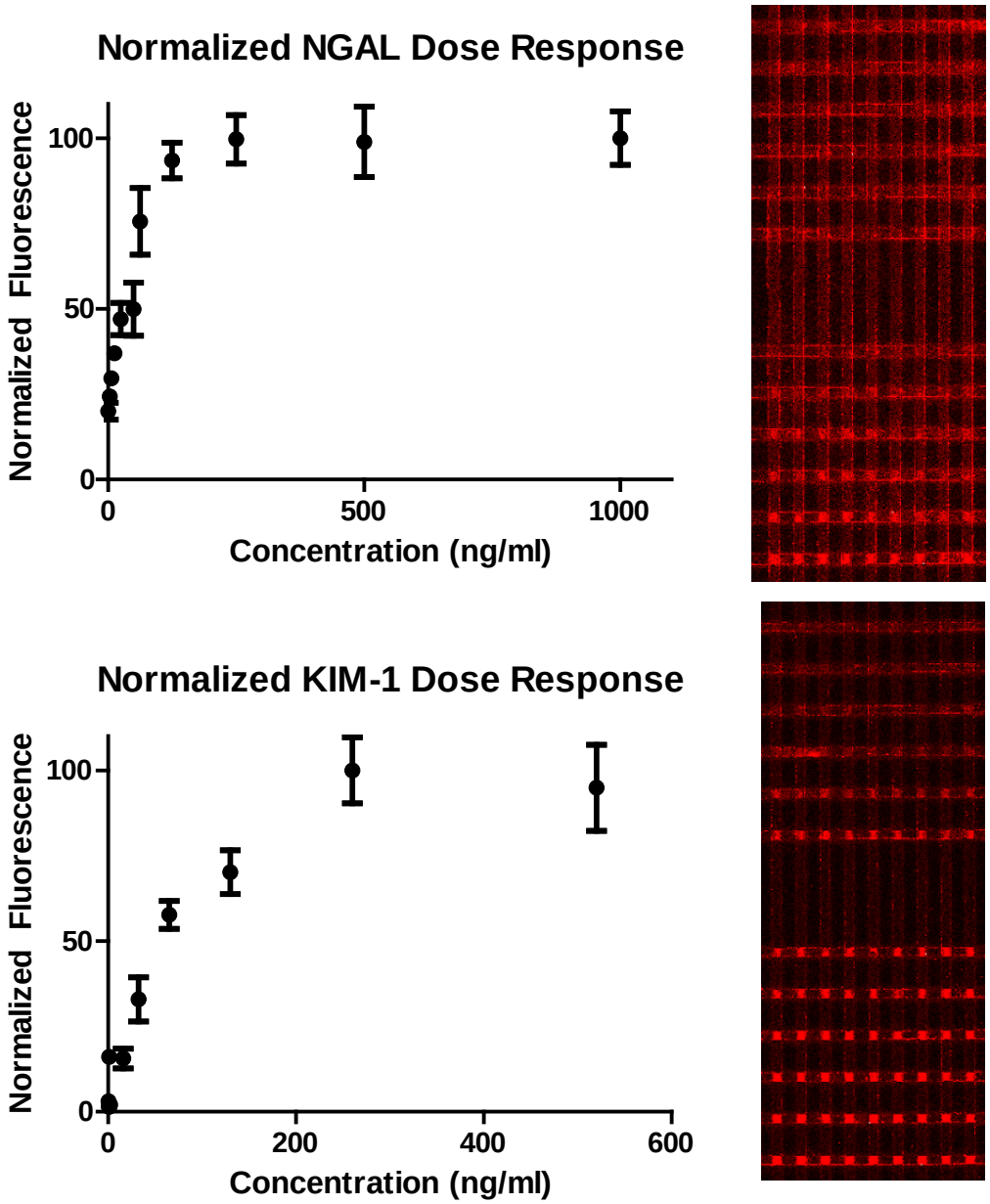

Figure 24. Normalized dose response for KIM-1 and NGAL using planar surface fluorescent immunoassay. KIM-1: LOD 401 pg/mL, NGAL: LOD 6.3 ng/mL

Following individual characterization of each biomarker, multiplexing by detecting both KIM-1 and NGAL on the same slide was conducted (Figure 25). The mean fluorescence intensity at the highest concentration for KIM-1 is about six times higher than the mean fluorescence intensity at the highest concentration for NGAL.

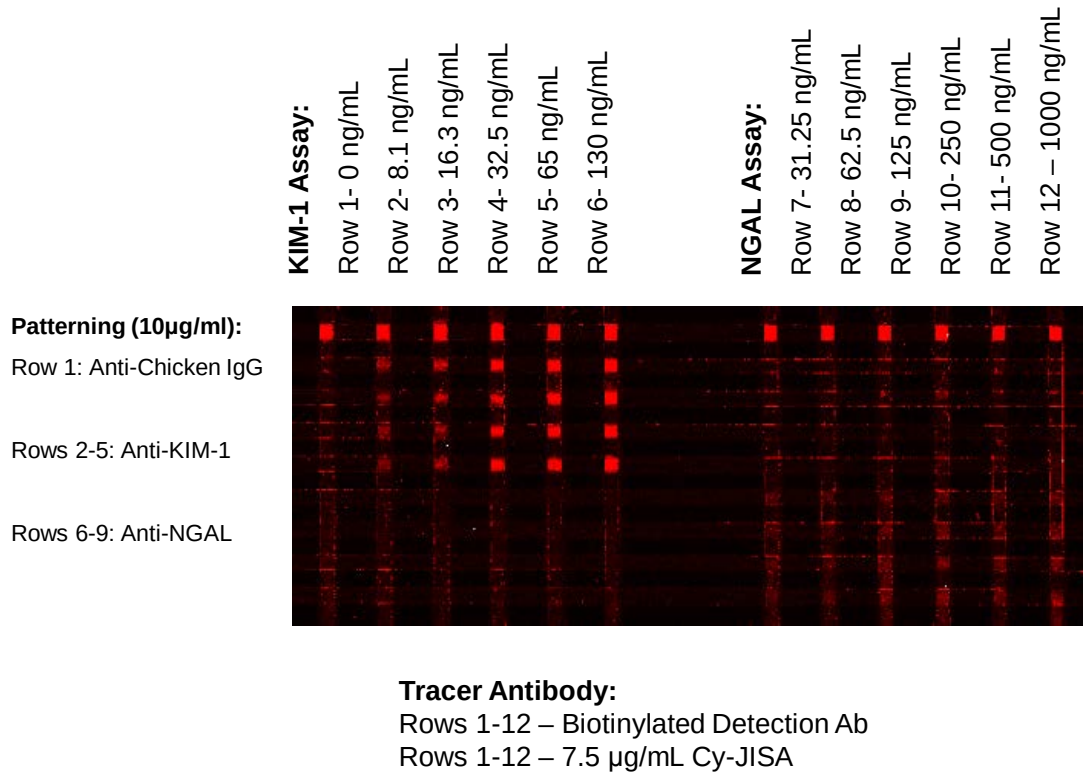

Figure 25. Image of planar surface fluorescent immunoassay: multiplexed detection of KIM-1 and NGAL using JacksonImmuno Streptavidin-Cy5 as detection label

This finding may be due to the different kinds of antibodies employed for each biomarker's detection. The capture antibody for NGAL and the detection antibody for NGAL are both polyclonal. However, the capture antibody for KIM-1 is monoclonal and the detection antibody for KIM-1 is polyclonal. Due to the higher specificity of monoclonal antibodies compared to polyclonal antibodies, assays using monoclonal antibodies are oftentimes less sensitive. The specificity of antibodies for their target may be one of the contributing factors for why NGAL detection differs from KIM-1 detection.

Another reason why the system does not perform equally when detecting KIM-1 and NGAL is because the size of the antigens and their antibodies are different and each protein is composed of a different combination of amino acids. The capture antibody of NGAL may alter its conformation due to binding the glass slide, which could adversely affect its interaction with the analyte.

Unspiked Commercial Urine & Plasma from Rats

96-well plate ELISA

Comparisons of the multiplexed platform with standard technology (ELISA) allows for a comprehensive evaluation of the performance of the platform with respect to clinically-relevant analytes. Experiments were conducted using unspiked, pure control urine or plasma to determine the baseline level of KIM-1 and NGAL. Since the background signal of the biomarkers were high, diluting the matrix was necessary. The buffer dose-response curves were used to determine the background level of KIM-1 and NGAL in the control samples.

Pure plasma and urine (wells 12 and 11) and 3X dilutions of each biological matrix (wells 10 to 2) using PBS as the diluent were prepared to determine the baseline level of KIM-1 and NGAL present in control samples (Figure 26). Well 12 was patterned with the opposite capture antibody and exposed to 100% of the biological matrix to assess cross-reactivity. Well 1 was exposed to PBS rather than diluted plasma or urine. Standard curves for KIM-1 and NGAL spiked in PBS are also shown in the figure for comparison. The mean absorbance of NGAL or KIM-1 in plasma was

compared to the respective standard curve in PBS for determination of the baseline levels. Results are reported in Table 10. Diluting plasma 243 times (well 6 in Figure 26A) was suitable for determining the concentration of NGAL from the standard curve (well 10 in Figure 26A), whereas diluting plasma 9 times (well 9 in Figure 26A) was adequate for determining the concentration of KIM-1 using the standard curve (well 9 in Figure 26A). Diluting urine 243 times (well 6 in Figure 26B) was suitable for determining the concentration of NGAL from the standard curve (well 8 in Figure 26B), whereas diluting urine 3 times (well 10 in Figure 26B) was adequate for determining the concentration of KIM-1 using the standard curve (well 7 in Figure 26B). Results showed that the baseline level of KIM-1 in either matrix was comparable (558 pg/ml in urine and 750 pg/ml in plasma) (Figure 26). NGAL detection in plasma and urine showed similar baseline levels, with NGAL in plasma (pNGAL) slightly higher (607 ng/ml) than urinary NGAL (uNGAL; 456 ng/ml). These results suggest that the amount of NGAL and KIM-1 have different baseline levels in plasma and urine; this may be due to the natural disparity of this protein in plasma and urine. Since NGAL is expressed in both the distal and proximal tubule, but KIM-1 is expressed only in the proximal tubule of the kidneys, it is reasonable to expect the baseline level of NGAL to be higher than that of KIM-1 [180]. Additionally, it is reasonable to expect pNGAL to be higher than uNGAL because pNGAL is implicated in innate immunity.

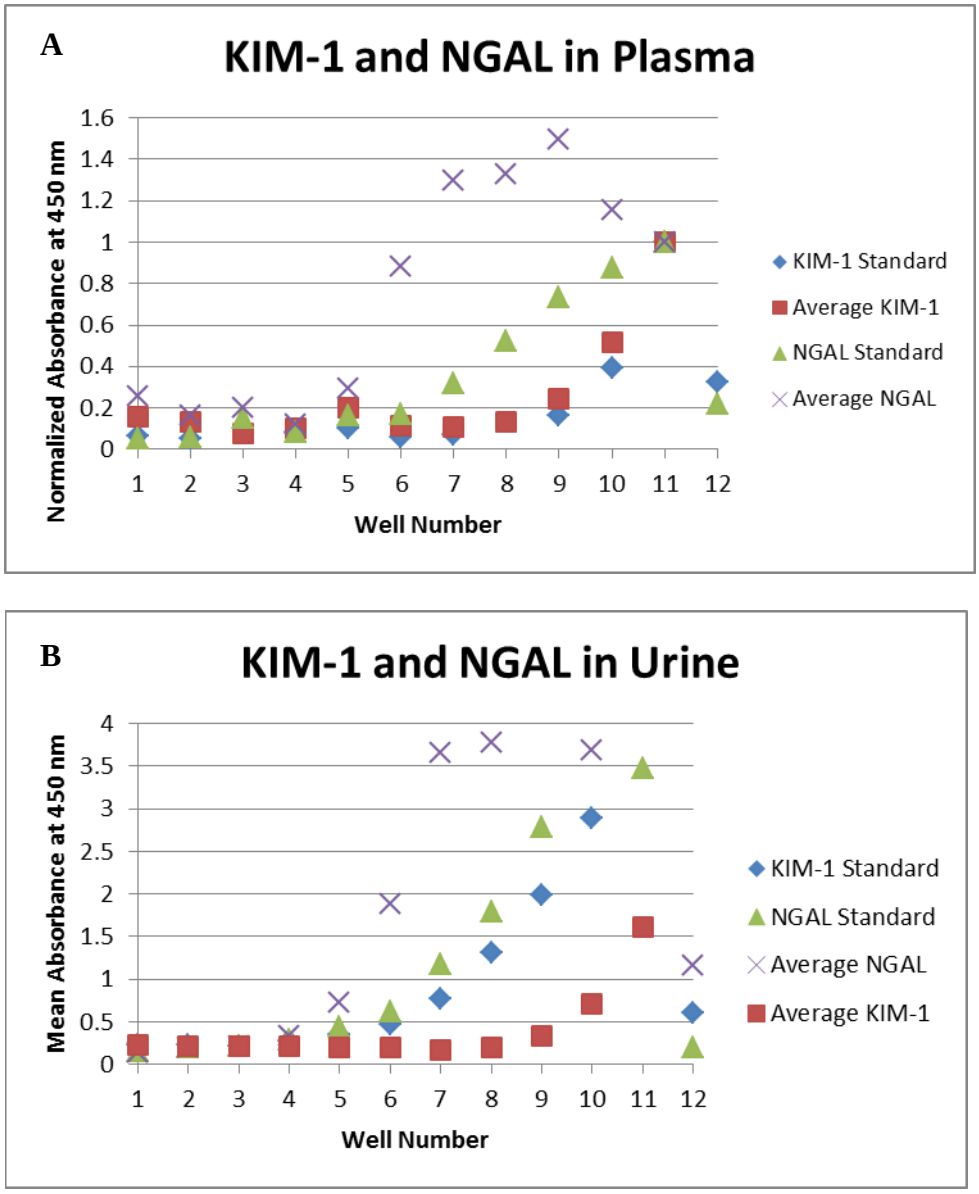

Figure 26. Colorimetric ELISA microtiter plate detection of KIM-1 and NGAL at various dilutions of (A) plasma or (B) urine. Standard curves for KIM-1 and NGAL spiked into PBS are shown as the blue diamond and green triangle, respectively. Well 12 was exposed to the opposite capture antibody (e.g. anti-NGAL for the KIM-1 standard curve). 100% of the matrix and 3X dilutions of the matrix in PBS are shown in wells 11→2. Well 1 was exposed to PBS. N = 3; average %SD is 24.5.

The baseline levels of KIM-1 and NGAL in urine and plasma did not agree with the baseline levels obtained by the Meso Scale platform (Table 10). However, these specimens did not come from the same source. The urine and plasma used for the colorimetric studies were obtained from rat samples provided by a company, Bioreclammation. The studies conducted on the Meso Scale instrument were obtained by in-house IACUC animal procedures. These results highlight the variability of KIM-1 and NGAL that may be present in healthy control rats.

Table 10. LOD comparison of AKI Biomarkers among platforms. LODs are reported for the planar surface fluorescent immunoassay and colorimetric assays in buffer. All other values are average concentrations of control rat samples. The known human reference intervals are shown.

Biomarker	Planar Fluorescent Surface Immunoassay	Colorimetric Microtiter Plate	Meso Scale (Obese Wistar Rat)	Meso Scale (Lean Wistar Rat)	Meso Scale (Sprague Dawley Rat)	Human Reference Interval
PBS KIM-1	LOD 401 pg/ml	LOD 3.9 pg/ml	N/A	N/A	N/A	N/A
PBS NGAL	LOD 6.3 ng/ml	LOD 19.5 pg/ml	N/A	N/A	N/A	N/A
Urinary KIM-1	0.5 ng/ml	558 pg/ml	1.78 ng/ml	0.17 ng/ml	1.01 ng/ml	500-1000 pg/ml [182]
Urinary NGAL	125 ng/ml	456 ng/ml	331 µg/ml	41 µg/ml	211.77 ng/ml	>150 ng/ml diseased [186, 187]
Plasma KIM-1	1 ng/ml	750 pg/ml	N/A	N/A	N/A	N/A
Plasma NGAL	63 ng/ml	607 ng/ml	N/A	N/A	N/A	N/A

Planar Surface Fluorescent Immunoassay

Studies were conducted to ascertain whether the planar surface fluorescent immunoassay platform is capable of simultaneously detecting and quantifying KIM-1 and NGAL in urine and plasma.

Planar surface fluorescent immunoassays were conducted using 100% control urine and 100% control plasma as the matrix. Figure 27 shows an image of a slide that was probed for KIM-1 and NGAL. This slide shows a minimal fluorescent signal in the KIM-1 region, indicating that the background level of KIM-1 in either urine or plasma is below the level detectable by this platform. Due to the lower sensitivity of the slides as compared to ELISA, the background level of KIM-1 was not an issue for detecting elevated levels of this biomarker. NGAL, on the other hand had a relatively high background level, demonstrating that level of NGAL is either naturally high in these matrices. There may also be interfering molecules in plasma and urine that non-specifically bind to the polyclonal NGAL antibody, as evidenced by Figure 28. The background levels on KIM-1 and NGAL in urine and plasma are shown in Table 10. The level of KIM-1 in plasma and urine agrees with the baseline levels in these matrices as obtained by ELISA. uNGAL and pNGAL, however, do not agree with baseline levels obtained via colorimetric 96-well plate detection and some reasons for this discrepancy are discussed in the Discussion section.

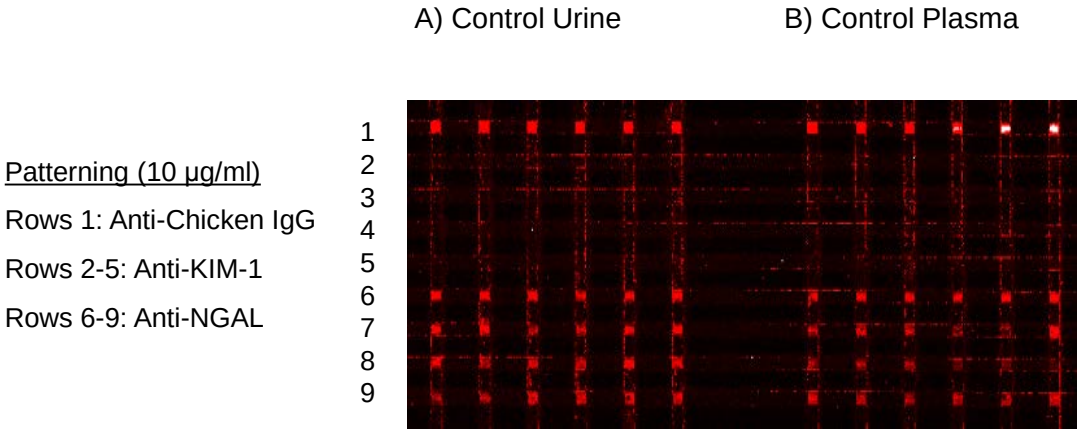

Figure 27. Images of KIM-1 and NGAL detection in unspiked commercial control (A) urine or (B) plasma using planar surface fluorescent immunoassays. Capture antibodies were patterned onto the surface and exposed to the 100% of the matrix (urine or plasma), followed by the biotinylated detection antibodies and Cy5-Streptavidin. Chicken IgG was used as a positive control

Spiked Commercial Urine & Plasma from Rats

Dilutions of urine and plasma were prepared at 100%, 50%, 25%, 10%, and 1% using PBS as the diluent. These solutions were then spiked with NGAL or KIM-1 in a region that is clinically relevant as described in the Methods Section to carry out experiments using planar surface fluorescent immunoassays. As shown in Figure 28, urine diluted to 50% and plasma diluted to 10% is best for detecting KIM-1 in the clinical range with both achieving a LOD of 2 ng/mL. In contrast, urine at 1% and plasma at 1% is best for detecting NGAL in the clinical range with LODs of 31 ng/mL and 63 ng/mL. The dilution for the biological matrix was deemed optimal when it approximated the biomarker standard in PBS. The fact that urine and plasma need to be diluted in buffer prior to conducting an assay is expected as other researchers have also needed to dilute these biological matrices 10X to obtain results for KIM-1 and NGAL using rat samples. LODs for KIM-1 and NGAL when spiked into diluted plasma and urine are shown in Table 11.

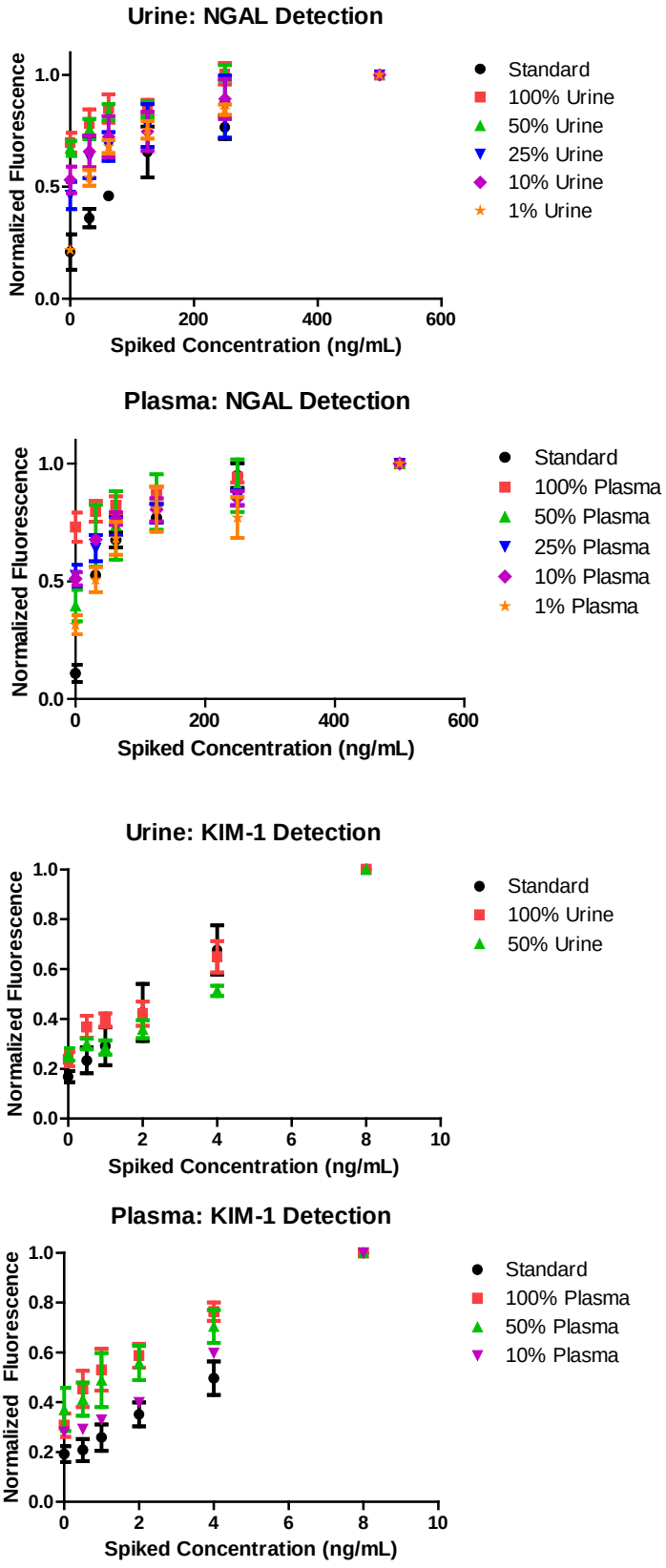

Figure 28. Detection of NGAL or KIM-1 spiked into control plasma or control urine using planar surface fluorescent immunoassay

Table 11. LOD of NGAL and KIM-1 when spiked into diluted urine or plasma and detected with planar surface fluorescent immunoassays

Biomarker	Biological Matrix	Dilution of Matrix	LOD
NGAL	Urine	1%	31 ng/ml
NGAL	Plasma	1%	63 ng/ml
KIM-1	Urine	50%	2 ng/ml
KIM-1	Plasma	10%	2 ng/ml

Rat Urine and Plasma Samples

Planar surface fluorescent assays were conducted using urine from rats exposed to a known nephrotoxicant, Gentamicin, at 0, 50, 100, 200, or 300 mg/kg. Results shown in Figure 29 are for 100% urine (i.e. no dilutions in PBS were conducted). This slide image illustrates that NGAL can be detected in rat urine even at high doses of exposure to the antibiotic. Although the level of NGAL in urine after exposure to 300 mg/kg is expected to be markedly higher than the control level, the detection system (GenePix 4000B) can still discern the signal, which has not reached its maximum. Consequently, planar surface fluorescent immunoassays can be used to detect renal injury biomarkers above baseline levels, including after exposure to nephrotoxicants.

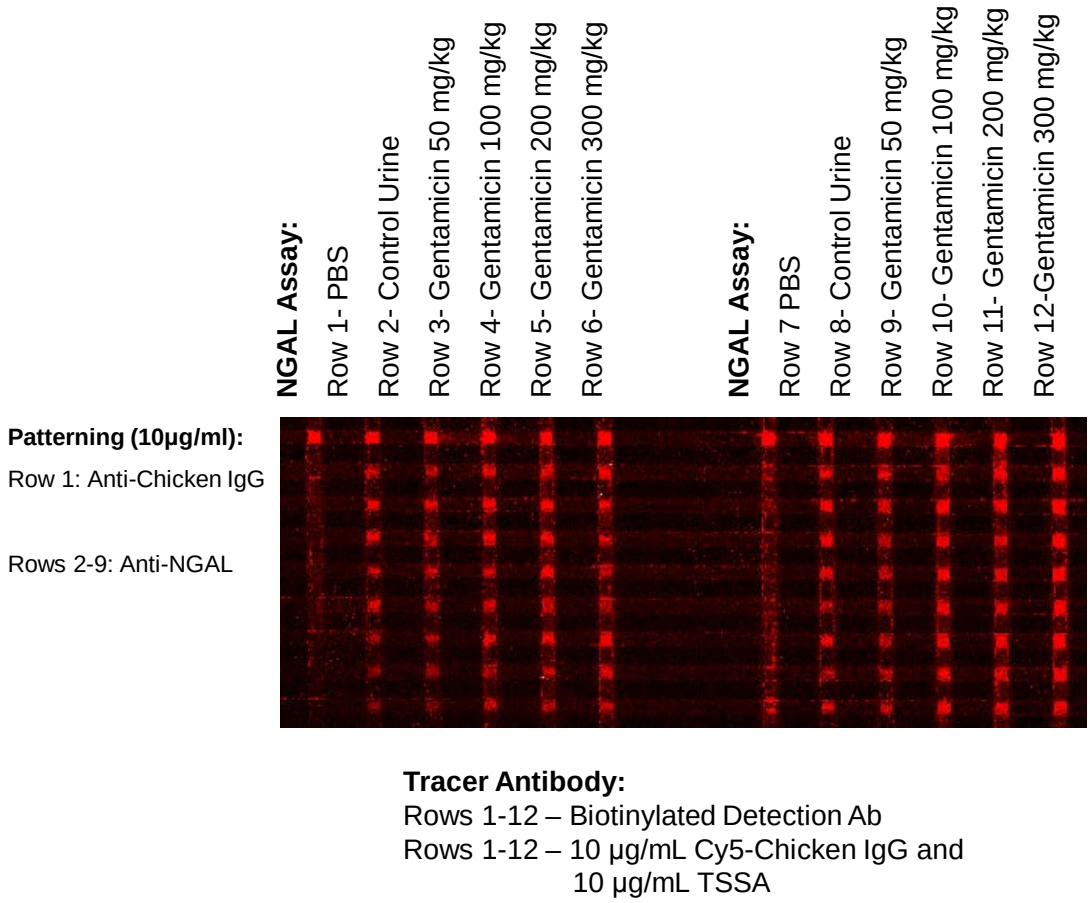

Figure 29. NGAL detection in urine from rats exposed to 0, 50, 100, 200, or 300 mg/kg of Gentamicin, a known nephrotoxicant

Discussion

The objective of this chapter was to demonstrate the applicability of planar surface fluorescent immunoassays to a real-world public health need for renal injury biomarker detection. We showed that the developed platform can detect both KIM-1 and NGAL in a multiplexed format in buffer as well as in urine and plasma, but detection in biological matrices requires dilution in order to obtain reliable results. We compared our results to standard 96-well plate colorimetric assays and noted

discrepancies between the two methods, which will be discussed in more detail below. Since there are no widely-accepted, clinically-relevant levels of KIM-1 and NGAL that indicate pathology, we cannot state with certainty that our platform would be useful for healthcare needs. Once the medical community develops consensus regarding the levels of these biomarkers that indicate disease, more tests can be conducted on the platform to determine its relevance for AKI intervention.

Microtiter Plate Fluorescent Immunoassays

As shown in the Results section, planar surface fluorescent immunoassays were compared to colorimetric assays using 96-well plates rather than direct comparison to microtiter plate fluorescent immunoassays. Baseline levels of KIM-1 in urine and plasma as determined by ELISA were comparable to the levels obtained using the planar surface fluorescent immunoassay. However, this was not the case for detection of NGAL in urine and plasma. This difference may be due to a variety of reasons including the fact that ELISA is more sensitive and less susceptible to matrix effects than the planar surface fluorescent immunoassay. Baseline level differences are expected when using two different platforms for NGAL detection because unlike KIM-1, NGAL has presented discrepancies in the absolute values of this biomarker when comparing Meso Scale technology to Luminex xMAP technology. In this study, by Pavkovic, et al. reported there were systematic error and biases when calculating baseline levels of NGAL. This same inconsistency was reported by others who analyzed NGAL using the same platforms, but with samples from different AKI root causes. These differences shed light on the issue that baseline levels of

biomarkers may be platform-specific and that reference intervals may need to be determined for each detection system rather use of a global reference interval.

In addition to ELISA, microtiter plate fluorescent immunoassays were conducted for KIM-1 and NGAL and these experiments data did not yield meaningful results. A fluorescent detection method was applied to detection of KIM-1 and NGAL in urine and plasma using 96-well plates and all experimental steps were the same as with the colorimetric assays, with the exception of Streptavidin-HRP, which was replaced with Streptavidin-Cy5. Some reasons why results the fluorescent studies were uninformative are: the assay is not sensitive enough for fluorescent detection, the assay performs better when amplification is possible, as with the colorimetric detection method, and the antibodies and proteins were optimized for colorimetric detection rather than fluorescent detection. Certain antibodies raised for a particular assay (e.g. ELISA) may not recognize the same antigen because the conformation of the antibody may be altered when used in a different assay [17]. Previous studies in our laboratory have demonstrated that fluorescent detection LODs are about 2 - 3 orders of magnitude higher than colorimetric assays. In addition to fluorescent detection not being as sensitive as colorimetric detection, renal biomarkers, especially NGAL, may be harder to detect because the capture antibody and detection antibody are polyclonal, rather than monoclonal. A monoclonal antibody, such as that used for KIM-1, has higher specificity and may have a resulting higher sensitivity.

Amplification of the signal, which is made possible by the enzymatic conversion of substrate into product in ELISA detection methods, is not available for direct Cy5 or biotin-antibody/Streptavidin-Cy5 fluorescent formats. One method for signal amplification is to use a polymer with amines, which can be biotinylated or conjugated to a dye. A polymer, poly(allylamine hydrochloride), was conjugated to biotin and Cy5 and used in a sandwich assay (the biotinylated detection antibody was exposed to streptavidin, followed by the Cy5-conjugated poly(allylamine hydrochloride)). Despite this attempt to amplify the fluorescent signal, this method did not yield meaningful results over the full dose response. An amplification strategy that has been shown to amplify the signal up to 1000-fold could be tested in future studies [17]. This technique applies enzymes and substrates in a coupled cycle where the product of the conventional enzyme-substrate reaction is not detected; rather, two recycling enzymes convert this product to a new form and back to the old form many times. The products from substrate 2 and 3 may be detected as fluorescent, colored, or luminescent. Another potential method for amplifying the fluorescent signal, which may be studied in the future, is to use a product called ELAST that is available by Perkin Elmer. This product uses biotinylated antibodies to amplify the signal. Still, another method that could be tested is enzyme-generated fluorophores, which may be used in conjunction with time-resolved fluorescence [17]. A variety of salicyl phosphates can be used as substrates for alkaline phosphatase (AP). AP produces fluorophores when chelated with lanthanides in the presence of ethylene triamine tetra-acetic acid (EDTA). This technique combines amplification of an enzyme with a very sensitive signal generation system. Even

though we could not compare our results for renal biomarker detection using planar surface fluorescent immunoassays to microtiter plate fluorescent immunoassays, based on previous characterization experiments shown in Chapters 3 and 4, we believe the two platforms would be expected to perform similarly.

Planar Surface Fluorescent Immunoassays

The developed planar surface fluorescent immunoassays demonstrated clinical utility for detecting both KIM-1 and NGAL in the known clinical range for urine and plasma. Although a background level of each of the biological matrices was detected, the assays performed on par with the standards in PBS when either urine or plasma was diluted. Detection of KIM-1 showed the greatest congruence with experiments conducted in buffer and diluting urine to 50% was adequate to detect this biomarker when spiked into solution. Detection of NGAL in urine showed the highest background and diluting the matrix to 1% was needed. This is because the baseline level of NGAL in control animals is quite high, around 125 ng/mL in urine and 63 ng/mL in plasma. However, despite the baseline levels of NGAL in each biological matrix, when diluting plasma or urine with PBS, the background signal is still above that of using PBS as the matrix.

These results suggest that some component of urine or plasma interferes with the assay. If there were no molecules interfering with the assay, we would expect that with each increasing dilution of the biological matrix, the dose response curves would become closer to the dose response curves in buffer and that the background levels

would decline in a predictable manner. However, since this is not the case and the background level of 1% of urine or plasma is still high, we can conclude that there are negative effects due to the matrix used. The source of this matrix effect could be due to molecules naturally-present in the matrix or chemicals or other substances that may have been used in the sample collection devices [17]. Some molecules that are known to cause background fluorescence in plasma are NADH and bilirubin, among other proteins [17]. The antibodies used in the assay may be low-affinity antibodies, which are more susceptible to sample interferences and matrix effects. To address the issue of background fluorescence, experiments could be conducted using time-resolved fluorescence where measurement of the emitted light occurs after a time gap following excitation of the fluorophore, however, this would require special labels such as terbium chelates. Antibody fragments could also be tested rather than the full antibodies, which could lower the non-specific binding.

As mentioned, the baseline level of NGAL in urine was determined to be 125 ng/mL, which is double the level of NGAL in plasma (63 ng/mL). These results are in agreement with the level of 150 ng/mL reported in the literature [187]. The level of KIM-1 was found to be 500 ng/mL and 1 ng/mL in urine and plasma, respectively. These levels agree with the reported range of 500 – 1000 pg/mL found in the literature [182]. Therefore, even though the clinically-relevant levels of these biomarkers have not been completely established by the medical community, based upon current knowledge, this platform is suitable for use in a clinical setting for

measuring KIM-1 and NGAL in either plasma or urine because our platform can measure these analytes above the baseline levels.

The LOD for detecting spiked NGAL in urine at a 1% dilution was 31 ng/mL. The LOD for detecting spiked NGAL in plasma at a 1% dilution was 63 ng/mL. The LOD for detecting spiked KIM-1 in urine at a 50% dilution was 2 ng/mL. The LOD for detecting spiked KIM-1 in plasma at a 10% dilution was 2 ng/mL. These results (Table 11) demonstrate that when the biological matrix is diluted, a LOD below the baseline level for NGAL (Table 10) can be achieved, meaning that the platform can detect increases in this biomarker and potentially the diseased state of a patient. The baseline levels of KIM-1 in plasma and urine (Table 10) are below the LOD, but detection at 2 ng/mL may be the lowest level needed to change clinical management of AKI. A rise in 1-1.5 ng/mL above baseline may not indicate a large enough rise in the biomarker to indicate disease, so this LOD may be adequate. More clinical data is needed to determine the pathological range for KIM-1.

One limitation to the experiments conducted with the planar surface fluorescent immunoassays is that the biological matrices were diluted prior to spiking the standard into the samples. This procedure was conducted as a way to save reagents and supplies. However, spiking the standard into the 100% biological matrix followed by diluting the sample may be a more appropriate way to measure the biomarkers in samples. Further studies may be warranted to investigate this spiking protocol.

Comparisons to Results in the Literature

As described in the Background section of this chapter, the literature has widely varying data regarding the levels of these biomarkers obtained in rats and humans. Table 10 shows the comparison of the levels of KIM-1 and NGAL in rats, as detected on the tested platforms: planar surface fluorescent immunoassays, colorimetric ELISA 96 well plate studies, Meso Scale evaluations of both obese and lean Wistar rats and normal Sprague Dawley rats. As shown in the table, when experiments were conducted in PBS and spiked with either KIM-1 or NGAL, the LODs using colorimetric assays involving microtiter plates were lower than the LODs using planar surface fluorescent immunoassays. Despite the fact that the LODs are higher for the planar surface fluorescent immunoassays, they are still distinctly lower than the baseline levels of the biomarkers, as detected by the planar surface fluorescent immunoassays, the colorimetric experiments, and the MesoScale experiments involving three different species of rats.

Despite the public health concern of detecting and characterizing AKI biomarkers, relevant ranges for both humans and rats have not yet been established for NGAL and KIM-1 in plasma or urine, following various doses of nephrotoxic drugs, or other exposure to agents that may cause AKI. As more information is known regarding potential relevant ranges of these biomarkers, if any, the context of our results can be better explained with regard to clinical relevance. Our research investigated the possibility of a quatitative assay for AKI biomarker determination. However, future studies may indicate that semi-qualitative devices may be sufficient to determine the

presence of NGAL and KIM-1 as negative, low positive, medium positive, or high positive [17]. Alternatively, qualitative assays may be sufficient to detect an elevated concentration of an analyte. It is still too early to state the clinical significance of our work for diagnosing AKI, but we have demonstrated that detection of KIM-1 and NGAL is possible using the developed planar surface fluorescent immunoassay.

One study by Zhang, et al. demonstrated a multiplexed electrochemiluminescent immunoassay for detection of four renal biomarkers in urine [24]. These experiments demonstrated imprecision below 15%, required 25 µl of sample, and took 5 hours to run. Reported LODs were 2.29 pg/mL and 0.02 ng/mL for KIM-1 and NGAL, respectively. They discovered that NGAL is higher in females and that reliance upon a reference interval may not be appropriate due to the individual variation in expression and concentration, particularly for NGAL. For example, researchers have reported values of NGAL as low as 3.2 pg/mL and as high as 3.0 µg/mL. Furthermore, NGAL in normal adults has been reported with a median from 12 to 38 ng/mL with an upper limit of 107 to 396 ng/mL and an intra-individual variability of 84 to 142%. Efforts to normalize markers with respect to urinary creatinine are flawed due to varied excretion rates. The overall conclusion of this study was that clinical strategies for AKI detection vary based on the biomarkers used because of the biological variability and baseline levels among patients. Serial measurements of patient biomarker levels may be superior to comparison to a reference interval.

While one of the issues with personalized medicine is the intrinsic individual variation, which may require many repeat measurements of biomarkers over time, there is still great promise for future developments that could outweigh this potential drawback. Nevertheless, based on the known cut-off levels of KIM-1 and NGAL in plasma and urine and the LODs of the planar surface fluorescent immunoassay, we can conclude that the platform performs within the known clinically-relevant ranges.

Conclusion

The planar surface fluorescent immunoassay platform is a viable option for KIM-1 and NGAL biomarker detection, which are implicated in early identification of AKI. These studies show that the platform can be applied to detection of AKI biomarkers present in biological matrices such as urine and plasma and can be detected within the known clinically-relevant limits. Our demonstration of NGAL detection in rat urine after exposure to a nephrotoxicant indicates that our platform may be useful for evaluation of clinical samples.

While the planar surface fluorescent immunoassay LODs were not as low for either biomarker as compared to ELISA, the LODs were adequate to detect KIM-1 and NGAL in rat plasma and urine in a multiplexed fashion at clinically relevant levels. These biomarkers were abundantly present in control rats, making a very low LOD unimportant. Rats treated with gentamicin, a nephrotoxic drug, had even higher concentrations of KIM-1 and NGAL, which were detectable with the newly

developed platform using diluted samples. The planar surface fluorescent immunoassay was compared to Meso Scale chemiluminescent detection methods. Results showed that different types of rats under investigation (e.g. species and whether they were lean or obese) had varied levels of the biomarkers in both control and nephrotoxicant exposure experiments. This data demonstrates a large dynamic range is paramount for detecting AKI biomarkers. As more studies are conducted to fully characterize KIM-1 and NGAL, devices can be fine-tuned to detect the appropriate range in concentrations. Nevertheless, our results showed that detection of NGAL and KIM-1 is possible using planar surface fluorescent immunoassays, and pending further clinical studies, this device could be adjusted for detection within the newly-established relevant clinical ranges.

Novelty of Work

Our evaluation of planar surface fluorescent immunoassays bolstered the use of this platform for actual biosensing needs with respect to existing sensing strategies. These results represent the first instance of a planar surface fluorescent immunoassay using very low volumes of either urine or plasma for analysis of renal injury biomarkers. This platform was shown to detect levels of AKI biomarkers present in control rat plasma and urine as well as gentamicin-treated rat urine. Although dilution of the biological matrices may be needed for analysis, we can detect elevations in KIM-1 and NGAL above baseline levels. It was previously unknown what the LOD and dynamic range would be for detecting these biomarkers using fluorescent methods. Our results showed that microtiter plates may be suitable for AKI biomarker detection if colorimetric ELISA methods are employed. However, use of fluorescent immunoassays using microtiter plates was unsuccessful. This work showed that the planar surface fluorescent immunoassays may be a viable alternative for detection of AKI biomarkers where use of small volumes is advantageous and where standard microtiter plate fluorescent experiments fail. These results show the promise of using this type of detection system in instances where fluorescence is the ideal method of detection, and where large volumes are not obtainable. Although this platform was applied to detection of other AKI biomarkers present in plasma or urine, planar surface fluorescent immunoassays may also be used to detect proteins implicated in other diseases or other non-clinical applications.

Chapter 6: Spatial and Spectral Multiplexing using Quantum Dots

Abstract

The simultaneous detection of two analytes, chicken IgY (IgG) and Staphylococcal enterotoxin B (SEB), in a single well of a 96-well plate is demonstrated using luminescent semiconductor quantum dot nanocrystal (QD) tracers. One light source can serve as the excitation source for detecting two distinct signals from analytes when using these unique labels. The QD-labeled antibodies were prepared via sulfhydryl-reactive chemistry using a facile protocol that took <3 h. Dose response curves for each target were evaluated in a single immunoassay format and compared to Cy5, a fluorophore commonly used in fluorescent immunoassays, and found to be equivalent. Immunoassays were then performed in a duplex format, demonstrating multiplex detection in a single well with limits of detection equivalent to the single assay format: 9.8 ng/mL chicken IgG and 7.8 ng/mL SEB. Immunoassays were further developed to demonstrate a triplex format to detect chicken IgG, mouse IgG, and SEB with LODs of 10 ng/mL, 5 ng/mL, and 2 ng/mL, respectively. In addition to demonstrating the multiplexing capability within a single well of microtiter plates, this technique was applied to planar surface fluorescent immunoassays. Spectral multiplexing within a single spot was achieved with a novel detection platform involving an evanescent wave scanner, which makes this platform more amenable to a POC environment.

Background

Antibodies demonstrate the highest levels of specificity and affinity compared to other synthetically produced molecules such as aptamers and molecularly imprinted polymers [144]. It has been demonstrated that up to nine antibodies can be spotted within a single well of a 96-well microtiter plate, but five of the nine assays were statistically different when compared to individually run assays [10]. The main problem with conducting multiplexed assays is the overlap of emission wavelengths among common organic dye labels [18, 144]. In order to circumvent this problem and avoid creating complicated assays, QDs can be used because of their distinct emission wavelengths.

Common methods for conjugating QD nanocrystals (NCs) to antibodies include targeting the antibody amine groups using EDC/NHS chemistry or glutaraldehyde, or using the popular biotin/streptavidin interaction. These methods are not ideal because they often require multiple trials to create a viable conjugate and conjugation can often result in undesirable cross-linking and subsequent aggregation and mixed avidity of the final product [18, 144]. Furthermore, biotin-avidin chemistry requires labeling of both molecules, which makes this technique more time-intensive. To avoid these complications, targeting less prevalent molecules on antibodies such as sulfhydryl groups can lead to more uniform final products [144]. Our collaborators developed a new conjugation method that requires only one step to conjugate maleimide-activated QD NCs to the exposed cysteine residues of reduced antibodies.

This procedure results in very minimal aggregation, if any, and can be completed in less than 3 hours, which improves upon previous methods.

Fluorescent Immunoassays

Fluorescent immunoassays are a common method for detecting protein analytes and will therefore serve as the basis for comparison to the newly-developed platform discussed in previous chapters. Comparison between standard sensing methodologies and new sensing strategies was facilitated by using the same analytes, e.g. the same antibody sources and stock solutions. By keeping all samples consistent among platforms, differences in performance characteristics are more likely to be attributed to the alternate technique. The analytes used were chicken IgG and SEB because they have been shown to have no cross-reactivity and because they are highly selective.

Quantum Dots

QDs were employed as tracers because of their inherent and unique optical and electrical properties, which are due to their size [191]. A variety of different QDs can be excited at the same excitation wavelength because they have broad excitation bandwidths, yet they have narrow emission bandwidths, with the emission wavelengths very specific to the type and size of QD core material [92]. QDs are made up of nanometer-sized semiconductor materials. The dimensions of the QDs enable the materials' excitons that are confined spatially in three dimensions (quantum confinement) to "collapse the continuous density of states in a bulk solid

into discrete electronic states of the nanocrystal" [192]. The two CdSe/ZnS core/shell nanocrystals (aka QD NCs) used in this study had a maximum emission at 605 ± 3 nm (NC 605) and 650 ± 3 nm (NC 650) and distinct photoluminescent spectra (Figure 30) [144]. The ZnS surface of the QD electronically isolates the CdSe core, allowing QDs to be photostable and have a high quantum yield [193]. Poly(ethylene glycol) (PEG) was used to cover the exterior of the eBiosciences nanocrystals (NC) used in this study to facilitate solubility in water. PEG is soluble in organic and aqueous media and becomes covered in water molecules, thereby preventing non-specific protein adsorption [194]. The surface of the PEG coating was further functionalized with a reactive maleimide (using proprietary techniques) that allowed conjugation to the antibodies' exposed cysteine residues.

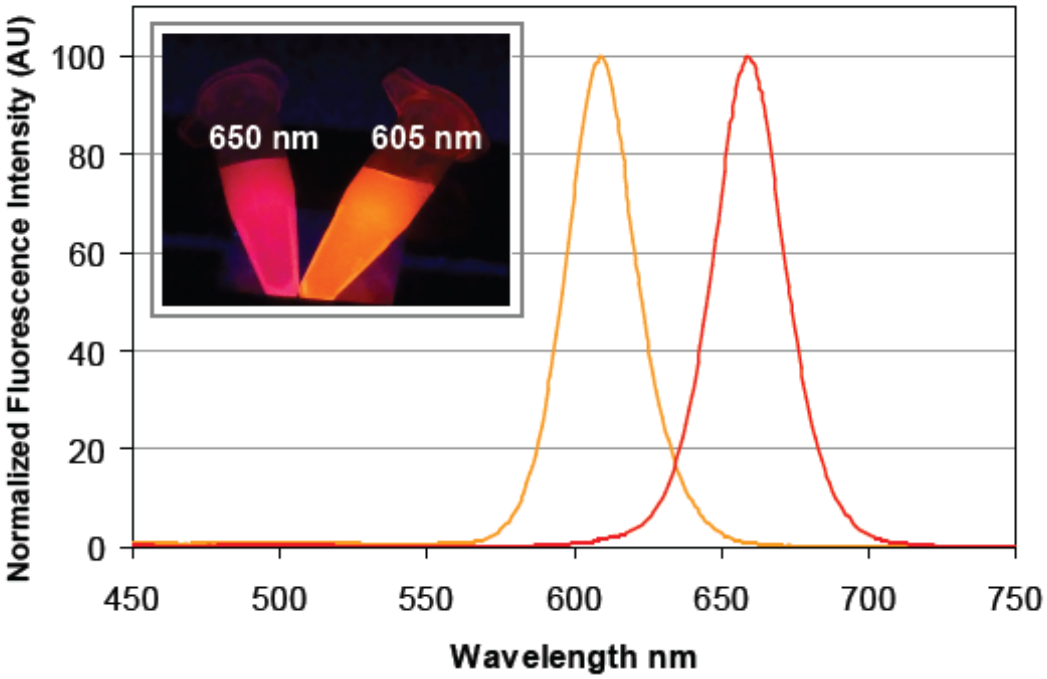

Figure 30. Photoluminescence spectra for nanocrystals (eFluor® NC 605 and NC 650, Ex @ 400 nm). Insert shows an image of the NCs in solution following UV 365 nm excitation [144]

Planar Surface Fluorescent Immunoassays

Planar surface fluorescent immunoassays were conducted similarly in previous chapters, except with the use of QDs as tracers. The Gene Pix 4000B slide scanner used in the work described in previous chapters is not suitable for investigation of other tracers such as QDs because the excitation wavelengths and emission filters cannot be tuned. As a result, an in-house developed detection system involving an evanescent waveguide was used to image the slides using QD tracers. This technique marks the first step in transitioning the planar surface fluorescent immunoassay from a traditional bench-top laboratory technique to a field-deployable device.

Methods

Materials

Staphylococcal enterotoxin B (SEB) and affinity purified rabbit anti-SEB were purchased from Toxin Technology Inc. (Sarasota, FL). Rabbit anti-Chicken IgG (IgY), Chicken IgG, Goat anti-mouse IgG and mouse IgG were purchased from Jackson ImmunoResearch Laboratories Inc (West Grove, PA). Phosphate buffered saline (PBS), Phosphate buffered saline with Tween (PBST), methanol, potassium hydroxide, toluene, ethanol, dimethyl sulfoxide, (3-mercaptopropyl)triethoxysilane, 4-meleimidobutyric acid N-hydroxysuccinimide ester, J. Melvin Freed Brand Microscope Slides, Plain, Corning Costar® flat bottom high binding white 96-well assay plates, Thermal Seal® sealing film for 96-well plates and bovine serum albumin (BSA) were obtained from Sigma-Aldrich (St. Louis, MO). Millipore Amicon® Ultra centrifugal filter devices 100 kDa were purchased from Millipore

Corporation (Billerica, MA). The quantum dot nanocrystals (NC) eF525-maleimde, eF605-maleimde and eF650-maleimde where a gift from our collaborators eBioscience (San Diego, CA), along with their proprietary Conjugation and Purification Buffers. Doubly distilled water (ddW) was used throughout the experiments and was prepared in house using a Nanopure Diamond™ water purification system (Barnstead, Dubuque, IA). The 800 nm QDs (Qdot® 800 ITK™ Streptavidin Conjugate Kit) were supplied by Invitrogen (Grand Island, NY). A 800 nm bandpass filter (85% transmission, 12.5 mm diameter) and a 605 nm bandpass filter (15 nm bandpass, 12.5 mm diameter) was obtained from Edmund Optics (Barrington, NJ). Impact-Resistant Polycarbonate was obtained from McMaster-Carr (Robbinsville, NJ). A 438 nm PN 156 1 watt laser was obtained from Hangzhou BrandNew Technology Co., Ltd (Zhejang, China). A Mead Deep Sky Imager PRO III CCD camera was obtained from Adirondack Video Astronomy (Hudson Falls, NY). Clear acrylic was obtained from Piedmont Plastics (Elkridge, MD). Fluid handling chips were designed in CorelDraw X4 (Corel Corp. Ontario, Canada) and micromachined using a computer controlled Epilog Legend CO2 65 W laser cutter (Epilog, Golden, CO). 3M 9770 adhesive transfer tape was used to hold together the layers of the planar surface fluorescent immunoassay. A REGLO Digital pump, appropriate connectors, and tubing were obtained from Ismatec (Wertheim, Germany). Appropriate connectors for the tubing were obtained from Cole Parmer (Vermon Hills, IL). CCD image intensities were analyzed using ImageJ software, developed and distributed freely by NIH (http://rsb.info.nih.gov/ij/download.html). Data was analyzed using Microsoft Excel (Microsoft, Redmond, WA).

QD Labeling Method

In this study, we used QD-labeled antibodies that were created using sulfhydryl-reactive chemistry in which disulfide bonds present on antibodies become reduced, allowing for conjugation to the QDs (Figure 31). The distinct photoluminescence spectra for the two different-colored QDs used in the study are shown in Figure 30.

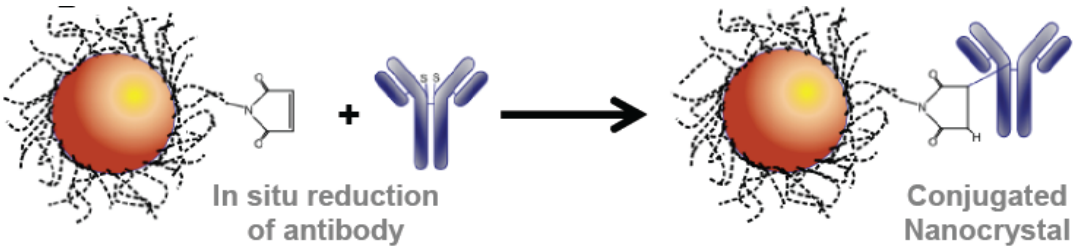

Figure 31. Sulfhydryl-reactive chemistry. The disulfide bond present on the antibody is reduced when exposed to the *in situ* reducing agent and conjugated to the nanocrystal [144]

Antibodies were labeled with the QDs using the sulfhydryl-reactive conjugation instructions provided by the manufacturer. Briefly lyophilized nanocrystals were reconstituted in 200 µL Conjugation Buffer by heating the mixture on high in a microwave for 5-10 s, repeated 3-4 times as necessary. A total of 200 µg of antibody was then added to the QDs and the reaction incubated for 2 hr. at RT on a shaker. For the microtiter plate immunoassay triplex studies eF525-maleimde, eF605-maleimde and eF650-maleimde NCs were conjugated to rabbit anti-chicken IgG, goat anti-mouse IgG and rabbit anti-SEB, respectively. For the planar surface fluorescent immunoassays, eF605-maleimde NCs were conjugated to rabbit anti-chicken IgG. The reaction was stopped after 2 h by adding 0.7 µL Quencher directly to the mixture,

vortexing and incubating for an additional 10 min on the shaker. The resulting antibody conjugated QDs were purified using a 100 KDa centrifugal filter unit. The reaction mixture was added to a centrifugal filter unit (pre-equilibrated with Purification Buffer) and the volume increased to a total of 1 ml using Purification Buffer, before being spun at 1,000g for 10 min (Beckman CS-6KR Centrifuge). Once the sample volume had reduced to ~0.1 ml an additional 1 ml of Purification Buffer was added and the spin repeated, this process was repeated a total of 4 times. The NC-antibody conjugate was then transferred to a 1.5 ml microcentrifuge tube and spun at 7 krpm for 5 min to remove any aggregates. The purified NC-antibody conjugate was characterized using UV-visible spectroscopy (Ultrospec™ 2100 Pro UV/Visible Spectrophotometer GE Healthcare, Piscataway, NJ) and stored at 4 °C prior to use for up to 12 months.

Labeling Antibodies with Cy5 Dye

Antibodies were labeled with a Cy5 dye via their primary amines [144]. The rabbit (Rb) anti-SEB and Rb anti-chicken IgG were prepared at 0.5 mg/mL (total of 600 µ L) in PBS. One vial of Cy5 was resuspended in 50 µ L DMSO. Then, 7.5 µL of the Cy5 was added to the antibody solution for incubation at room temperature (RT) for ~30 min. Any unincorporated dye was removed by using a Zebra™ desalt spin column. An Amersham Biosciences Ultrospec 2100 pro UV/visible Spectrophotometer (GE Healthcare, Piscataway, NJ, USA) was used to measure the absorbance of the purified Cy5-labeleled antibody at 280 and 650 nm. Final antibody

concentration and dye-to-antibody ratio were determined, following the manufacturer's instructions.

Microtiter Plate Fluorescent Immunoassays

The microtiter plate fluorescent immunoassays were conducted in a sandwich format (Figure 32). In this format, capture antibodies were immobilized onto the surface of the wells. For the single assay studies, only a single capture antibody species was immobilized onto the surface (using 50 µL per well). In these experiments, either 10 µg/mL of Rb-anti-chicken IgG, goat anti-mouse IgG, or rabbit anti-SEB were immobilized in one well. For the multiplex studies, a mixture of all capture antibodies were combined together to yield a total 50 µL for well incubation. Microtiter wells were functionalized with antibodies against chicken IgG at 7.5 µg/mL and SEB at 2.5 µg/mL for duplex immunoassays. For the triplex studies, 4 µg/mL rabbit anti-chicken IgG, 4 µg/mL goat anti-mouse IgG, and 2 µg/mL rabbit anti-SEB in PBS were used. These final concentrations were optimized based on some preliminary studies. To allow ample time for the capture antibodies to adsorb to the plate, the plate was sealed with Thermal Seal® sealing film and incubated for ~1 hr. at RT and then overnight at 4 ^{o}C.

The 96-well plates used in this study were Corning Costar flat bottom high-binding polystyrene plates that have an ionic/hydrophobic chemistry that enables them to bind to the capture antibodies. No preparation was required to prepare the surface of each

well to ensure binding to the capture antibodies. The antibodies randomly oriented themselves and attached to the surface.

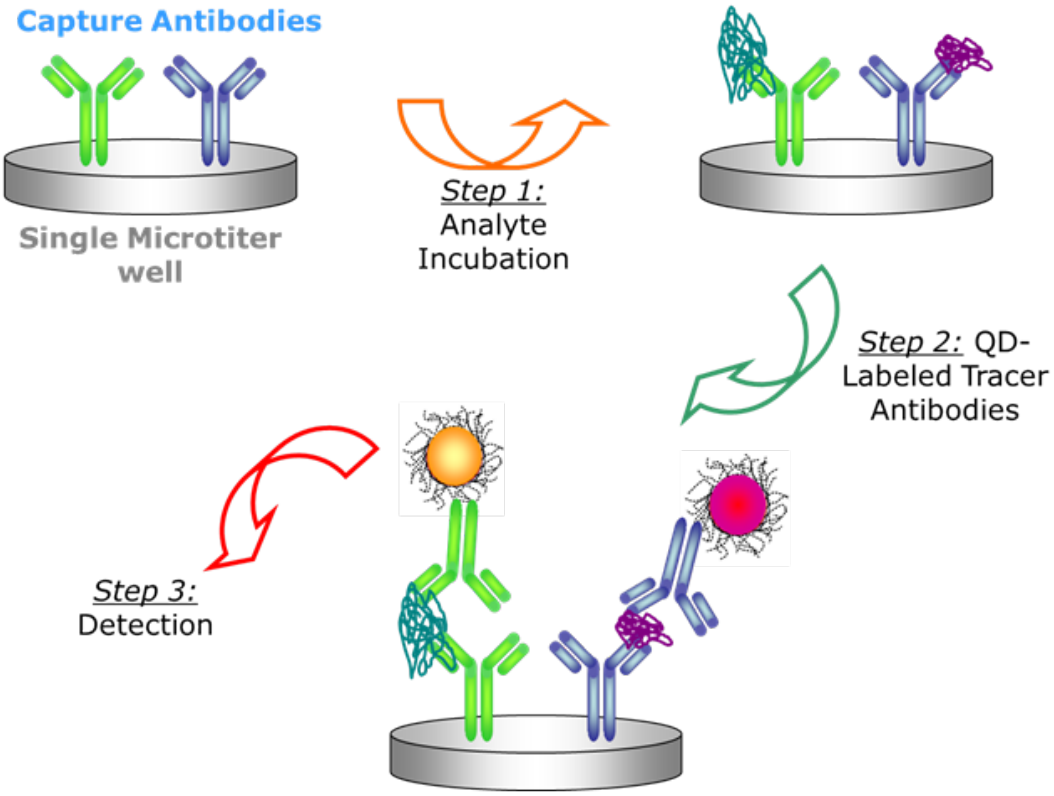

Figure 32. Sandwich assay format involving QDs [144]. Analytes are distinguished based on color even in the same well of a 96-well plate or within the same spot of a planar surface fluorescent immunoassay

The following day, the wells were emptied and washed four times with 200 µL/well ddH_2O. The surface was blocked with 200 µL per well of a blocking buffer (1% BSA and PBS) to prevent non-specific binding to the surface. The plate was placed on a rocker for ~1.5 hr. at RT during blocking (The Belly Dancer, Stovall LifeScience, Inc, Greensboro, NC, USA).

The next step of the immunoassay was to expose the wells to the sample containing the target antigen (50 µL/well) for 1.5 hr. on a rocker, followed by several washes to remove any non-specific binding (4 x 200 µL/well). The singleplex immunoassays were exposed to samples of either chicken IgG (0–2.5 µg/mL) or SEB (0-0.5 µg/mL) in 0.1% BSA + PBS. To complete the sandwich immunoassay, the optimized QD tracers were composed of NC605-Rb-anti-chicken IgG at 1:400 dilution or NC650-Rb-anti-SEB at 1:100 dilution. The organic dye tracers were either Cy5-Rb-anti-chicken IgG (10 µg/mL) or Cy5-Rb-anti-SEB (10 µg/mL). Each well was exposed to 50 µL of the tracer (in 0.1% BSA + PBS) for 1 hr. on the rocker. Lastly, the wells were washed with 2 x 200 µL/well PBS followed by 2 x 200 µL/well ddH_2O and dried with air.

For the duplex and triplex immunoassays, the samples involved were the same as those used in the singleplex, except they were mixed prior to well exposure. For duplex studies, for wells 1-12, analyte concentrations increased from 0-2.5 µg/ml for chicken IgG and decreased from 0.5 µg/ml – 0 for SEB. For triplex studies, for wells 1-12, target analyte concentrations increased from 0 – 2.5 µg/ml for chicken IgG and from 0-0.5 µg/ml for SEB and decreased from 2.5 – 0 µg/ml for mouse IgG. The

same procedure described above was used, except in this case, only the QD tracers were used. Following all methods described above, including washes to ensure that antibodies are only bound through specific biorecognition events, the fluorescence, which is an indication of the amount of target analyte present, was detected. Fluorescence intensity measurements were collected using a Tecan Infinite M1000 Dual Monochromator Multifunctional Plate Reader (Tecan, Research Triangle Park, NC) simultaneously using 400 nm as the excitation wavelength for both QDs. The plate reader detects fluorescence at the emission wavelengths specific to the labels used. Emission wavelengths were collected at 605 nm and 650 nm for the NC605 and NC650, respectively. In our studies, the mean fluorescence was determined using the TECAN plate reader, which is coupled to a computer for outputting quantitative data. Data was analyzed and interpreted using Microsoft Excel and/or Prism statistical software.

Negative controls were always present for each assay to determine whether the assay was performing appropriately. For example, a negative control involved exposing some wells of the 96-well plate solely to buffer instead of samples was used. In this case, the capture antibodies were not exposed to the analyte, but were exposed to the tracer combination.

Planar Surface Fluorescent Immunoassays

All of the steps for fabrication, assembly, and experimentation are the same as in Chapter 3. Beginning at 800 ng/ml, 50% serial dilutions of SEB and chicken IgG were used as the samples. However, instead of using Cy5 dyes, QD tracers were

employed. For chicken IgG detection, a dilution of 1:100 of eF605-maleimde NCs was used. For SEB detection, a detection antibody conjugated to biotin, followed by 15 nM 800 nm SA-QDs were used. The first tracer (eF605-maleimide NC) was exposed to the surface for 1 hr. at RT in a humid chamber, covered with aluminum foil. Following 3X PBST washes, the biotinylated SEB antibody was exposed to the surface for 1 hr. at RT in a humid chamber, covered with aluminum foil. Following 3X PBST washes, the 800 nm QDs were exposed to the surface for 1 hr. at RT in a humid chamber, covered with aluminum foil. Following exposure to the 800 nm QDs, 3 washes with PBST were conducted. The slides were imaged using the evanescent wave detection system.

Evanescent Wave Detection System

Because the GenePix4000B is not optimized for QD imaging, a new system was developed in-house to image slides using an evanescent wave scanner. This device involves the use of a blue light source combined with a CCD camera and filters to generate a small and potentially portable fluorescence detection platform [44, 195, 196]. The chameleon 1.3 MP Mono was purchased from Point Grey Research. A 605 nm bandpass filter and 800 nm bandpass filter, both with 15 nm bandpass and 12.5 mm diameter were purchased from Edmund Optics. A laser at 400 nm was used to excite quantum dots. These filters were chosen to improve the rejection of light scattered by the laser and thereby reduce the background noise. This platform was designed to read the photon emissions from this excitation while minimizing other photon sources (e.g. background fluorescence from the slide and external light).

Light from a laser was used as the excitation source for these studies. In order to ensure laser excitation of all points on the slide, the laser beam was passed through a line generator (Figure 33). The beam was then injected into the side of the slide (the planar surface serves as a waveguide) and propagates through the slide due to total internal reflection fluorescence (TIRF). ,. Normally, due to the interface of two different media with incongruent refractive indices, light from the higher refractive index medium is both refracted and reflected. However, in the case of this developed system, the angle of incidence of the laser hitting the glass slide is greater than the critical angle, causing all of the light to be reflected and none to be refracted due to total internal reflection. At the point of reflection, a standing wave known as an evanescent wave is generated that penetrates into the lower refractive index medium with an exponential decay. The evanescent wave interacts with the surface species immobilized at the interface and therefore excites the quantum dots that are bound to analytes on the planar surface and the subsequent fluorescence emission is measured using the CCD camera. Several angles of injection were tested for the evenness of the propagating laser beam along the longer portion of the slide. The optimum angle of injection was determined to be 45º from the bottom of the slide.

The injection of the laser beam produced an uneven background fluorescence that complicated reading the signal. The laser beam from the line generator had a Gaussian intensity profile (Figure 34A). The resulting beam still produced uneven lateral background fluorescence (Figure 34B). Since the laser beam scattered as it

propagated along the slide, another glass slide was added in front of the assay slide such that the laser propagated through both slides. The result (Figure 34C) shows even lateral background fluorescence. The linear trend in background fluorescence in the direction of laser propagation was then corrected for during data analysis.

The slides were imaged in a dark room to prevent interference from external light sources. The apparatus was shielded from remaining sources of light by a black acrylic box.

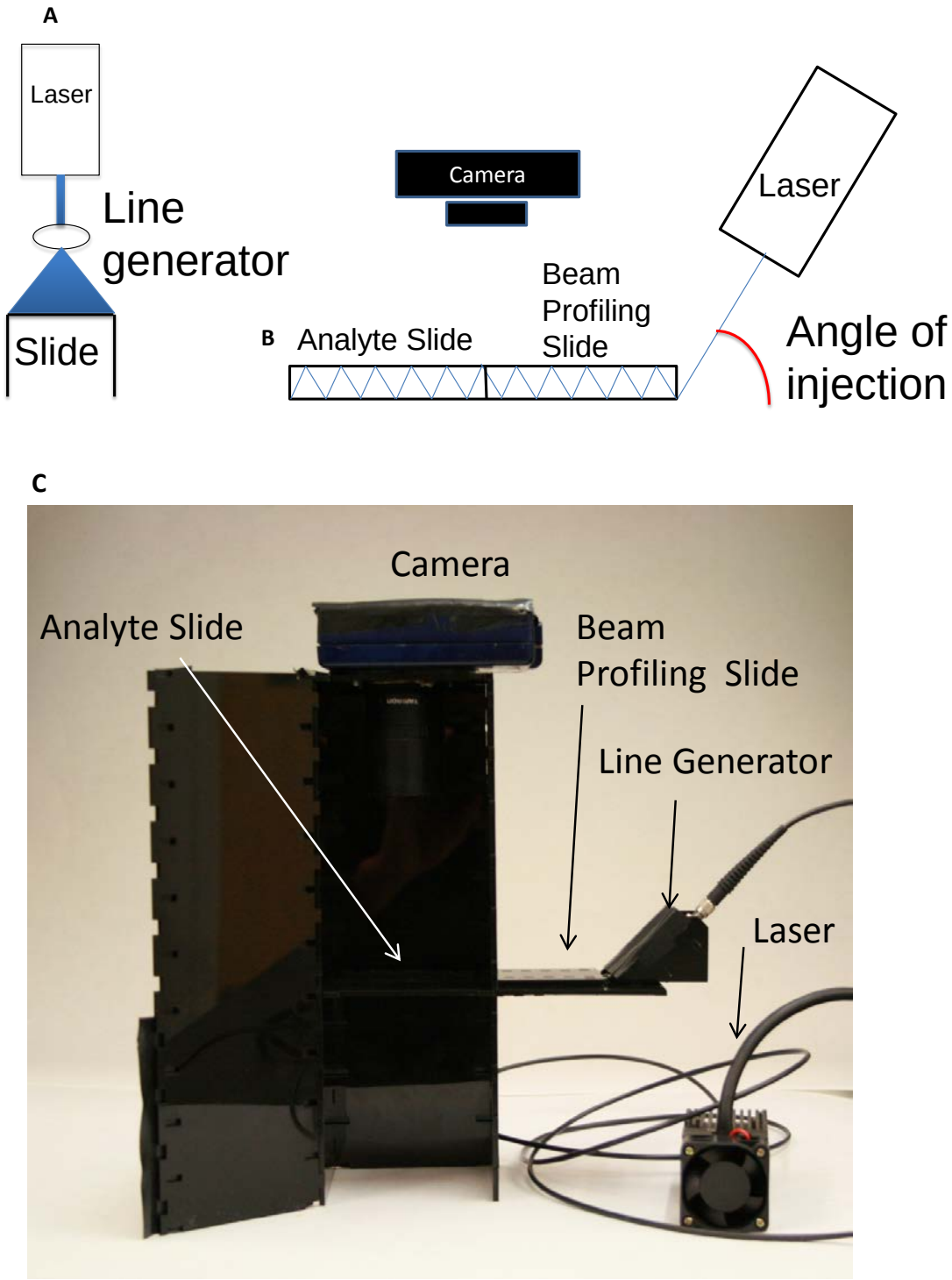

Figure 33. POC evanescent waveguide detection scheme. (A) schematic of laser injection featuring line generator, (B) schematic of experimental set-up for imaging, (C) image of detection platform

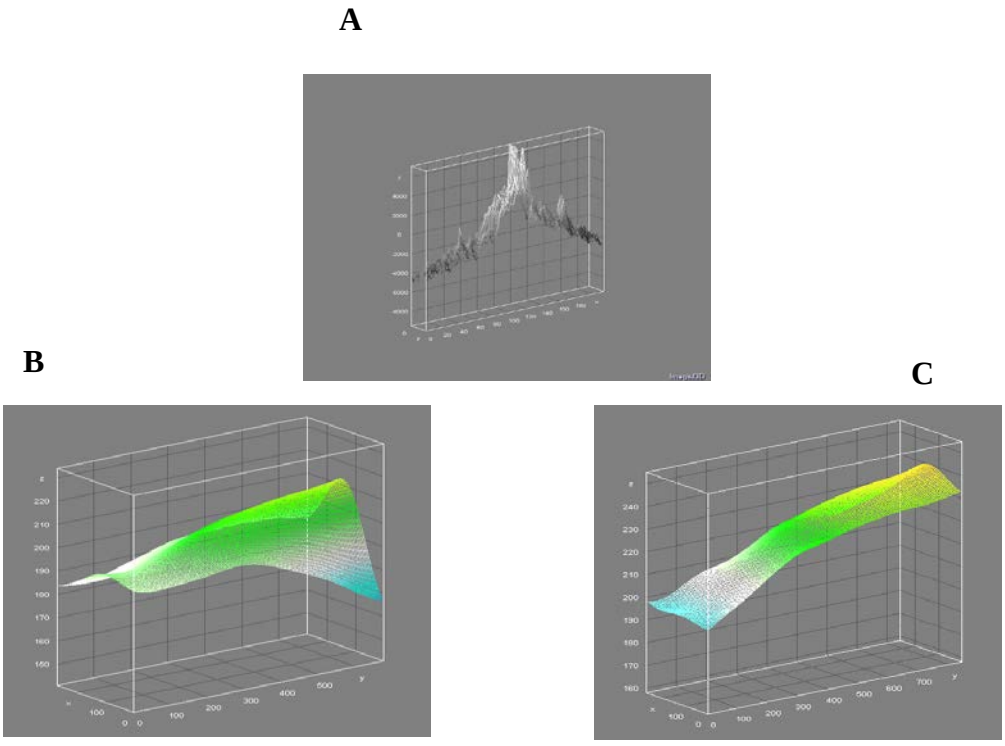

Figure 34. Slide background fluorescence. (A) Intensity profile of laser beam out of the line generator, (B) intensity profile of background fluorescence on blank slides using one-slide method, or (C) two-slide method

Results

Results have indicated that multiplexing of antibodies within a single well of a white, high-binding, 96-well microtiter plate is possible when using semiconductor QD tracers [144]. We have also shown how QDs can be employed for both spatial and spectral multiplexing using planar surface fluorescent immunoassays.

Microtiter Plate

Single Immunoassays

Dose response curves for the singleplex chicken IgG immunoassay and SEB immunoassay for both the methods of detection—Cy5 tracer or QD tracer are shown in Figure 35. The different tracers show similar curves for each analyte using the four-parameter logistic model commonly used for immunoassay dose response curves. A statistical comparison of the fit parameters was conducted and at the 99% confidence level (t-test, $p > 0.01$), the parameters that determine the EC_{50} value and slope for each analyte were not significantly different between the two tracers. The reported LODs (signal greater than three standard deviations above the background signal) are shown in Table 12. While the LOD for the Cy5 tracer was slightly better than the LOD for the NC 605 for the chicken IgG immunoassay, the LODs were the same regardless of the tracer for the SEB immunoassay. There results, combined with the dose response curves shown in Figure 35, indicate that the new QD conjugation method employed here was controlled in a manner to retain appropriate binding activity.

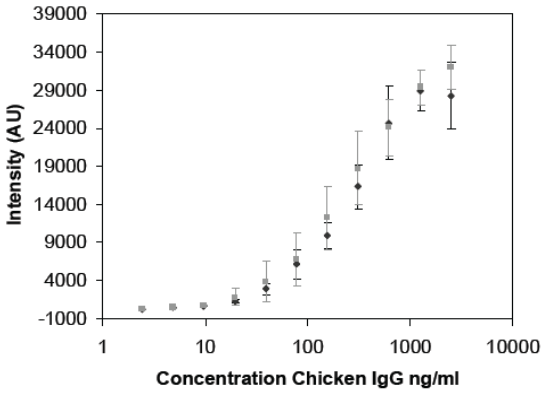

(A)

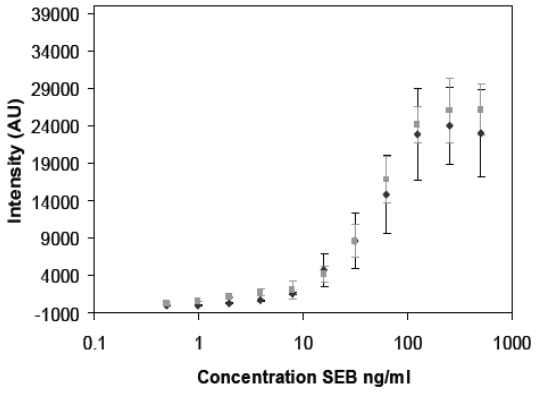

(B)

Figure 35. Single NC tracers versus Cy5 tracer [144]. (A) chicken immunoassay. (B) SEB immunoassay. NC tracer is represented as the grey square, while the Cy5 tracer is represented by the black diamond

Table 12. LOD of chicken IgG and SEB from dose response studies involving either single or duplex formats with organic or nanocrystal quantum dot (NC) tracers [144]

Target	Tracer	Format	LOD (ng/ml)	n
Chicken IgG	Cy5	Single	4.9	8
	NC605	Single	9.8	8
	NC605	Duplex	9.8	4
SEB	Cy5	Single	7.8	4
	NC650	Single	7.8	4
	NC650	Duplex	7.8	4

Duplex Immunoassays

In these experiments, sandwich assays (Figure 32) were used to immobilize both capture antibodies onto the surface with an optimized ratio of 7.5:2.5 of Rb-anti-chicken IgG and Rb-anti-SEB. The chicken IgG sample was increased from 0 to 2,500 ng/mL while the SEB was decreased from 500 to 0 ng/mL to create the target samples.

Dose response curves for the duplex formats are shown in Figure 36 for Chicken IgG and SEB immunoassays, respectively. As displayed in A, when the concentration of the analyte increases in ng/mL, the corresponding intensity of the QD emission increases. This figure shows the spectral separation of the QD emissions over a wide range of sample concentrations (ng/mL). In the single format, 10 µg/mL was used for the capture antibody, but in the duplex format, 7.5 µg/ml was used for the Anti-chicken IgG capture antibodies and 2.5 µg/mL was used for the anti-SEB capture antibodies. During capture antibody ratio optimization studies, comparison of the chicken IgG/SEB ratios 7.5/2.5 and 9/1 give very similar dose response curves and the LOD is the same for both. Figure 36 (B, C) demonstrates the intensity data versus concentration for each antigen in the duplex and singleplex format involving NC tracers. The LOD for SEB in the duplex, 7.8 ng/mL, was equivalent to the value obtained by the single assay format using either QDs or Cy5. The LOD for chicken IgG in the duplex, 9.8 ng/mL, was the same for single assay; however, when using the Cy5 label, the LOD was 4.9 ng/mL. These results show that duplexing did not hinder the sensitivity of the assays.

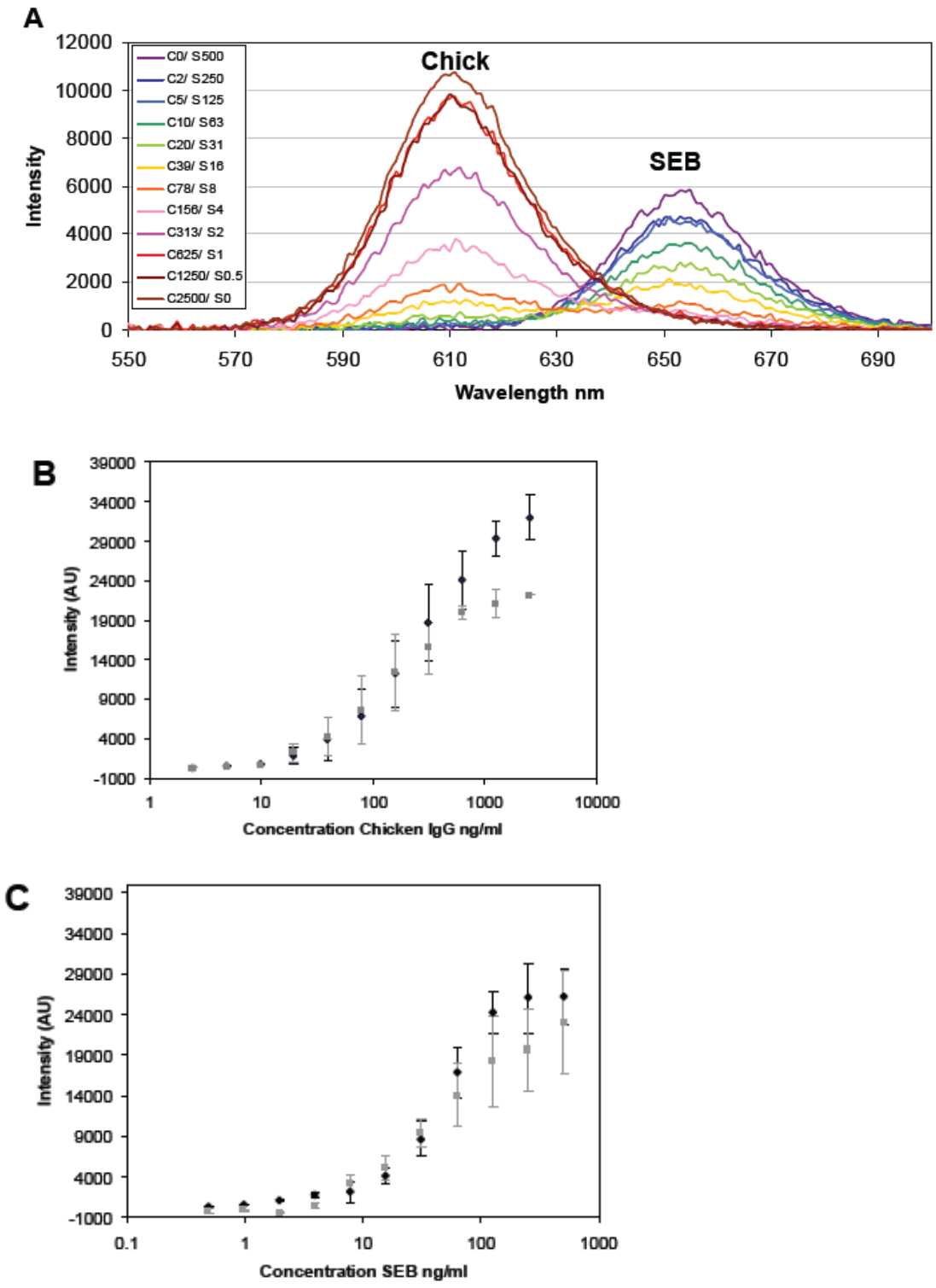

Figure 36. Duplex immunoassay data [143]. (A) intensity vs. wavelength curves for chicken & SEB concentrations (B) Dose response curve for chicken immunoassay in single (black) or duplex (grey) format (C) Dose response curve for SEB in either single (black) or duplex (grey) format [144]

Triplex Immunoassays

After success of the duplex was shown using microtiter plates, the duplex was extended to demonstrate a triplex with a lower LOD than previously found for SEB [18]. In addition to the analytes used in the duplex, chicken IgG and SEB, a second immunoglobulin, mouse IgG was detected simultaneously. Both IgGs are ~150 kD, while SEB is ~28kD. For these studies, the same QDs used in the duplex were used for chicken IgG and SEB, and a QD with maximum emission spectra at 525 nm was used for mouse IgG detection. In this study, chicken IgG was increased from 0 to 2500 ng/mL and SEB was increased from 0 to 500 ng/mL while mouse IgG was decreased from 2500 to 0 ng/mL. As seen in Figure 37, the data obtained from the plate reader shows that there is no cross-reactivity between the analytes and all analytes can be detected within the same well. Figure 37 shows the raw data (A), fitted data (B), fluorescence intensity wavelength scans, and (C) normalized data. In Figure 37A, deconvoluted data is shown from 78 ng/mL chicken IgG, 39 ng/mL mouse IgG, and 15 ng/mL SEB. Figure 37B shows the full fitted spectra for all twelve wells exposed to all mixed concentrations of analytes. Figure 37C shows the normalized intensity versus concentration. The LOD for the triplex is 10 ng/ml, 5 ng/ml, and 2 ng/ml for the chicken IgG, mouse IgG, and SEB, respectively. As demonstrated, the analyte concentrations are clearly distinct from one another, even before deconvolution.

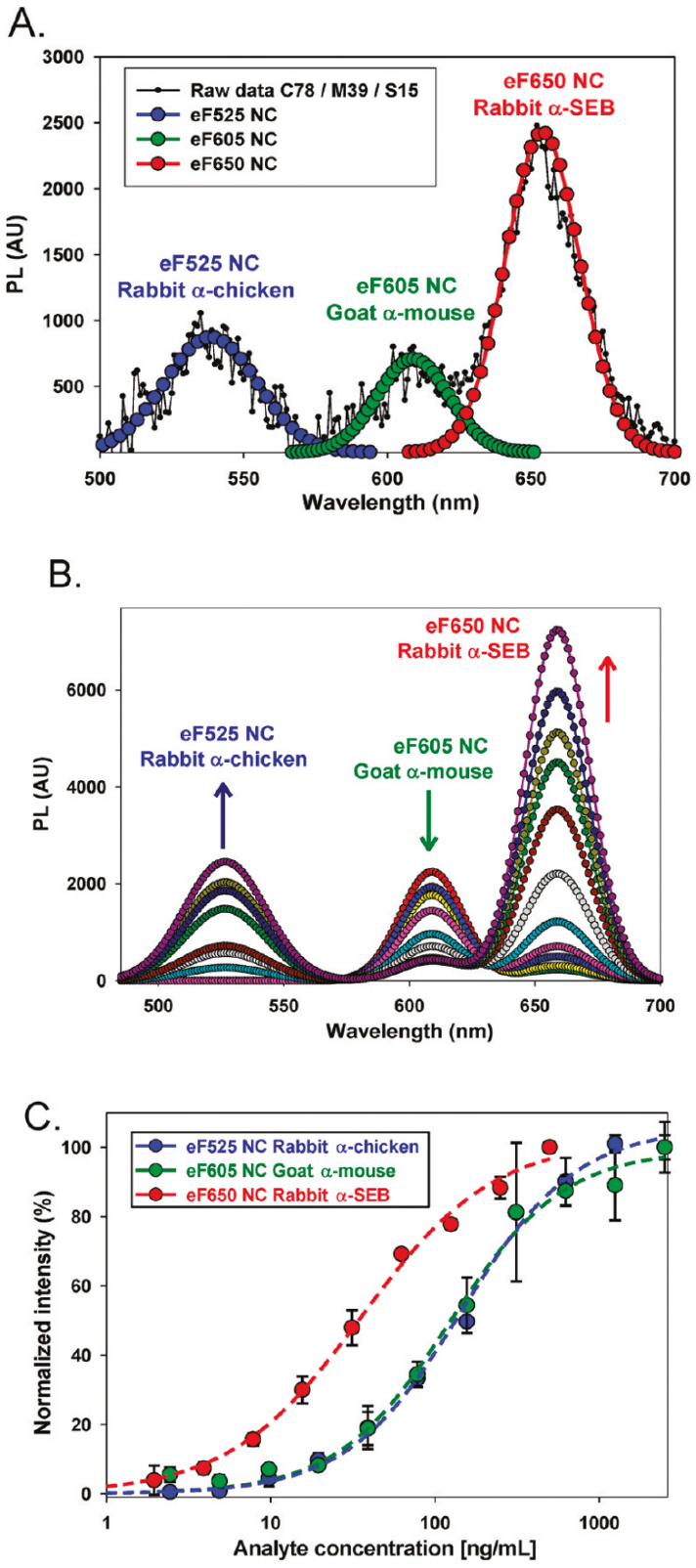

Figure 37. Simultaneous triplex immunoassay of a 96 well plate. (A) raw data from one well, (B) Fitted Data from twelve wells (50% serial dilutions), (C) normalized data with respect to the highest concentration measured [18]

Planar Surface Fluorescent Immunoassays

Singleplex Immunoassays

Figure 38 illustrates the sandwich assay format used in these studies involving QDs. As shown in the figure, a direct assay was used for chicken IgG detection (QD-anti-chicken IgG antibodies bound to chicken IgG) and an indirect assay (Bt-antibody/SA-QDs) was used for SEB detection. When a sandwich assay was performed using 50% serial dilutions of SEB beginning at 800 ng/mL, followed by exposure to 10 μg/mL biotinylated anti-SEB and 15 nM 800 nm Streptavidin-QDs for detection, the signal was obtained using the developed evanescent waveguide and had a resulting LOD of 3 ng/mL. When a sandwich assay was performed with 50% serial dilutions of chicken IgG beginning at 800 ng/mL and exposed to 655 nm QDs conjugated to anti-chicken IgG (1:100 dilution), the LOD was 3 ng/mL. Figure 39 shows two singleplex immunoassay images. Slide A in the figure shows a sandwich assay where the target analyte is SEB, which is detected using biotinylated Rb-anti-SEB antibodies along with streptavidin-conjugated 800 nm QDs. Slide B in the figure shows a sandwich assay where the target analyte is chicken IgG, which is detected using 605 nm QDs conjugated to Rb-anti-chicken IgG. Detection of SEB and chicken IgG using Cy5 tracers and imaged with the GenePix (Table 7) achieved LODs one order of magnitude lower than that achieved using QDs and the evanescent waveguide detection system. However, with improvements to make the detection platform "light-tight", we believe we can achieve comparable LODs compared to Cy5 detection using the GenePix.

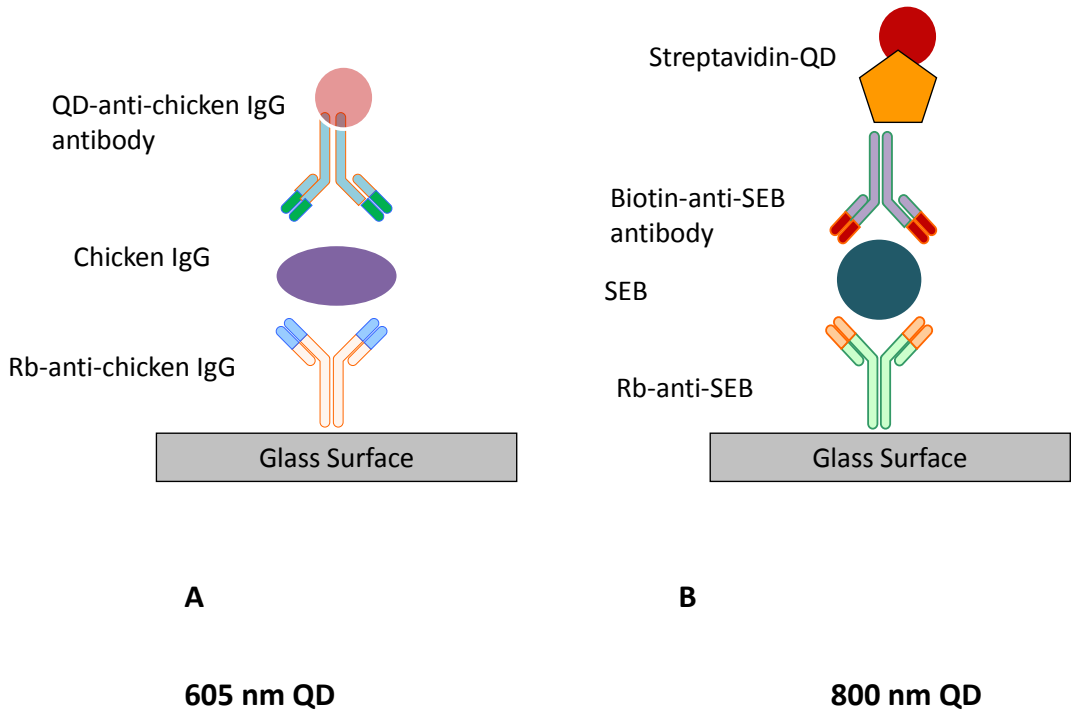

Figure 38. Sandwich assay format employed for planar surface fluorescent immunoassay involving 800 nm QDs for SEB detection and 605 nm QDs for chicken IgG detection

A

Patterning:
Columns 1-9: Columns 4-6: α-SEB (10 µg/ml)

Assay:
Row A: PBS
Rows L → B: 800 ng/mL SEB → 50% serial dilutions

All rows: 10 µg/ml Biotin-α-SEB, 800 nm QD-SA (15 nM)

B

Patterning:
Columns 1-9: α-Chicken IgG (10 µg/ml)

Assay:
Row A: PBS
Rows B → L: 800 ng/mL Chicken IgG → 50% serial dilutions

All rows: 1:100 dilution of 605 nm QD-α-Chicken IgG

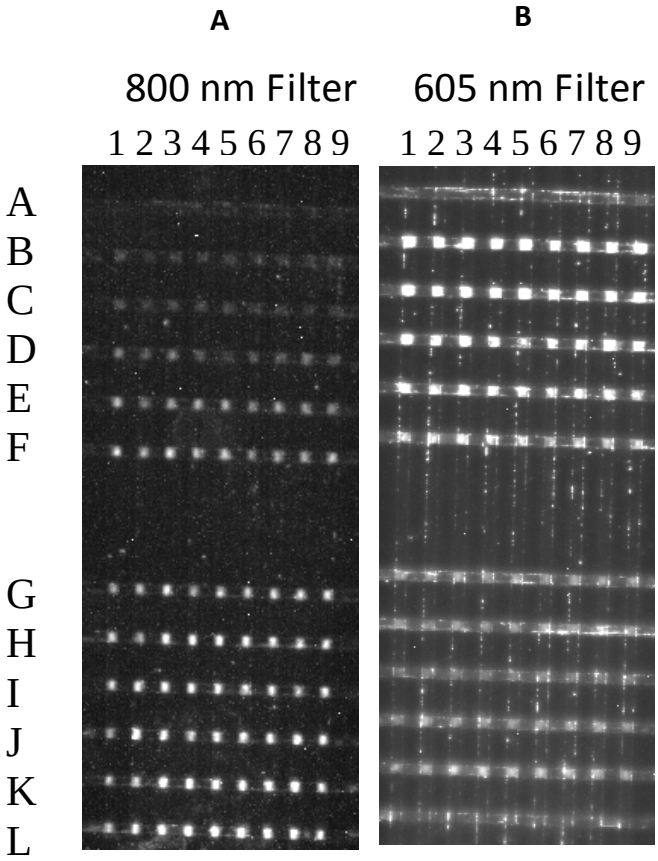

Figure 39. Singleplex immunoassays using planar surface fluorescent immunoassays imaged with evanescent waveguide detection system. Chicken IgG was detected using 605 nm QDs and SEB was detected using 800 nm QDs

Duplex Immunoassays

Figure 38 illustrates the sandwich assay format used in these studies involving QDs, which is the same as that used in the singleplex studies. When a duplex was conducted on a single immunoassay by detecting both SEB and chicken IgG using a sandwich format, the LODs for SEB and chicken IgG were 0.78 ng/mL and 3 ng/mL, respectively. These results were obtained when each capture antibody was patterned for only one single analyte. The LOD for SEB is on the same order of magnitude as the LOD obtained when using Cy5 tracers, but the LOD for chicken IgG is an order of magnitude larger than that obtained for a Cy5 tracer (Table 7).

Figure 40 shows two images of the same slide imaged using two different filters. The 800 nm bandpass filter was used to capture the signal from the 800 nm QD, corresponding to the presence of SEB, while the 605 nm bandpass filter was used to capture the signal from the 605 nm QD, corresponding to the presence of chicken IgG. As shown in the figure, the signal from the 605 nm QD is blocked when the 800 nm filter is used for imaging, and vice versa.

Patterning:
Columns 1-4: Columns 4-6: α-SEB (10 µg/ml)
Columns 5-9: α-Chicken IgG (10 µg/ml)

Assay:
Row A: PBS
Rows L → B: 800 ng/mL SEB → 50% serial dilutions
Rows B → L: 800 ng/mL Chicken IgG → 50% serial dilutions

All rows: 10 µg/ml Biotin-α-SEB, 800 nm QD-SA (15 nM)
All rows: 1:100 dilution of 605 nm QD-α-Chicken IgG

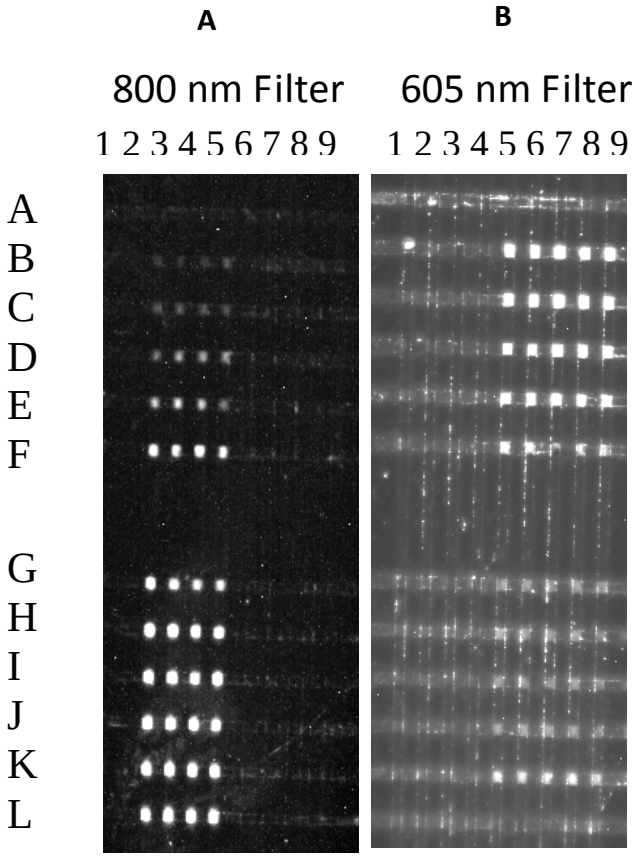

Figure 40. Duplex immunoassays using planar surface fluorescent immunoassays imaged with evanescent waveguide detection system. Chicken IgG was detected using 605 nm QDs and SEB was detected using 800 nm QDs

Duplex Immunoassays: Multiplexing within the same spot

Figure 38 illustrates the sandwich assay format used in the studies involving QDs for both spatial and spectral multiplexing. Note that this is the same format as that used in the duplex experiments that employed only spatial multiplexing. When both analytes were detected in a single spot (capture antibodies for both SEB and chicken IgG were mixed together), the LODs for SEB and chicken IgG were 1.6 ng/mL and 25 ng/mL, respectively. An image of a representative slide imaged with the 800 nm filter and the 605 nm filter is shown in Figure 41. The slide imaged with the 800 nm filter shows bright spots where SEB is patterned as well as where SEB and chicken IgG are patterned together, but there is no signal obtained in the region where chicken IgG is patterned alone. Likewise, the slide imaged at with the 605 nm filter shows a signal where chicken IgG is patterned alone, as well as where chicken IgG and SEB are patterned together, but there is no signal obtained in the region where SEB is patterned alone. A quantitative analysis of these images is shown in Figure 42. When only SEB antibodies are patterned onto the surface, the signal from the 800 nm QD shows a remarkable increase in the signal to noise ratio as compared to when both antibodies are patterned onto the surface. In contrast, the signal of chicken IgG from the 605 nm QD is comparable when both antibodies are patterned onto the surface or when only chicken IgG antibodies are patterned onto the surface. The assays conducted with the 605 nm QDs are not as sensitive as the assays conducted with the 800 nm QDs due to the higher observed autofluorescence of the slide, which cannot be fully blocked with the 605 nm filter.

Patterning:
Columns 1-3: Mixed α-SEB (2.5 µg/ml) and α-Chicken IgG (7.5 µg/ml)
Columns 4-6: α-SEB (10 µg/ml)
Columns 7-9: α-Chicken IgG (10 µg/ml)

Assay:
Row A: PBS
Rows B → L: 800 ng/mL SEB → 50% serial dilutions
Rows L → B: 800 ng/mL Chicken IgG → 50% serial dilutions

All rows: 10 µg/ml Biotin-α-SEB, 800 nm QD-SA (15 nM)
All rows: 1:100 dilution of 605 nm QD-α-Chicken IgG

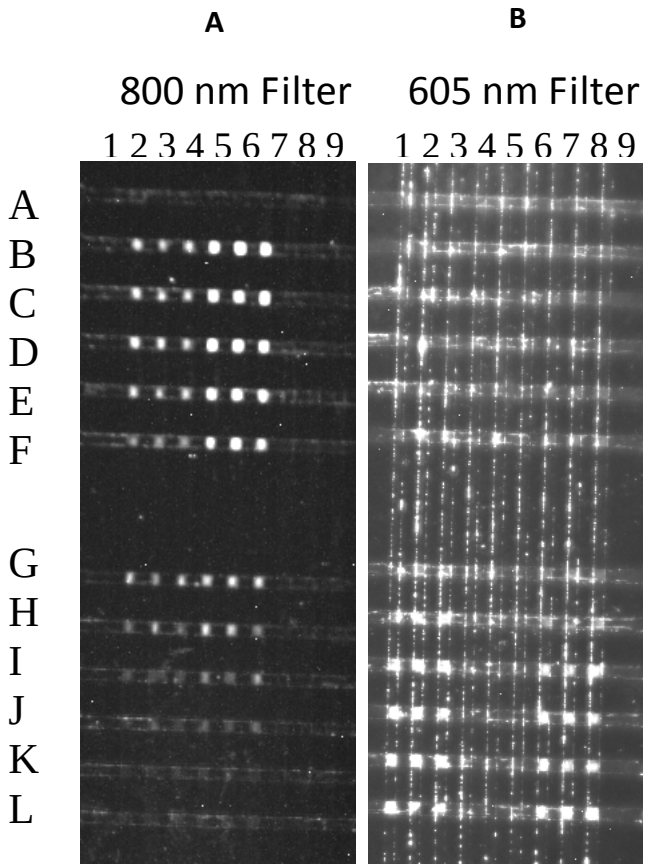

Figure 41. Spatial and spectral multiplexing using planar surface fluorescent immunoassays imaged with evanescent waveguide detection system. Chicken IgG was detected using 605 nm QDs and SEB was detected using 800 nm QDs.

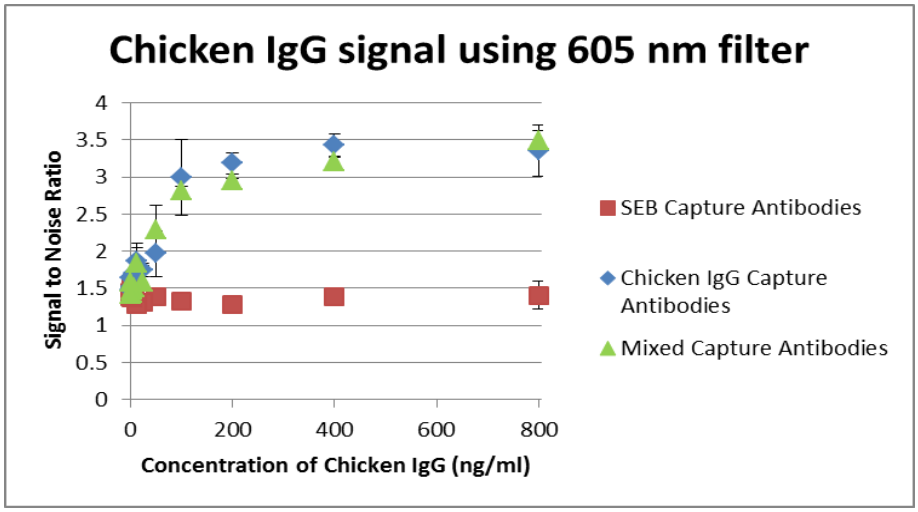

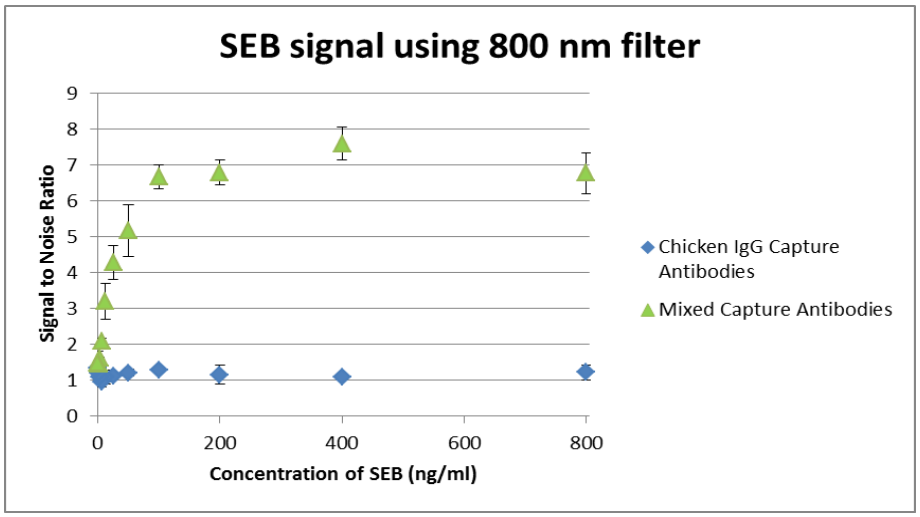

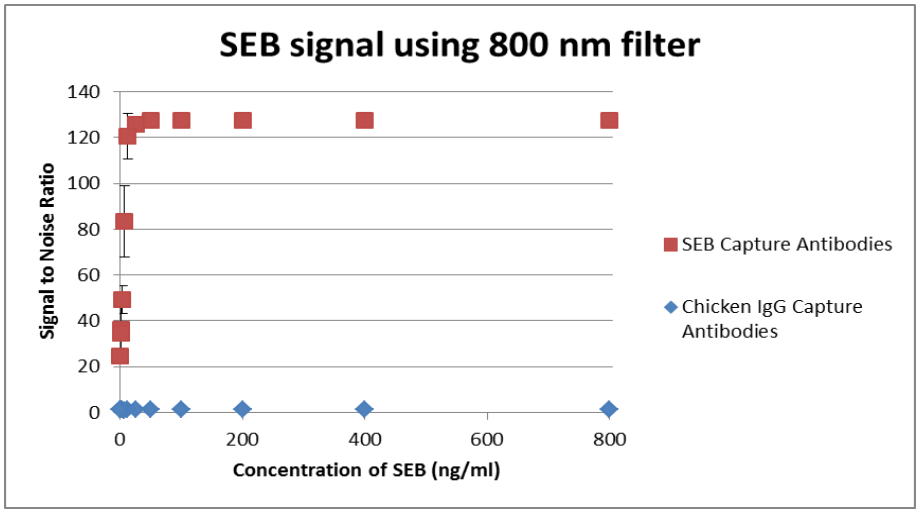

Figure 42. Quantitative data of spatial and spectral multiplexing using planar surface fluorescent immunoassays. Chicken IgG was detected using 605 nm QDs and SEB was detected using 800 nm QDs.

Evanescent Waveguide Detection System

While the fluorescent label, Cy5 has been used in spatial multiplex studies involving the GenePix for imaging, other tracer labels such as QDs were tested in order to demonstrate spectral multiplexing. In order to image these slides, a new evanescent waveguide detection system was created to pair specific filter sets with the QDs labels employed in the assays. As mentioned in Chapter 2, use of QDs makes the immunoassay more amenable to a POC environment because one excitation source can be used to excite multiple QDs that emit at distinct wavelengths, which simplifies the platform design. Using the evanescent waveguide method, there was a high level of background that was spatially uneven across the slide. To minimize some of the noise that is caused by a residue from the vinyl template that adheres to the slide, the process for creating the templates on the Epilog printer was revised. When the laser cutter operates, some pieces of material that falls through the grate can still be exposed to the laser cutter as it continues its operation. Those pieces of material below the grate that are exposed to the laser can give off some smoke as they burn. The smoke can adversely affect the even-ness of the bottom layer of the material as it is being cut. To avoid any interaction of smoke with the material being cut, a sacrificial layer of acrylic was used to absorb the effects of exposure to smoke. This process was shown to decrease the background of the slide.

The combined cost of the materials and devices in this platform were much less expensive than the plate reader. The platform was also decidedly lighter, and therefore could be more portable than the plate reader. This study was an initial

proof-of-concept that could be used to detect more than two analytes in each spot, assuming the quantum dots were spectrally distinct from one another and that appropriate filter sets were used to detect the signal from each analyte.

Discussion

The objective of this chapter was to evaluate the multiplexing capability of QDs using microtiter plates and planar surface fluorescent immunoassays. We demonstrated that multiplexing is possible within a single well of a 96-well plate by detecting three distinct proteins using spectrally distinct QDs. We also showed how an in-house evanescent waveguide detection system can be used for planar surface fluorescent immunoassay multiplexing not only spatially, but also spectrally.

Quantum Dot Conjugation Chemistry

Bioconjugation chemistries have contributed greatly to improvements in fluorescence techniques ranging from biological research to medical diagnostics [18]. This is particularly true in the case of attaching proteins to fluorescent nanomaterials, such as the QD NCs used in this study. A variety of approaches exist, such as use of a heterobifunctional succinimide ester-maleimide crosslinker with amine-thiol reactivity to introduce maleimide groups to an amine functionalized NC. Typical nanomaterial bioconjugation approaches involve multiple preparation steps and long durations of time to complete and may render the biological region of the antibody

partially inactive and/or be detrimental to the nanomaterial unique properties [197]. However, in the method developed by our collaborators and demonstrated in this work, only specific sites for attachment (the cysteine residues exposed under mildly reducing conditions) are engaged in the conjugation of the antibody to the maleimide activated NC. This approach should leave the binding region of the antibody available to engage in biorecognition events. Another advantage of this method is that the conjugation reaction occurs *in situ* with only a few steps and relatively quickly, without requiring excess components for completion or purification of antibody fragments. Other advantages of this chemistry are its non-reactivity toward other functional groups and its stability in aqueous solution.

Quantum Dot Immunoassay Detection Technique

In contrast to the technique employed here, performing a similar experiment with traditional fluorophores such as Cy3 and Cy5 would have required the use of two different excitation wavelengths and either instrumentation containing parallel excitation sources or a computer capable of serial data acquisition at different signals. Use of NC avoids these complications as an excitation wavelength of 400 nm was used to excite both tracers due to the broad adsorption profile characteristic of these semiconducting nanomaterials.

Although quite low LODs for SEB have been reported in the literature (e.g. 4 ng/mL to <2.5 fg/mL), the aim of the experiments was to demonstrate a proof-of-concept for the QD labeling and multiplexing [144]. The LOD for SEB achieved in this study

was 15 times lower than the 30 ng/ml found in a previous 4-color QD immunoassay [198]. This study suggests that the QD-antibody constructs can differentiate among varying sizes of different proteins [18]. We directly compared the fluorophore, Cy5, with QDs and demonstrated that although the sensitivity is equivalent regardless of the label, the use of QDs allows for multiplexed detection, which is not as easily accomplished using traditional dyes due to their much broader fluorescence emission profiles relative to QDs. Improvements to this assay, along with use of high-affinity antibodies may improve the sensitivity in both single and multiplexed formats. Furthermore, due to the discrete spectral separation of QDs by 50 nm, immunoassays using up to 5 different tracers in the range of 450 – 540 nm may be possible.

Some issues may limit the applicability of multiplexing in QD-immunoassay formats. One drawback is the cross-reactivity among antibodies for a particular antigen. Employing monoclonal antibodies to afford the most specificity could help overcome this limitation. Another impediment is the ability to resolve QD emissions that are in close range of one another, although researchers have shown that spectral deconvolution methods used during data analysis can address this issue [199]. Selecting quantum dots that are spectrally diverse in addition to using state-of-the art instrumentation with higher resolution could help avoid the second constraint.

POC Development

While this work demonstrated the potential for multiplexing, the usefulness of the device for a POC application has not yet been realized. In order for this device to be

useful for a company to scale-up production, all steps should be automated. The process of patterning antibodies onto the surface can be automated as well as performing an assay and analyzing results. Automation can increase the assay performance, robustness, and reliability [117]. Components can be fabricated inexpensively by replication, which can make the device more cost-effective. If the planar surface fluorescent immunoassay were to be scaled up for manufacturing and use, storage conditions over ranges in temperature and humidity would need to be tested to determine the most appropriate shelf life using traditional testing and accelerated shelf life testing [200, 201] and additional processing steps may be needed in this case.

Besides automation, development of a pseudo-POC device could build upon previous work with microfluidics [48, 50, 202]. Currently, two systems exist for this platform—one for performing the assay, and one for imaging and data analysis. Ideally, the experimental procedures and the detection systems would be integrated to create one fully-fledge, self-contained device that requires minimal user interaction. In addition, the box containing the camera and other associated imaging components could be concealed in a box that is more “light tight” to avoid any other intrusion of external sources of light.

Conclusion

This work is one of only a few examples of multiplexing three distinct biological analytes within a single well of a microtiter plate using QDs. The NC-antibody constructs with emissions centered at 605 nm, 650 nm, and 525 nm were able to differentiate among two closely related IgGs and between small and large proteins when they are all present in the same mixture [18]. Spectral and spatial multiplexing was also demonstrated using planar surface fluorescent immunoassays for detection of chicken IgG and SEB within the same spot. Theoretically, spatial and spectral multiplexing can be extended beyond three analytes with either platform so long as distinct QDs are employed and the signals can be analyzed separately. The newly-developed detection system featuring an evanescent waveguide can be used "in the field" because it is lightweight, small, and self-contained. Further work regarding integration of the assay with detection mechanisms may make this system even more favorable. For example, color cameras such as those used in cellular phones could potentially be used and applied in rugged settings.

Traditional labeling methods for attaching antibodies to QDs are complex, prone to aggregation and loss of product, but the method used in this study took less than 3 hours [144]. This process used the thiols present in the hinge regions of reduced antibodies to conjugate nanocrystals with activated maleimide groups. Careful control as demonstrated by this conjugation method is important for the long-term needs of bionanotechnology.

QD-based dose response curves were shown for both SEB and chicken IgG in a single format (microtiter plates) and were statistically equivalent (99% confidence level) compared to Cy5 singleplex assays [144]. While other platforms for detecting SEB such as ELISA, cantilever methods, and SPR may be more sensitive than this QD platform, they often involve multiple steps and specialized equipment. The microtiter plate immunoassays were then developed for simultaneous duplexing with LODs of 9.8 ng/mL for chicken IgG and 7.8 ng/mL for SEB. Building upon these results, a triplex was demonstrated with mouse IgG. Our LOD for SEB is 15 times lower than a recent previously reported QD immunoassay [198]. These novel outcomes regarding multiplexing and a very low LOD have not been demonstrated in the literature prior to the release of our two papers in *Sensors* and *ACS Nano.* The studies involving a duplex and triplex suggest promise for multiplexing with greater than three configurations because of the large spectral window that could be accessed with more diverse QD materials, which can span the UV to IR range [144]. Spatial and spectral multiplexing were also demonstrated using planar surface fluorescent immunoassays with LODs of 25 ng/mL for chicken IgG and 1.6 ng/mL for SEB. Furthermore, these results, along with those previously published, show promise that multiplexed fluorescent immunoassays could be used in other immunoassay formats, such as in reverse phase or in displacement assays [18, 203].

Scientific Impact

Since publication, our first paper, *Optimizing two-color semiconductor nanocrystal immunoassays in a single well microtiter plate formats*, has been cited five times [93, 95, 204-206]. Morales-Narvaez, et al. noted that our work, along with others, demonstrates that QDs have better performance in solid phase as compared to liquid phase, and this makes them particularly useful as reporters [93]. These researchers also conducted biomarker screening experiments for Alzheimer's Disease using antibody microarrays, demonstrating the real-world applicability of using QDs in a multiplexed fashion for a true clinical need.

A second publication that featured our peer-reviewed work was in a review article published by Petryayeva, et al. [204]. This review discussed the use of QDs in assays, bioprobes, and biosensors, and in applications such as for fluorescence imaging, microscopy, spectroscopy, and imaging. Petryayeva, et al. cited our work in another publication regarding the use of Fluorescence Resonance Energy Transfer (FRET) and QDs in a microtiter plate format [205]. This paper demonstrated the use of QDs as donors in FRET, which were paired with either Cy3 or Alexa Fluor 647 as acceptors in experiments to discern between fully complementary DNA and single base mismatches.

A fourth paper that cited our original work is a review by Samir, et al., which highlights the use of QDs for various biomedical applications [95]. This review discusses the relevance of QDs for *in vitro* diagnostics and imaging.

Lastly, the fifth paper that cited our paper, *Optimizing two-color semiconductor nanocrystal immunoassays in a single well microtiter plate formats,* was written by Anderson, et al., who reported the use of single domain antibodies that self-assembled onto QDs [206]. The antibody-QD conjugates were used in fluoroimmunoassays as well as in SPR to detect ricin.

Our second paper, *Reactive Semiconductor Nanocrystals for Chemoselective Biolabeling and Multiplexed Analysis,* has been cited twenty times since its publication in 2011 [144, 197, 204, 207-223]. One paper discussed the use of nanomaterials in medicine and the potential adverse effects that may be associated with health such as toxicity, genotoxicity, and allergic reactions as well as issues related to exposure to physiological environments such as material corrosion and aggregation or non-specific adsorption of biomolecules [213]. Other papers discussed the delivery of QDs to a wide range of different cell types with implications for drug delivery and *in vivo* labeling [207, 223], while a third paper involved the use of single cell imaging [214]. One paper investigated functionalization of nanoparticles with biological molecules and another research group focused on designing petidyl linkers [197, 208]. A review paper published by Javier Vela cited our paper in his discussion of semiconductor nanocrystals [217]. In another review paper, Tyrakowski, et al. described the use of QDs for biological sensing and highlighted recent advances in QD technology [221]. Vannoy, et al., found our work helpful in his studies regarding competitive displacement assays involving QDs as FRET donors [216] and Nonat, et al., cited our work with regard to intramolecular

energy transfer [212]. Research involving doping QDs with ligands and imaging have also relied upon our previous work [210, 215]. Furthermore, our work has been cited by researchers investigating QDs for multiplexed biosensors and aptamer sensors involving chemiluminescence [209, 211]. In two other papers, researchers demonstrated how QDs can form a complex with a photosensitizer, chlorin e(6) and demonstrated that this complex can become localized within the plasma membrane and endocytic vesicles of cancer cells [219, 220]. In another paper, our work was cited with regard to controlling spacing of QDs as they attach to gold nanorods in solution, which may be useful for biological sensing and optical communication [218]. Wegner, et al. demonstrated an immunoassay involving QDs for potential clinical use to detect prostate specific antigen using low volumes of serum [222].

Our two papers regarding the use of QDs in multiplexing have been well-accepted by the scientific community as demonstrated by the number of publications that have cited our work. Scientists have found our work useful for determining the properties of QDs, for *in vivo* and *in vitro* applications, and for incorporation into review papers.

We anticipate that achievements of our work using microtiter plates portends the scientific impact of the application of QDs to spatial and spectral multiplexing using planar surface fluorescent immunoassays. The planar surface fluorescent platform and its associated in-house developed detection system (in combination with QDs) containing an evanescent waveguide signify a novel way to detect multiple proteins using a cost-effective approach. Likewise, the detection system is fabricated from

acrylic and other cheap components, including the camera that was installed into the device. The combined cost of the materials and devices in this platform were much less expensive than a conventional plate reader. The detection platform requires only a laptop computer and battery for operation and could therefore be used in remote locations. This new imaging technique is more suitable for a POC environment because of its greater portability compared to that of a standard plate or slide reader. Conventional instruments have photomultiplier tubes and other components that are sensitive to vibrations that may be caused by jostling or placement on an uneven surface. This developed detection system is also more immune to jostling that could surely arise due to POC use.

Chapter 7: Summary

This work discussed the ability to develop Point-of-Care (POC) platforms capable of multiplexing (detecting multiple analytes simultaneously) for personalized medicine. Specifically, optical sensor platforms can be used to aid in diagnosis of disease or determination of proper therapy. The overall goal of this work was to develop and evaluate a new multiplexed immunoassay for protein detection.

A new method for protein multiplexing, planar surface fluorescent immunoassays, was developed with the advantages of using less sample/reagent volume and being amenable to a POC environment. This new platform was designed and fabricated in-house and applied for detection of SEB and chicken IgG. These analytes were used to optimize the platform because they are commonly used in the literature, thus allowing us to compare performance to existing technologies. The platform was characterized by evaluating a variety of immobilization techniques, capture antibody concentrations, and detection labels. The performance of the platform was characterized over a range of concentrations to demonstrate full dose response curves and reproducibility. Variations among slides and within slides were investigated for systematic errors, and analyses revealed that discrepancies were random. The LODs and dynamic ranges were comparable for standard fluorescent plate experiments for model protein analytes.

The newly developed multiplexed method, planar surface fluorescent immunoassays, was applied to real-world diagnostics by quantifying Acute Kidney Injury (AKI)

biomarkers. The two biomarkers selected for these studies were Kidney Injury Marker-1 (KIM-1) and Neutrophil Gelatinase-Associated Lipocalin (NGAL) due to their promise for potential earlier and more specific diagnosis of AKI compared to traditional markers [24-26]. Studies were compared to colorimetric 96-well plate assays in buffer (fluorescence detection was not available) and physiologically-relevant matrices such as urine and plasma. Urine samples from Sprague Dawley rats treated with varying levels of exposure to gentamicin, a known nephrotoxicant, were evaluated with planar surface fluorescent immunoassays. This work demonstrated the applicability of planar surface fluorescent immunoassays to detection of biomarkers for a real public health need, Acute Kidney Injury.

A technique was developed using microtiter plates for protein multiplexing of two, and then three analytes using luminescent semiconductor quantum dot nanocrystal (NC) tracers. SEB, chicken IgG, and mouse IgG were all detected simultaneously with LODs 15 times lower than the 30 ng/ml found in a previous 4-color QD immunoassay [198]. These results were published and cited by numerous other research groups in peer-reviewed publications. Our work has been featured in both review papers and original research papers regarding the use of QDs for various sensing applications.

A novel detection system using an evanescent waveguide and appropriate filters was employed for detection of chicken IgG and SEB using Quantum Dots. The results presented demonstrate a proof-of-concept where multiplexing was achieved both

spatially and spectrally. Detection of more than two analytes in a single spot is possible if spectrally-diverse QDs are paired with appropriate filter sets that can detect the emission of each of the QDs. This detection system is more amenable to a POC environment compared to the standard slide reader, the GenePix 4000B, which is a large instrument. These results demonstrated the potential for this assay to be applied for true "in the field" use. While the developed platform is not a true biosensor because it is not stand-alone device, requires washing [224], and cannot be reused [110], these new methods have the potential to be incorporated into an analytical device. The washing steps and other liquid handling procedures can eventually be automated.

Chapter 8: Scientific Impact of Work

The significance of this work is many-fold. First, a promising optical sensor platform—planar surface fluorescent immunoassays— was created and a comprehensive analysis was conducted to illustrate its use for multiplexing with low sample volumes. Second, this new platform was applied to a real-world public health concern: detection of two novel Acute Kidney Injury (AKI) biomarkers, Kidney Injury Marker-1 (KIM-1) and Neutrophil Gelatinase-Associated Lipocalin (NGAL). This study represents the first assessment of these biomarkers using low volumes of urine and plasma, as there are no known current publications regarding this topic. We demonstrated detection of these biomarkers above baseline levels, including after exposure to a nephrotoxicant. Third, a novel method for multiplexing three analytes using microtiter plates and QDs was demonstrated. This method allowed for a significantly lower LOD for SEB than what had previously been reported in the literature using a comparable technique. Finally, a novel detection system was created using an evanescent waveguide for imaging two analytes within a single spot on the planar surface fluorescent immunoassay. Creation of this system portends how the planar surface fluorescent immunoassays could transition into a POC device where many analytes can be distinguished both spatially and spectrally.

Therefore, this project contributed to our scientific knowledge by providing a unique multiplexed optical sensor that performs better than existing platforms due to its miniaturized format, low sample volume requirements, and its POC amenability.

This platform was applied to detection of emerging AKI biomarkers, which could eventually aid in improving medical interventions and treatment.

This work has demonstrated the potential of using a planar surface fluorescent immunoassay for clinical *in vitro* diagnostic applications and personalized medicine. As the fields of microfluidics and nanotechnology and biomaterials develop, assay formats will become simpler and more accessible. Use of POC devices to meet a variety of clinical needs such as diagnosing diseases, determining prognosis, and selecting the best therapy, is on the horizon.

Future Directions

Improvements in Experimental Techniques

This work focused on the need for detecting numerous proteins simultaneously using optical sensors. Microtiter plate fluorescent immunoassays as well as planar surface fluorescent immunoassays were shown to be capable of multiplexing, but improvements could be made to both techniques. Microtiter plate experiments require relatively large volumes of reagents and samples and rely upon large laboratory instrumentation. These drawbacks limit the utility of this type of assay for a POC environment. On the other hand, planar surface fluorescent immunoassays use much smaller volumes, but still rely upon skilled laboratory personnel to carry out the methods. Development of this assay for actual clinical use would require automation of the immobilization chemistry, automation of the template production (used in patterning and performing the assay), and automation of data analysis to minimize

user interaction. Future work can also evaluate the potential for storage of slides in a dry setting at room temperature so that the device is ready for use at any time.

The current design of the planar surface fluorescent immunoassay can be improved in terms of limit of detection, sample throughput, and analyte throughput. According to Surinova, et al., the device would currently be classified as having a high LOD, and low sample and analyte throughput [225]. Improving the LOD to below 1 ng/mL and increasing the sample throughput to more than 1000/day and analyte throughput to more than 100 would make this new technology more attractive for future development.

Point-of-Care Development

The planar surface fluorescent immunoassay was used for detection of multiple protein analytes both spatially and spectrally by employing QDs as tracers and an evanescent wave scanner for imaging. Detection of more than two analytes in a single spot would make this device more desirable for point-of-care development. In order to realize the application of this sensor for clinical use, further studies demonstrating detection of many analytes by pairing each with different QDs should be conducted. The limit to the number of analytes that may be detected within a single spot depends upon the diversity of the QDs and the availability of distinct filters that can block out other wavelengths.

Another avenue for future work is to develop an easier way for discerning concentrations with a digital interface. Integration of the assay platform with the detection system featuring a digital readout for each spot on the slide would assist with interpretation of results. Further development of a handheld, self-contained POC device using an evanescent wave scanner or other technology would be instrumental in the potential marketability of the device. It may be possible to use CCDs or alternate cameras used in camera phones or smartphones for the design of a POC device that can deconvolute signals from different QDs.

Acute Kidney Injury Biomarker Panel

More studies are needed to determine definitively whether or not a normal reference interval is appropriate for assessing levels of KIM-1 and NGAL in plasma and urine. Currently, no reference ranges for these markers have been accepted or recognized by the medical community. Some studies indicate that reference intervals may not be appropriate for these biomarkers and that monitoring levels of these proteins over time may provide more useful clues regarding a person's health status [24]. More research is needed so that the medical community can confidently know the best way to interpret these biomarker measurements. With this knowledge, the scientific community can design medical devices more appropriately to detect AKI biomarkers using proper specifications.

Since only two biomarkers were investigated with regard to assessing renal injury, incorporation of additional biomarkers into the study design may be useful. Some

traditional biomarkers used for renal damage detection that could be included in future studies are N-acetyl-β-glucosaminidase, a urinary enzyme located in the lysosomes of the proximal tubules and γ-glutamyltransferase, a protein located on the outer membrane of the kidney [180]. These markers are very good indicators of early renal damage, but could not be tested in our studies because measurements need to be taken at the time of urine collection, making retrospective measurements impossible. Future studies would require ongoing animal studies for data collection.

Examples of some novel biomarkers that have already been qualified and may indicate damage to different regions of the kidney are albumin (glomerulus) and TFF-3 (distal tube), to name a few (Figure 43) [180]. Cystatin C may be of particular interest because it is independent of muscle mass, gender, and age, and can indicate damage in both the glomerulus and proximal tubule of the kidney. Another protein that could have significant use for incorporation into a POC device is β2-microglobulin because it is stable over a large range of pH and can also indicate damage to both the glomerulus and proximal tubule. Assessment of total urinary protein may provide insight regarding kidney damage, but this could be challenging to assess using a miniaturized optical sensor platform due to space limitations. There are numerous other qualified biomarkers as well as those that are considered "exploratory" that might be worthwhile for testing. Investigating detection of additional biomarkers may yield clinical results that have greater utility.

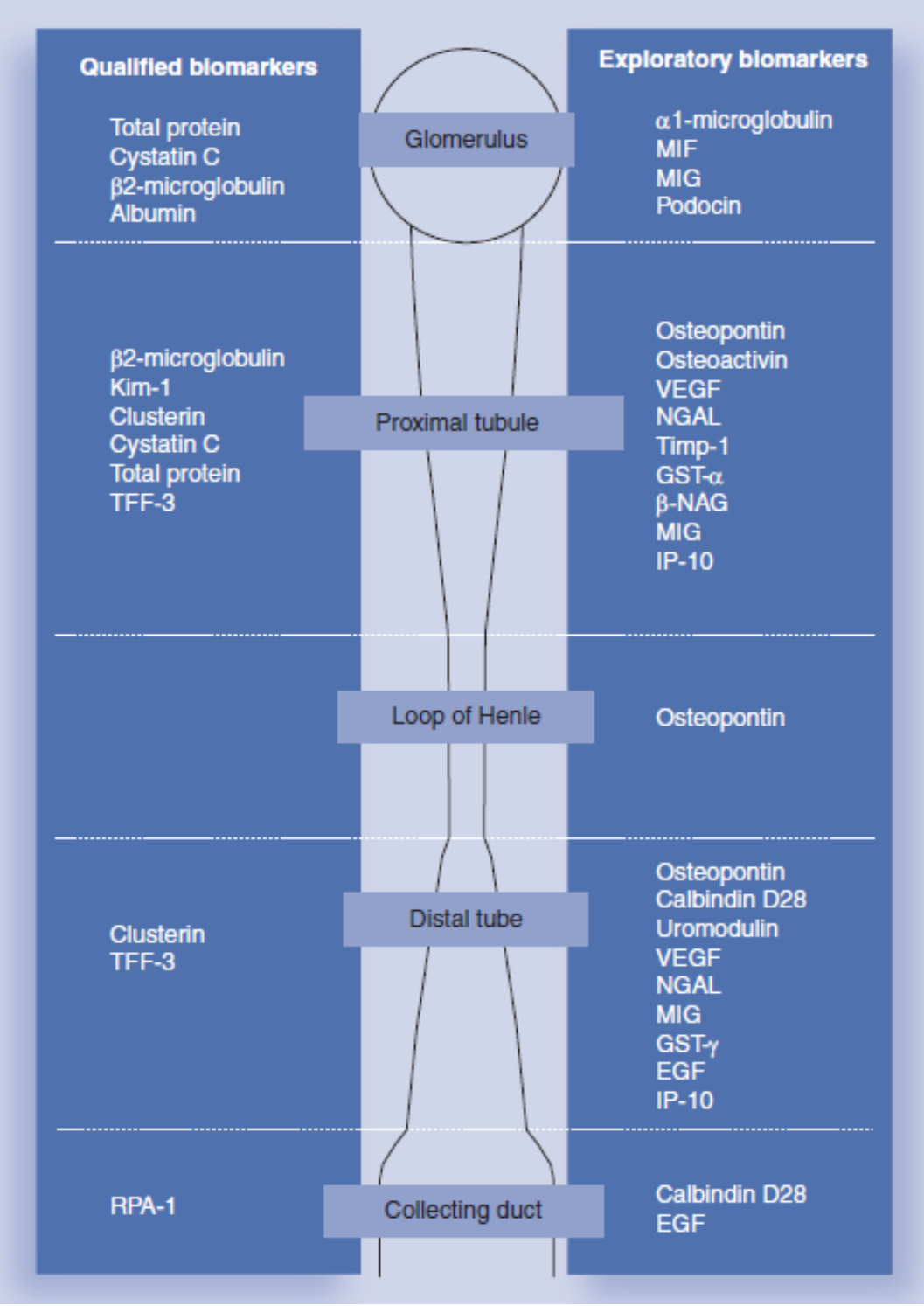

Figure 43. Qualified and exploratory kidney biomarkers and region of detection within the nephron [180]

More experiments are needed to demonstrate the effectiveness of biomarkers by testing retrospective samples with known disease outcomes, prospective samples from the intended patient population, and random samples from a target population [225]. Not only is it important to multiplex more biomarkers, it is important to test their usability in other biosensing contexts besides the planar surface fluorescent immunoassays developed in this work [180]. Further studies can provide greater insight into the understanding of kidney disease as well as improve the performance of new biomarkers.

While this work focused on the public health concern of detecting Acute Kidney Injury biomarkers that can indicate damage earlier than current techniques, this technology may be applied to detecting other types of clinically-relevant biomarkers as well. Planar surface fluorescent immunoassays may also be useful for detecting analytes for environmental monitoring, to ensure food safety, to aid in drug enforcement activities, and for defense needs.

Appendices

Appendix A: Variation of fluorescence at different concentrations using various Cy5-avidin labels (Chapter 3)

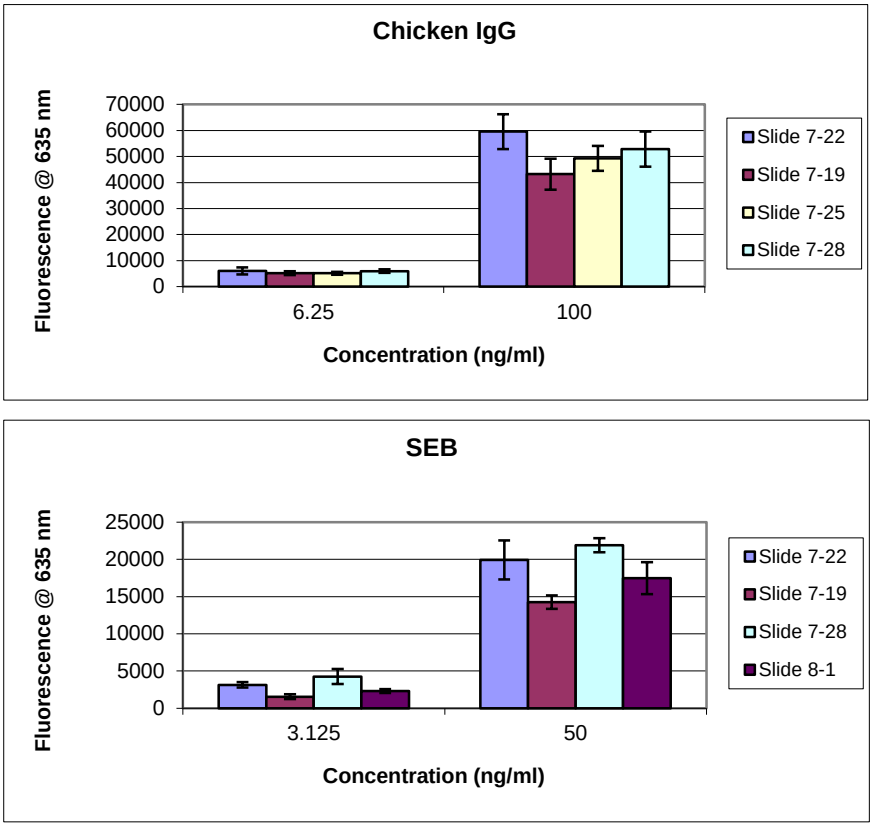

Figure 44. Variation of fluorescence among slides at low and high concentrations for chicken IgG or SEB sandwich assays using JacksonImmuno Streptavidin

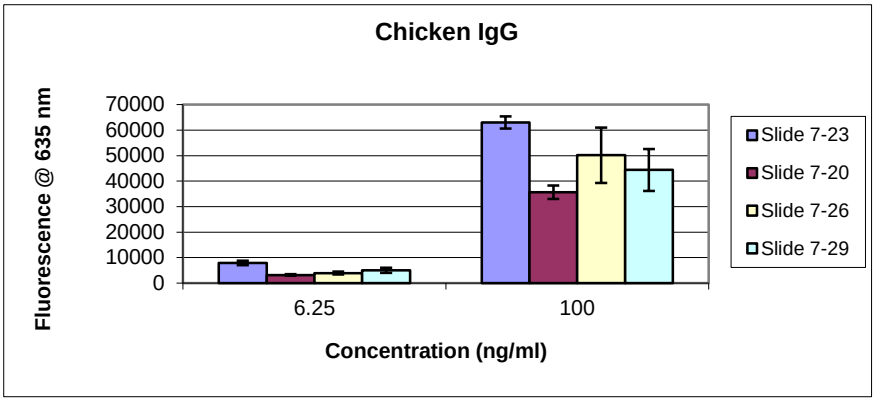

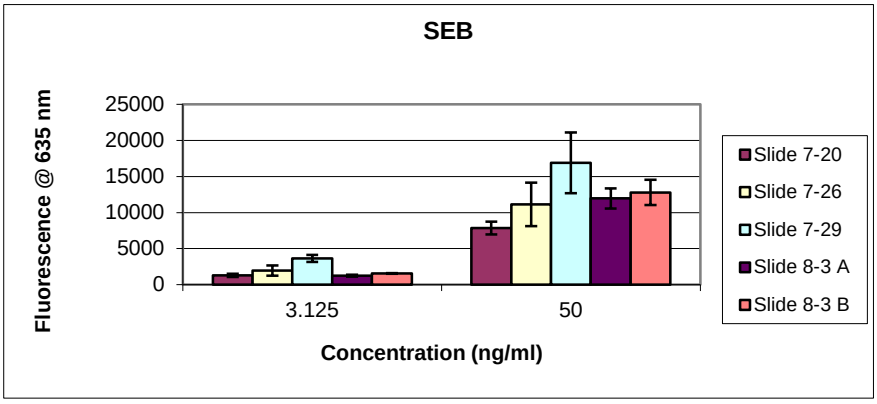

Figure 45. Variation of fluorescence among slides at low and high concentrations for chicken IgG or SEB sandwich assays using ThermoScientific NeutrAvidin

Appendix B: Spatial Analysis of Planar Surface Fluorescent Immunoassays (Chapter 4)

A spatial analysis was conducted on all 108 spots per slide to determine whether specific spots on the slide have a greater probability of having more variability than others (Schematic 1). The purpose of the analysis was to elucidate whether there are inconsistencies in the surface functionalization and if so, whether this inconsistency typically shows up in the same regions of the slide. This analysis was conducted on both raw data and normalized data. Data was normalized to the corresponding spot on the slide exposed to the highest concentration of the analyte. An average of replicates at the highest concentration was used to normalize each spot exposed to the highest concentration. This was necessary to avoid a value of 1.0 for all of the spots exposed to the highest concentration so that variability between these spots could be ascertained. Standard deviations were obtained at all corresponding spots exposed to a particular concentration of antigen among slides. Of the four or five spots exposed to the same concentration of analyte, the spot with the lowest and highest standard deviations were identified. Out of the six concentrations per analyte per slide, the probability of one particular spot having the highest or lowest standard deviation is x/6. Those percentages were converted to probabilities. Even though certain spots may look like they have a high probability for being variable, when the total number of slides analyzed per tracer is taken into account, at most, only 30% of all of the slides analyzed had high variances at the same spot number. Therefore, this analysis revealed that there is no systematic error for the variation between spots. Rather, the variation is random.

Another spatial analysis was conducted to determine overall how replicate spots differ from one another on one slide (Schematic 2). This analysis revealed the average intra-slide variation for each particular tracer. In this analysis, replicate spots exposed to the same concentration of antigen and the same tracer were analyzed using raw data in one analysis and normalized data in separate analysis. Each set of spots exposed to the same concentration of antigen on one slide have an average and a standard deviation among the replicate spots. Using these values, a percent standard deviation was obtained for each set of spots exposed to the same concentration per slide. Then, each of the percent standard deviations at a particular concentration were averaged to obtain one overall percent standard deviation per slide. Finally, each percent standard deviation per slide was averaged to obtain one value per tracer. Overall, each analyte had an average percent standard deviation of roughly 20%, which is adequate for a biological assay.

In addition to an analysis among replicate spots described above, another analysis was conducted based on the average of replicate spots compared to other slides exposed to the same tracer, Cy5 (Schematic 3). This analysis revealed the average inter-slide variation for each particular tracer. The purpose of this analysis was to determine how much one set of spots differ from another set of spots regardless of the exposure to a specific concentration of the antigen. In this analysis, the average fluorescence (or normalized fluorescence) at the highest concentration and the standard deviation among replicate spots exposed to the same concentration of analyte were obtained. The percent standard deviation (standard deviation/mean) was

obtained for each concentration of analyte. These values were averaged to determine the overall percent standard deviation for each tracer. Overall, each analyte had an average standard deviation of roughly 20%, which is adequate for a biological assay. Therefore, this analysis bolsters the argument that variation among spots is not affected by spatial position. Rather, variation is consistent regardless of exposure to a different concentration of analyte.

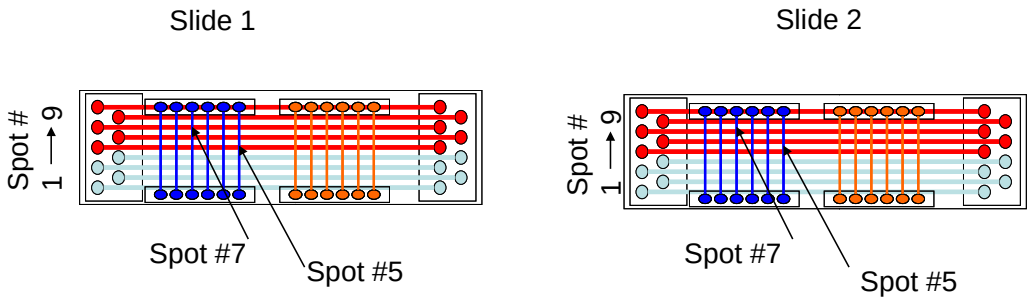

Schematic 1

Analysis Among Replicate Spots (How do they differ?)

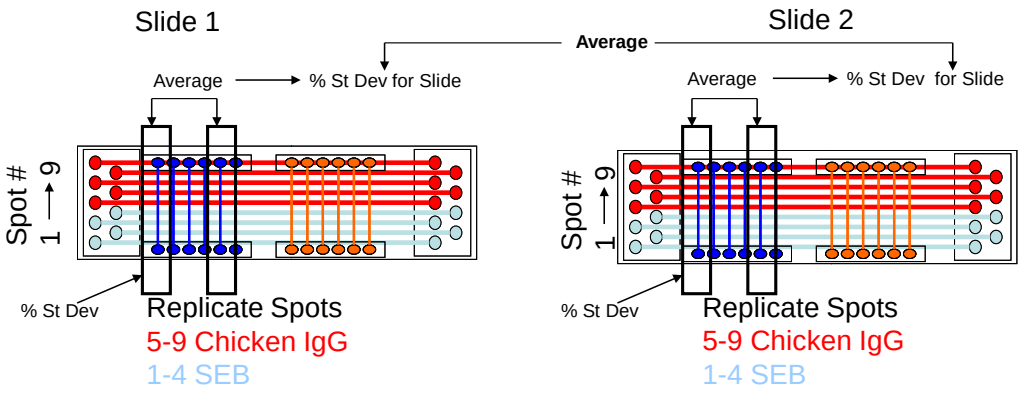

Intra-Slide Variation
1) Calculate % Standard Deviation among replicate spots
2) Average % Standard Deviations at each concentration on one slide
3) Obtain one % standard deviation for each slide
4) Average % standard deviations among slides to obtain one overall variance

Schematic 2

Analysis on Average of Replicate Spots
(How do sets of spots differ?)

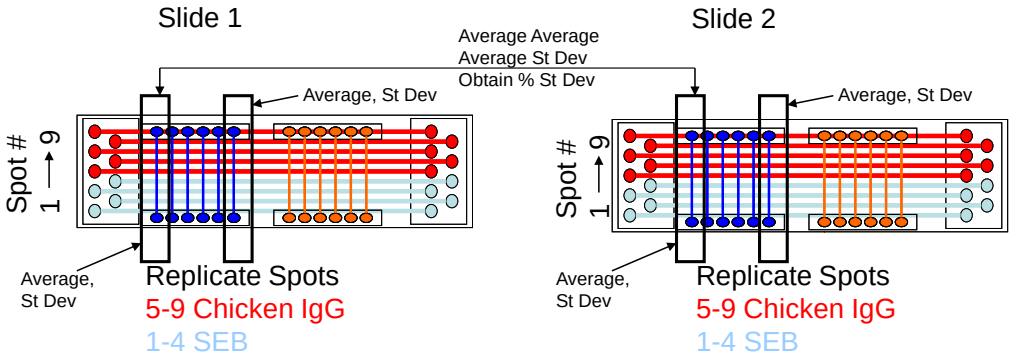

Inter-Slide Variation

1) Calculate average fluorescence and standard deviation at each concentration of analyte per slide
2) Average the fluorescence at each concentration among slides
3) Average the standard deviations at each concentration among slides
4) Calculate the % standard deviation using the values above to obtain one % standard deviation per concentration
5) Average percent standard deviations to obtain one overall variance

Schematic 3

Bibliography

1. Frank, R. and R. Hargreaves, *Clinical biomarkers in drug discovery and development.* Nature Reviews Drug Discovery, 2003. **2**(7): p. 566-580.
2. Phan, J.H., et al., *Convergence of biomarkers, bioinformatics and nanotechnology for individualized cancer treatment.* Trends in Biotechnology, 2009. **27**(6): p. 350-358.
3. Marrer, E. and F. Dieterle, *Impact of biomarker development on drug safety assessment.* Toxicology and Applied Pharmacology, 2010. **243**(2): p. 167-179.
4. Yu, X.B., N. Schneiderhan-Marra, and T.O. Joos, *Protein Microarrays for Personalized Medicine.* Clinical Chemistry, 2010. **56**(3): p. 376-387.
5. Blair, E.D., *Molecular diagnostics and personalized medicine: value-assessed opportunities for multiple stakeholders.* Personalized Medicine, 2010. **7**(2): p. 143-161.
6. Sapsford, K.E., et al., *Biomarkers to improve the benefit/risk balance for approved therapeutics: a US FDA perspective on personalized medicine.* Therapeutic delivery, 2010. **1**(5): p. 631-41.
7. Gubala, V., et al., *Point of Care Diagnostics: Status and Future.* Analytical Chemistry, 2012. **84**(2): p. 487-515.
8. Atkinson, A.J., et al., *Biomarkers and surrogate endpoints: Preferred definitions and conceptual framework.* Clinical Pharmacology & Therapeutics, 2001. **69**(3): p. 89-95.
9. Aggarwal, B.B., et al., *Models for prevention and treatment of cancer: problems vs promises.* Biochemical pharmacology, 2009. **78**(9): p. 1083-1094.
10. Donzella, V. and F. Crea, *Optical biosensors to analyze novel biomarkers in oncology.* Journal of Biophotonics. **4**(6): p. 442-452.
11. Wu, A.H.B., N. Babic, and K.T.J. Yeo, *Implementation of pharmacogenomics into the clinical practice of therapeutics: issues for the clinician and the laboratorian.* Personalized Medicine, 2009. **6**(3): p. 315-327.
12. Chau, C.H., et al., *Validation of Analytic Methods for Biomarkers Used in Drug Development.* Clinical Cancer Research, 2008. **14**(19): p. 5967-5976.
13. Apweiler, R., et al., *Approaching clinical proteomics: current state and future fields of application in fluid proteomics.* Clinical Chemistry and Laboratory Medicine, 2009. **47**(6): p. 724-744.
14. Regnier, F.E., et al., *Protein-Based Multiplex Assays: Mock Presubmissions to the US Food and Drug Administration.* Clinical Chemistry, 2010. **56**(2): p. 165-171.
15. Rodriguez, H., et al., *Analytical Validation of Protein-Based Multiplex Assays: A Workshop Report by the NCI-FDA Interagency Oncology Task Force on Molecular Diagnostics.* Clinical Chemistry, 2010. **56**(2): p. 237-243.
16. Lee, J.-R., et al., *Emerging protein array technologies for proteomics.* Expert Review of Proteomics, 2013. **10**(1): p. 65-75.
17. Wild, D.G., *The Immunoassay Handbook: Theory and applications of ligand binding, ELISA and related techniques*. 2013: Access Online via Elsevier.

18. Jennings, T.L., et al., *Reactive Semiconductor Nanocrystals for Chemoselective Biolabeling and Multiplexed Analysis.* ACS nano.
19. Varghese, S.S., et al., *FRET for lab-on-a-chip devices - current trends and future prospects.* Lab Chip, 2010. **10**(11): p. 1355-64.
20. Verch, T. and R. Bakhtiar, *Miniaturized immunoassays: moving beyond the microplate.* Bioanalysis, 2012. **4**(2): p. 177-88.
21. Yager, P., G.J. Domingo, and J. Gerdes, *Point-of-care diagnostics for global health.* Annual Review of Biomedical Engineering, 2008. **10**: p. 107-144.
22. Ligler, F.S., *Perspective on optical biosensors and integrated sensor systems.* Anal Chem, 2009. **81**(2): p. 519-26.
23. Rios, A., M. Zougagh, and M. Avila, *Miniaturization through lab-on-a-chip: utopia or reality for routine laboratories? A review.* Anal Chim Acta, 2012. **740**: p. 1-11.
24. Zhang, X.C., et al., *Analytical and biological validation of a multiplex immunoassay for acute kidney. injury biomarkers.* Clinica Chimica Acta, 2013. **415**: p. 88-93.
25. Sinha, V., L.M. Vence, and A.K. Salahudeen, *Urinary Tubular Protein-Based Biomarkers in the Rodent Model of Cisplatin Nephrotoxicity: A Comparative Analysis of Serum Creatinine, Renal Histology, and Urinary KIM-1, NGAL, and NAG in the Initiation, Maintenance, and Recovery Phases of Acute Kidney Injury.* Journal of Investigative Medicine, 2013. **61**(3): p. 564-568.
26. Hoffmann, D., et al., *Evaluation of a urinary kidney biomarker panel in rat models of acute and subchronic nephrotoxicity.* Toxicology. **277**(1-3): p. 49-58.
27. Klaassen, C., *Casarett & Doull's Toxicology: The Basic Science of Poisons, Seventh Edition*. McGraw Hill professional. 2007: Mcgraw-hill.
28. Han, M., et al., *Renal neutrophil gelatinase associated lipocalin expression in lipopolysaccharide-induced acute kidney injury in the rat.* Bmc Nephrology, 2012. **13**.
29. Amato, A.A., et al., *Harrison's Principles of Internal Medicine. 18th Edition*. 2012.
30. Delehanty, J.B. and F.S. Ligler, *A microarray immunoassay for simultaneous detection of proteins and bacteria.* Analytical Chemistry, 2002. **74**(21): p. 5681-5687.
31. VanMeter, A., et al., *Reverse-phase protein microarrays: application to biomarker discovery and translational medicine.* Expert Review of Molecular Diagnostics, 2007. **7**(5): p. 625-633.
32. Taitt, C.R., et al., *Array Biosensor for Toxin Detection: Continued Advances.* Sensors, 2008. **8**(12): p. 8361-8377.
33. Wilson, B., L.A. Liotta, and E. Petricoin, *Monitoring proteins and protein networks using reverse phase protein arrays.* Disease Markers. **28**(4): p. 225-232.
34. Samanta, D. and A. Sarkar, *Immobilization of bio-macromolecules on self-assembled monolayers: methods and sensor applications.* Chemical Society Reviews. **40**(5): p. 2567-2592.

35. Rapkiewicz, A., et al., *The needle in the haystack: Application of breast fine-needle aspirate samples to quantitative protein microarray technology.* Cancer Cytopathology, 2007. **111**(3): p. 173-184.
36. Balboni, I., et al., *Evaluation of microarray surfaces and arraying parameters for autoantibody profiling.* Clinical Immunology, 2008. **127**: p. S87-S87.
37. Balboni, I., et al., *Multiplexed protein array platforms for analysis of autoimmune diseases.* Annual Review of Immunology, 2006. **24**: p. 391-418.
38. Wong, D.S.Y. and G.K.H. Li, *The role of fine-needle aspiration cytology in the management of parotid tumors: A critical clinical appraisal.* Head and Neck-Journal for the Sciences and Specialties of the Head and Neck, 2000. **22**(5): p. 469-473.
39. Hughes, J.H. and M.B. Cohen, *Fine-needle aspiration of the pancreas.* Pathology (Philadelphia, Pa.), 1996. **4**(2): p. 389-407.
40. Al-Khafaji, B.M., B.R. Nestok, and R.L. Katz, *Fine-needle aspiration of 154 parotid masses with histologic correlation - Ten-year experience at the University of Texas MD Anderson Cancer Center.* Cancer Cytopathology, 1998. **84**(3): p. 153-159.
41. Florentine, B.D., et al., *The reliability of fine-needle aspiration biopsy as the initial diagnostic procedure for palpable masses - A 4-year experience of 730 patients from a community hospital-based outpatient aspiration biopsy clinic.* Cancer, 2006. **107**(2): p. 406-416.
42. Frates, M.C., et al., *Management of thyroid nodules detected at US: Society of Radiologists in Ultrasound consensus conference statement.* Ultrasound quarterly, 2006. **22**(4): p. 231.
43. Osuchowski, M.F. and D.G. Remick, *The repetitive use of samples to measure multiple cytokines: The sequential ELISA.* Methods, 2006. **38**(4): p. 304-311.
44. Sapsford, K.E., et al., *Miniaturized 96-well ELISA chips for staphylococcal enterotoxin B detection using portable colorimetric detector.* Analytical and Bioanalytical Chemistry, 2009. **394**(2): p. 499-505.
45. Thangawng, A.L., et al., *A hard microflow cytometer using groove-generated sheath flow for multiplexed bead and cell assays.* Analytical and Bioanalytical Chemistry. **398**(5): p. 1871-1881.
46. Godin, J., et al., *Microfluidics and photonics for Bio System on a Chip: A review of advancements in technology towards a microfluidic flow cytometry chip.* Journal of Biophotonics, 2008. **1**(5): p. 355-376.
47. Sencan, I., et al., *Spectral Demultiplexing in Holographic and Fluorescent On-chip Microscopy.* Scientific Reports, 2014. **4**.
48. Golden, J.P., et al., *A portable automated multianalyte biosensor.* Talanta, 2005. **65**(5): p. 1078-1085.
49. Arlett, J.L., E.B. Myers, and M.L. Roukes, *Comparative advantages of mechanical biosensors.* Nature Nanotechnology. **6**(4): p. 203-215.
50. King, K.D., et al., *Automated fiber optic biosensor for multiplexed immunoassays.* Environmental Science & Technology, 2000. **34**(13): p. 2845-2850.

51. Abbas, A., M.J. Linman, and Q.A. Cheng, *New trends in instrumental design for surface plasmon resonance-based biosensors.* Biosensors & Bioelectronics. **26**(5): p. 1815-1824.
52. Kumar, M.A., S. Jung, and T. Ji, *Protein Biosensors Based on Polymer Nanowires, Carbon Nanotubes and Zinc Oxide Nanorods.* Sensors. **11**(5): p. 5087-5111.
53. Buchapudi, K.R., et al., *Microcantilever biosensors for chemicals and bioorganisms.* Analyst. **136**(8): p. 1539-1556.
54. Anderson, G.P., B.M. Lingerfelt, and C.R. Taitt, *Eight analyte detection using a four-channel optical biosensor.* Sensor Letters, 2004. **2**(1): p. 18-24.
55. Washburn, A.L. and R.C. Bailey, *Photonics-on-a-chip: recent advances in integrated waveguides as enabling detection elements for real-world, lab-on-a-chip biosensing applications.* Analyst. **136**(2): p. 227-236.
56. Mittag, A. and A. Tarnok, *Recent Advances in Cytometry Applications: Preclinical, Clinical, and Cell Biology.* Methods in Cell Biology, Vol 103: Recent Advances in Cytometry, Part B: Advances in Applications, Fifth Edition. **103**: p. 3-20.
57. Golden, J.P., et al., *Multi-wavelength microflow cytometer using groove-generated sheath flow.* Lab on A Chip, 2009. **9**(13): p. 1942-1950.
58. Brauer, H.A., et al., *Biochips that sequentially capture and focus antigens for immunoaffinity MALDI-TOF MS: A new tool for biomarker verification.* Proteomics, 2010. **10**(21): p. 3922-3927.
59. Nelson, R.W., et al., *Mass spectrometric immunoassay.* Analytical chemistry, 1995. **67**(7): p. 1153-1158.
60. Chandra, H., P.J. Reddy, and S. Srivastava, *Protein microarrays and novel detection platforms.* Expert Review of Proteomics, 2011. **8**(1): p. 61-79.
61. El Khoury, G., et al., *Development of miniaturized immunoassay: Influence of surface chemistry and comparison with enzyme-linked immunosorbent assay and Western blot.* Analytical Biochemistry. **400**(1): p. 10-18.
62. Silvestri, A., et al., *Protein pathway biomarker analysis of human cancer reveals requirement for upfront cellular-enrichment processing.* Laboratory Investigation. **90**(5): p. 787-796.
63. Aebersold, R. and M. Mann, *Mass spectrometry-based proteomics.* Nature, 2003. **422**(6928): p. 198-207.
64. Sklar, L.A., et al., *Flow cytometric analysis of ligand-receptor interactions and molecular assemblies.* Annual Review of Biophysics and Biomolecular Structure, 2002. **31**: p. 97-119.
65. Laerum, O.D. and T. Farsund, *Clinical-Application of Flow-Cytometry - A Review.* Cytometry, 1981. **2**(1): p. 1-13.
66. Shoma, S., et al., *Development of a multiplexed bead-based immunoassay for the simultaneous detection of antibodies to 17 pneumococcal proteins.* European Journal of Clinical Microbiology & Infectious Diseases. **30**(4): p. 521-526.
67. van den Berg, S., et al., *A multiplex assay for the quantification of antibody responses in Staphylococcus aureus infections in mice.* Journal of Immunological Methods. **365**(1-2): p. 142-148.

68. Ravindranath, M.H., et al., *HLA-E monoclonal antibodies recognize shared peptide sequences on classical HLA class Ia: Relevance to human natural HLA antibodies.* Molecular Immunology. **47**(5): p. 1121-1131.
69. Liu, K.D., et al., *Serum Interleukin-6 and interleukin-8 are early biomarkers of acute kidney injury and predict prolonged mechanical ventilation in children undergoing cardiac surgery: a case-control study.* Critical Care, 2009. **13**(4).
70. de Keizer, W., et al., *Flow cytometric immunoassay for sulfonamides in raw milk.* Analytica Chimica Acta, 2008. **620**(1-2): p. 142-149.
71. Gibbs, J., *Selecting the Detection System - Colorimetric, Fluorescent, Luminescent Methods*, C. Incorporated, Editor 2001: Acton, MA. p. 1-14.
72. Lesch, H.P., et al., *Avidin-biotin technology in targeted therapy.* Expert Opinion on Drug Delivery, 2010. **7**(5): p. 551-564.
73. Wilchek, M., E.A. Bayer, and O. Livnah, *Essentials of biorecognition: The (strept)avidin-biotin system as a model for protein-protein and protein-ligand interaction.* Immunology Letters, 2006. **103**(1): p. 27-32.
74. Zempleni, J., S.S. Wijeratne, and Y.I. Hassan, *Biotin.* Biofactors, 2009. **35**(1): p. 36-46.
75. Liao, F., et al., *Homogeneous noncompetitive assay of protein via Forster-resonance-energy-transfer with tryptophan residue(s) as intrinsic donor(s) and fluorescent ligand as acceptor.* Biosensors & Bioelectronics, 2009. **25**(1): p. 112-117.
76. Oh, E., et al., *Inhibition assay of biomolecules based on fluorescence resonance energy transfer (FRET) between quantum dots and gold nanoparticles.* Journal of the American Chemical Society, 2005. **127**(10): p. 3270-3271.
77. Ji, E., D. Wu, and K.S. Schanze, *Intercalation-FRET Biosensor with a Helical Conjugated Polyelectrolyte.* Langmuir, 2010. **26**(18): p. 14427-14429.
78. Liu, L., et al., *Two-photon excitation fluorescence resonance energy transfer with small organic molecule as energy donor for bioassay.* Bioconjugate Chemistry, 2008. **19**(2): p. 574-579.
79. Büller, H.R., et al., *Enoxaparin followed by once-weekly idrabiotaparinux versus enoxaparin plus warfarin for patients with acute symptomatic pulmonary embolism: a randomised, double-blind, double-dummy, non-inferiority trial.* The Lancet. **379**(9811): p. 123-129.
80. Geissler, D., et al., *Quantum Dot Biosensors for Ultrasensitive Multiplexed Diagnostics.* Angewandte Chemie-International Edition, 2010. **49**(8): p. 1396-1401.
81. Charbonniere, L.J., et al., *Lanthanides to quantum dots resonance energy transfer in time-resolved fluoro-immunoassays and luminescence microscopy.* Journal of the American Chemical Society, 2006. **128**(39): p. 12800-12809.
82. Gu, J.-Q., et al., *Resonance energy transfer in steady-state and time-decay fluoro-immunoassays for lanthanide nanoparticles based on biotin and avidin affinity.* Journal of Physical Chemistry C, 2008. **112**(17): p. 6589-6593.
83. Soh, N., et al., *Sequential Injection Immunoassay for Environmental Measurements.* Analytical Sciences, 2011. **27**(11): p. 1069-1076.

84. Lin, C.H., et al., *Quantitative measurement of binding kinetics in sandwich assay using a fluorescence detection fiber-optic biosensor.* Analytical Biochemistry, 2009. **385**(2): p. 224-228.
85. Hage, D.S., *Immunoassays.* Analytical Chemistry, 1993. **65**(12): p. R420-R424.
86. Kambegawa, A., *[Enzyme labeling methods and it's specificities]*. Nippon rinsho.Japanese journal of clinical medicine, 1995. **53**(9): p. 2160-2167.
87. Coenen, D., et al., *Technical and diagnostic performance of 6 assays for the measurement of citrullinated protein/peptide antibodies in the diagnosis of rheumatoid arthritis.* Clinical Chemistry, 2007. **53**(3): p. 498-504.
88. Righetti, P.G., et al., *Quantitative proteomics: a review of different methodologies.* European Journal of Mass Spectrometry, 2004. **10**(3): p. 335-348.
89. Kricka, L.J., *Stains, labels and detection strategies for nucleic acids assays.* Annals of Clinical Biochemistry, 2002. **39**: p. 114-129.
90. Oleinikov, V.A., *Fluorescent semiconductor nanocrystals (quantum dots) in protein biochips.* Russian Journal of Bioorganic Chemistry. **37**(2): p. 151-167.
91. Resch-Genger, U., et al., *Quantum dots versus organic dyes as fluorescent labels.* Nat Meth, 2008. **5**(9): p. 763-775.
92. Sapsford, K.E., L. Berti, and I.L. Medintz, *Fluorescence resonance energy transfer - Concepts, applications and advances.* Minerva Biotecnologica, 2004. **16**(4): p. 247-273.
93. Morales-Narvaez, E., et al., *Signal Enhancement in Antibody Microarrays Using Quantum Dots Nanocrystals: Application to Potential Alzheimer's Disease Biomarker Screening.* Analytical Chemistry, 2012. **84**(15): p. 6821-6827.
94. Zhuang, Z., Q. Peng, and Y. Li, *Controlled synthesis of semiconductor nanostructures in the liquid phase.* Chem Soc Rev, 2011. **40**(11): p. 5492-513.
95. Samir, T.M., et al., *Quantum dots: heralding a brighter future for clinical diagnostics.* Nanomedicine, 2012. **7**(11): p. 1755-1769.
96. Han, J.H., et al., *Photonic Crystal Lab-On-a-Chip for Detecting Staphylococcal Enterotoxin B at Low Attomolar Concentration.* Analytical Chemistry, 2013. **85**(6): p. 3104-3109.
97. Salmain, M., et al., *Piezoelectric immunosensor for direct and rapid detection of staphylococcal enterotoxin A (SEA) at the ng level.* Biosensors & Bioelectronics, 2011. **29**(1): p. 140-144.
98. Vinayaka, A.C. and M.S. Thakur, *An immunoreactor-based competitive fluoroimmunoassay for monitoring staphylococcal enterotoxin B using bioconjugated quantum dots.* Analyst, 2012. **137**(18): p. 4343-4348.
99. Xue, P., et al., *Novel chemiluminescent assay for staphylococcal enterotoxin B.* Microchimica Acta, 2011. **174**(1-2): p. 167-174.
100. Dinges, M.M., P.M. Orwin, and P.M. Schlievert, *Exotoxins of Staphylococcus aureus.* Clinical microbiology reviews, 2000. **13**(1): p. 16.
101. *Bioterrorism Agents/Diseases*. [cited 2013 August 12, 2013]; Available from: http://www.bt.cdc.gov/agent/agentlist-category.asp.

102. Phillips, K.S. and Q. Cheng, *Microfluidic immunoassay for bacterial toxins with supported phospholipid bilayer membranes on poly(dimethylsiloxane).* Analytical Chemistry, 2005. **77**(1): p. 327-334.
103. Bakaltcheva, I.B., et al., *Multi-analyte explosive detection using a fiber optic biosensor.* Analytica Chimica Acta, 1999. **399**(1-2): p. 13-20.
104. Kattah, M.G., P.J. Utz, and I. Balboni, *Protein microarrays address the elephant in the room.* Clinical Chemistry, 2008. **54**(6): p. 937-939.
105. Choi, S., et al., *Microfluidic-based biosensors toward point-of-care detection of nucleic acids and proteins.* Microfluidics and Nanofluidics. **10**(2): p. 231-247.
106. Cunningham, B.T., *Photonic Crystal Surfaces as a General Purpose Platform for Label-Free and Fluorescent Assays.* Journal of the Association for Laboratory Automation. **15**(2): p. 120-135.
107. Mukundan, H., et al., *Waveguide-based biosensors for pathogen detection.* Sensors, 2009. **9**(7): p. 5783-5809.
108. Orellana, G. and D. Haigh, *New trends in fiber-optic chemical and biological sensors.* Current analytical chemistry, 2008. **4**(4): p. 273-295.
109. Leung, A., P.M. Shankar, and R. Mutharasan, *A review of fiber-optic biosensors.* Sensors and Actuators B: Chemical, 2007. **125**(2): p. 688-703.
110. Deiss, F., et al., *Nanostructured optical fibre arrays for high-density biochemical sensing and remote imaging.* Analytical and Bioanalytical Chemistry. **396**(1): p. 53-71.
111. Weiss, S.M., G. Rong, and J.L. Lawrie, *Current status and outlook for silicon-based optical biosensors.* Physica E: Low-dimensional Systems and Nanostructures, 2009. **41**(6): p. 1071-1075.
112. Walt, D.R., *Fibre optic microarrays.* Chem.Soc.Rev., 2009. **39**(1): p. 38-50.
113. Tam, J.M., L. Song, and D.R. Walt, *DNA detection on ultrahigh-density optical fiber-based nanoarrays.* Biosensors and Bioelectronics, 2009. **24**(8): p. 2488-2493.
114. Yu, X., et al., *Qantifying antibody binding on protein microarrays using microarray nonlinear calibration.* Biotechniques, 2013. **54**(5): p. 257-+.
115. Mustafa, S.A., J.D. Hoheisel, and M.S.S. Alhamdani, *Secretome profiling with antibody microarrays.* Molecular Biosystems, 2011. **7**(6): p. 1795-1801.
116. Stoll, D., et al., *Protein microarray technology.* Front Biosci, 2002. **7**: p. c13-32.
117. Hartmann, M., et al., *Protein microarrays for diagnostic assays.* Analytical and bioanalytical chemistry, 2009. **393**(5): p. 1407-1416.
118. Griffiths, J., *The way of the array.* AnAlytiCAl ChEmistry, 2007. **79**(23): p. 8833-8837.
119. Short, J.D., et al., *AMPK-Mediated Phosphorylation of Murine p27 at T197 Promotes Binding of 14-3-3 Proteins and Increases p27 Stability.* Molecular Carcinogenesis, 2010. **49**(5): p. 429-439.
120. Tang, J., et al., *Rapid and simultaneous detection of Ureaplasma parvum and Chlamydia trachomatis antibodies based on visual protein microarray using gold nanoparticles and silver enhancement.* Diagnostic Microbiology and Infectious Disease, 2010. **67**(2): p. 122-128.

121. Ghosh, G., A.G. Lee, and S.P. Palecek, *Hydrogel-based protein array for quantifying epidermal growth factor receptor activity in cell lysates.* Analytical Biochemistry, 2009. **393**(2): p. 205-214.
122. Hurst, R., et al., *Protein-protein interaction studies on protein arrays: Effect of detection strategies on signal-to-background ratios.* Analytical Biochemistry, 2009. **392**(1): p. 45-53.
123. Park, S., et al., *Carbohydrate microarrays.* Chemical Society Reviews, 2013. **42**(10): p. 4310-4326.
124. Nijdam, A.J., et al., *Application of Physicochemically Modified Silicon Substrates as Reverse-Phase Protein Microarrays.* Journal of Proteome Research, 2009. **8**(3): p. 1247-1254.
125. Hirlekar Schmid, A., et al., *Site-directed antibody immobilization on gold substrate for surface plasmon resonance sensors.* Sensors and Actuators B: Chemical, 2006. **113**(1): p. 297-303.
126. Weiping, Q., et al., *Site-directed immobilization of immunoglobulin G on 3-aminopropyltriethoxylsilane modified silicon wafer surfaces.* Materials Science and Engineering: C, 1999. **8–9**(0): p. 475-480.
127. Nijdam, A.J., et al., *Physicochemically modified silicon as a substrate for protein microarrays.* Biomaterials, 2007. **28**(3): p. 550-558.
128. Cretich, M., et al., *High Sensitivity Protein Assays on Microarray Silicon Slides.* Analytical Chemistry, 2009. **81**(13): p. 5197-5203.
129. Leatzow, D.M., et al., *Attachment of plastic fluidic components to glass sensing surfaces.* Biosensors and Bioelectronics, 2002. **17**(1): p. 105-110.
130. Rao, S.V., K.W. Anderson, and L.G. Bachas, *Oriented immobilization of proteins.* Mikrochimica Acta, 1998. **128**(3-4): p. 127-143.
131. Gregorius, K. and M. Theisen, *In situ deprotection: A method for covalent immobilization of peptides with well-defined orientation for use in solid phase immunoassays such as enzyme-linked immunosorbent assay.* Analytical Biochemistry, 2001. **299**(1): p. 84-91.
132. Rowe-Taitt, C.A., et al., *Simultaneous detection of six biohazardous agents using a planar waveguide array biosensor.* Biosensors and Bioelectronics, 2000. **15**(11–12): p. 579-589.
133. Bilitewski, U., et al., *Biochemical analysis with microfluidic systems.* Analytical and Bioanalytical Chemistry, 2003. **377**(3): p. 556-569.
134. Figeys, D., *Adapting arrays and lab-on-a-chip technology for proteomics.* Proteomics, 2002. **2**(4): p. 373-382.
135. Liu, W., et al., *SlipChip for immunoassays in nanoliter volumes.* Analytical chemistry, 2010. **82**(8): p. 3276-3282.
136. Wang, E., et al., *A portable fiberoptic ratiometric fluorescence analyzer provides rapid point-of-care determination of glomerular filtration rate in large animals.* Kidney international, 2011. **81**(1): p. 112-117.
137. *Research International: Bioidentification Systems*. 11/08/01/; Available from: http://www.resrchintl.com/Identify.html.
138. Lenz, D.E., A.A. Brimfield, and L.A. Cook, *Development of immunoassays for detection of chemical warfare agents*, in *Immunochemical Technology for*

Environmental Applications, D.S. Aga and E.M. Thurman, Editors. 1997. p. 77-86.
139. Singh, A.K., L.H. Stanker, and S.K. Sharma, *Botulinum neurotoxin: Where are we with detection technologies?* Critical Reviews in Microbiology, 2013. **39**(1): p. 43-56.
140. Bernard, A., B. Michel, and E. Delamarche, *Micromosaic immunoassays.* Analytical Chemistry, 2001. **73**(1): p. 8-12.
141. Murphy, B.M., D.S. Dandy, and C.S. Henry, *Analysis of oxidative stress biomarkers using a simultaneous competitive/non-competitive micromosaic immunoassay.* Analytica Chimica Acta, 2009. **640**(1–2): p. 1-6.
142. Jansen, H., et al., *A survey on the reactive ion etching of silicon in microtechnology.* Journal of micromechanics and microengineering, 1996. **6**(1): p. 14.
143. McDonald, J.C. and G.M. Whitesides, *Poly(dimethylsiloxane) as a Material for Fabricating Microfluidic Devices.* Accounts of Chemical Research, 2002. **35**(7): p. 491-499.
144. Sapsford, K.E., et al., *Optimizing Two-Color Semiconductor Nanocrystal Immunoassays in Single Well Microtiter Plate Formats.* Sensors, 2011. **11**(8): p. 7879-7891.
145. Chaubaroux, C., et al., *Collagen-Based Fibrillar Multilayer Films Cross-Linked by a Natural Agent.* Biomacromolecules, 2012. **13**(7): p. 2128-2135.
146. Jung, C.C., et al., *RAPTOR: A fluoroimmunoassay-based fiber optic sensor for detection of biological threats.* Ieee Sensors Journal, 2003. **3**(4): p. 352-360.
147. Chivers, C.E., et al., *How the biotin-streptavidin interaction was made even stronger: investigation via crystallography and a chimaeric tetramer.* Biochemical Journal. **435**: p. 55-63.
148. Sapsford, K.E. and F.S. Ligler, *Real-time analysis of protein adsorption to a variety of thin films.* Biosensors & Bioelectronics, 2004. **19**(9): p. 1045-1055.
149. Danczyk, R., et al., *Comparison of antibody functionality using different immobilization methods.* Biotechnology and bioengineering, 2003. **84**(2): p. 215-223.
150. Anderson, G.P. and C.R. Taitt, *Amplification of microsphere-based microarrays using catalyzed reporter deposition.* Biosensors & Bioelectronics, 2008. **24**(2): p. 324-328.
151. Kim, J.S., et al., *Multiplexed Detection of Bacteria and Toxins Using a Microflow Cytometer.* Analytical Chemistry, 2009. **81**(13): p. 5426-5432.
152. Kim, J.S., et al., *Multiplexed magnetic microsphere immunoassays for detection of pathogens in foods.* Sensing and instrumentation for food quality and safety, 2010. **4**(2): p. 73-81.
153. Pauly, D., et al., *Simultaneous quantification of five bacterial and plant toxins from complex matrices using a multiplexed fluorescent magnetic suspension assay.* Analyst, 2009. **134**(10): p. 2028-2039.
154. Simonova, M.A., et al., *Development of xMAP Assay for Detection of Six Protein Toxins.* Analytical Chemistry, 2012. **84**(15): p. 6326-6330.

155. Wang, J., et al., *Simultaneous detection of five biothreat agents in powder samples by a multiplexed suspension array.* Immunopharmacology and Immunotoxicology, 2009. **31**(3): p. 417-427.
156. Garber, E.A.E., K.V. Venkateswaran, and T.W. O'Brien, *Simultaneous Multiplex Detection and Confirmation of the Proteinaceous Toxins Abrin, Ricin, Botulinum Toxins, and Staphylococcus Enterotoxins A, B, and C in Food.* Journal of Agricultural and Food Chemistry, 2010. **58**(11): p. 6600-6607.
157. Parker, C.T., et al., *Comparison of genotypes of Salmonella enterica serovar Enteritidis phage type 30 and 9c strains isolated during three outbreaks associated with raw almonds.* Applied and environmental microbiology, 2010. **76**(11): p. 3723-3731.
158. Lee, J.H., et al., *High-Throughput Screening of Small Molecule Ligands Targeted to Live Bacteria Surface.* Analytical chemistry, 2013. **85**(7): p. 3508-3514.
159. Molina, D.M., et al., *Identification of immunodominant antigens of< i> Chlamydia trachomatis</i> using proteome microarrays.* Vaccine, 2010. **28**(17): p. 3014-3024.
160. Ng, A.C., U. Uddayasankar, and A. Wheeler, *Immunoassays in microfluidic systems.* Analytical and Bioanalytical Chemistry, 2010. **397**(3): p. 991-1007.
161. Dong, Y., K.S. Phillips, and Q. Cheng, *Immunosensing of Staphylococcus enterotoxin B (SEB) in milk with PDMS microfluidic systems using reinforced supported bilayer membranes (r-SBMs).* Lab on A Chip, 2006. **6**(5): p. 675-681.
162. Liu, F., et al., *Highly Sensitive Microplate Chemiluminescence Enzyme Immunoassay for the Determination of Staphylococcal Enterotoxin B Based on a Pair of Specific Monoclonal Antibodies and Its Application to Various Matrices.* Analytical Chemistry, 2010. **82**(18): p. 7758-7765.
163. Yacoub-George, E., et al., *Automated 10-channel capillary chip immunodetector for biological agents detection.* Biosensors & Bioelectronics, 2007. **22**(7): p. 1368-1375.
164. Yang, M., et al., *Carbon Nanotubes with Enhanced Chemiluminescence Immunoassay for CCD-Based Detection of Staphylococcal Enterotoxin B in Food.* Analytical Chemistry, 2008. **80**(22): p. 8532-8537.
165. Clarizia, L.J., et al., *Antibody orientation enhanced by selective polymer-protein noncovalent interactions.* Analytical and Bioanalytical Chemistry, 2009. **393**(5): p. 1531-1538.
166. Zengin, A. and T. Caykara, *Controlling immunoglobulin G orientation on a protein-A terminated bilayer system.* Materials Science & Engineering C-Materials for Biological Applications. **32**(5): p. 1107-1111.
167. Wen, X.F., H.Y. He, and L.J. Lee, *Specific antibody immobilization with biotin-poly(L-lysine)-g-poly(ethylene glycol) and protein A on microfluidic chips.* Journal of Immunological Methods, 2009. **350**(1-2): p. 97-105.
168. Kim, H., et al., *Analysis of direct immobilized recombinant protein G on a gold surface.* Ultramicroscopy, 2008. **108**(10): p. 1152-1156.

169. Bae, Y.M., et al., *Study on orientation of immunogrlobulin G on protein G layer.* Biosensors & Bioelectronics, 2005. **21**(1): p. 103-110.
170. Guo, S.L., et al., *A Fast Universal Immobilization of Immunoglobulin G at 4 degrees C for the Development of Array-based Immunoassays.* Plos One. **7**(12).
171. Kim, E.S., et al., *Synergistic effect of orientation and lateral spacing of protein G on an on-chip immunoassay.* Analyst. **137**(10): p. 2421-2430.
172. Shen, G.Y., et al., *Improvement of antibody immobilization using hyperbranched polymer and protein A.* Analytical Biochemistry. **409**(1): p. 22-27.
173. Farris, L.R. and M.J. McDonald, *Computational analysis of non-covalent polymer-protein interactions governing antibody orientation.* Analytical and Bioanalytical Chemistry, 2012. **402**(4): p. 1731-1736.
174. Ji, T., et al., *Increased Sensitivity in Antigen Detection with Fluorescent Latex Nanosphere-IgG Antibody Conjugates.* Bioconjugate Chemistry. **21**(3): p. 427-435.
175. Jia, L.L., et al., *An Attempt to Understand Kidney's Protein Handling Function by Comparing Plasma and Urine Proteomes.* Plos One, 2009. **4**(4).
176. Zhou, Y., et al., *Comparison of kidney injury molecule-1 and other nephrotoxicity biomarkers in urine and kidney following acute exposure to gentamicin, mercury, and chromium.* Toxicological sciences, 2008. **101**(1): p. 159.
177. Corradi, M., et al., *Early markers of nephrotoxicity in patients with metal-on-metal hip arthroplasty.* Clinical Orthopaedics and Related Research®, 2011. **469**(6): p. 1651-1659.
178. Martensson, J., et al., *Neutrophil gelatinase-associated lipocalin in adult septic patients with and without acute kidney injury.* Intensive Care Medicine, 2010. **36**(8): p. 1333-1340.
179. de Geus, H.R., et al., *Time of injury affects urinary biomarker predictive values for acute kidney injury in critically ill, non-septic patients.* BMC Nephrol, 2013. **14**(1): p. 273.
180. Fuchs, T.C. and P. Hewitt, *Preclinical perspective of urinary biomarkers for the detection of nephrotoxicity: what we know and what we need to know.* Biomarkers in Medicine, 2011. **5**(6): p. 763-779.
181. Anderson, N.L., et al., *The human plasma proteome.* Mol Cell Proteomics, 2004. **3**(4): p. 311-326.
182. Han, W.K., et al., *Kidney Injury Molecule-1 (KIM-1): a novel biomarker for human renal proximal tubule injury.* Kidney international, 2002. **62**(1): p. 237-244.
183. Martino, F.K., et al., *Neutrophil Gelatinase-Associated Lipocalin in the Early Diagnosis of Peritonitis: The Case of Neutrophil Gelatinase-Associated Lipocalin*, in *Peritoneal Dialysis - State-of-the-Art 2012*, C. Ronco, M.H. Rosner, and C. Crepaldi, Editors. 2012. p. 258-263.
184. Vashist, S.K., M. Saraswat, and H. Holthšfer, *Development of a Rapid Sandwich Enzyme Linked Immunoassay Procedure for the Highly Sensitive*

Detection of Human Lipocalin-2/NGAL. Procedia Chemistry, 2012. **6**(0): p. 141-148.
185. *Mayo Renal Laboratory Urinary NGAL Normals*. 2013 August 2009 [cited 2013 7/29/2013]; Available from: http://www.mayomedicallaboratories.com/articles/hottopics/transcripts/2009/2009-8b-renal-failure/8b-18.html.
186. Dent, C., et al., *Plasma neutrophil gelatinase-associated lipocalin predicts acute kidney injury, morbidity and mortality after pediatric cardiac surgery: a prospective uncontrolled cohort study.* Critical Care, 2007. **11**(6): p. R127.
187. Devarajan, P., *Review: Neutrophil gelatinase-associated lipocalin: A troponin-like biomarker for human acute kidney injury.* Nephrology, 2010. **15**(4): p. 419-428.
188. Hoffmann, D., et al., *Performance of Novel Kidney Biomarkers in Preclinical Toxicity Studies.* Toxicological sciences. **116**(1): p. 8-22.
189. Moreno-Navarrete, J.M., et al., *Metabolic endotoxemia and saturated fat contribute to circulating NGAL concentrations in subjects with insulin resistance.* International Journal of Obesity, 2010. **34**(2): p. 240-249.
190. Chew, S.T. and L.K. Ti, *Ethnicity and acute kidney injury: the correct definition of acute kidney injury?* Br J Anaesth, 2014. **112**(1): p. 177.
191. Rossetti, R., S. Nakahara, and L.E. Brus, *QUANTUM SIZE EFFECTS IN THE REDOX POTENTIALS, RESONANCE RAMAN-SPECTRA, AND ELECTRONIC-SPECTRA OF CDS CRYSTALLITES IN AQUEOUS-SOLUTION.* Journal of Chemical Physics, 1983. **79**(2): p. 1086-1088.
192. Murray, C.B., C.R. Kagan, and M.G. Bawendi, *Synthesis and characterization of monodisperse nanocrystals and close-packed nanocrystal assemblies.* Annual Review of Materials Science, 2000. **30**: p. 545-610.
193. Dabbousi, B.O., et al., *(CdSe)ZnS core-shell quantum dots: Synthesis and characterization of a size series of highly luminescent nanocrystallites.* Journal of Physical Chemistry B, 1997. **101**(46): p. 9463-9475.
194. Harris, J.M., *Poly (ethylene glycol) chemistry: biotechnical and biomedical applications*. 1992: Springer.
195. Sapsford, K.E., et al., *A fluorescence detection platform using spatial electroluminescent excitation for measuring botulinum neurotoxin A activity.* Biosensors & Bioelectronics, 2008. **24**(4): p. 618-625.
196. Sun, S., et al., *Multi-wavelength spatial LED illumination based detector for in vitro detection of botulinum neurotoxin A activity.* Sensors and Actuators B-Chemical. **146**(1): p. 297-306.
197. Sapsford, K.E., et al., *Functionalizing Nanoparticles with Biological Molecules: Developing Chemistries that Facilitate Nanotechnology.* Chemical Reviews, 2013. **113**(3): p. 1904-2074.
198. Goldman, E.R., et al., *Multiplexed toxin analysis using four colors of quantum dot fluororeagents.* Analytical Chemistry, 2004. **76**(3): p. 684-688.
199. Medintz, I.L., et al., *Multiplex Charge-Transfer Interactions between Quantum Dots and Peptide-Bridged Ruthenium Complexes.* Analytical Chemistry, 2009. **81**(12): p. 4831-4839.

200. *Cosmetics: Shelf Life/Expiration Date*. 2000 August 15, 2002 July 29, 2013]; Available from: http://www.fda.gov/Cosmetics/CosmeticLabelingLabelClaims/LabelClaimsandExpirationDating/ucm2005204.htm.
201. *Guidance for Federal Agencies and State and Local Governments Potassium Iodide Tablets Shelf Life Extension*. 2004 July 29, 2013]; Available from: http://www.fda.gov/downloads/Drugs/GuidanceComplianceRegulatoryInformation/Guidances/ucm080549.pdf
202. Chandrasekaran, A., et al., *Hybrid integrated silicon microfluidic platform for fluorescence based biodetection.* Sensors, 2007. **7**(9): p. 1901-1915.
203. Geho, D.H., et al., *Fluorescence-based analysis of cellular protein lysate arrays using quantum dots.* Methods in molecular biology (Clifton, N.J.), 2007. **374**: p. 229-237.
204. Petryayeva, E., W.R. Algar, and I.L. Medintz, *Quantum Dots in Bioanalysis: A Review of Applications Across Various Platforms for Fluorescence Spectroscopy and Imaging.* Applied Spectroscopy, 2013. **67**(3): p. 215-252.
205. Petryayeva, E., W.R. Algar, and U.J. Krull, *Adapting Fluorescence Resonance Energy Transfer with Quantum Dot Donors for Solid-Phase Hybridization Assays in Microtiter Plate Format.* Langmuir, 2013. **29**(3): p. 977-987.
206. Anderson, G.P., et al., *Single domain antibody–quantum dot conjugates for ricin detection by both fluoroimmunoassay and surface plasmon resonance.* Analytica Chimica Acta, 2013. **786**(0): p. 132-138.
207. Boeneman, K., et al., *Selecting Improved Peptidyl Motifs for Cytosolic Delivery of Disparate Protein and Nanoparticle Materials.* Acs Nano, 2013. **7**(5): p. 3778-3796.
208. Gemmill, K.B., et al., *Optimizing Protein Coordination to Quantum Dots with Designer Peptidyl Linkers.* Bioconjugate Chemistry, 2013. **24**(2): p. 269-281.
209. Hildebrandt, N., *Biofunctional Quantum Dots: Controlled Conjugation for Multiplexed Biosensors.* Acs Nano, 2011. **5**(7): p. 5286-5290.
210. Jennings, T.L., et al., *Simplistic Attachment and Multispectral Imaging with Semiconductor Nanocrystals.* Sensors, 2011. **11**(11): p. 10557-10570.
211. Liu, X., et al., *Chemiluminescence and Chemiluminescence Resonance Energy Transfer (CRET) Aptamer Sensors Using Catalytic Hemin/G-Quadruplexes.* Acs Nano, 2011. **5**(9): p. 7648-7655.
212. Nonat, A., et al., *Definition of an Intramolecular Eu-to-Eu Energy Transfer within a Discrete Eu2L Complex in Solution.* Chemistry-a European Journal, 2012. **18**(26): p. 8163-8173.
213. Pelaz, B., et al., *Interfacing Engineered Nanoparticles with Biological Systems: Anticipating Adverse NanoBio Interactions.* Small, 2013. **9**(9-10): p. 1573-1584.
214. Stender, A.S., et al., *Single Cell Optical Imaging and Spectroscopy.* Chemical Reviews, 2013. **113**(4): p. 2469-2527.
215. Tavasoli, E., et al., *Surface Doping Quantum Dots with Chemically Active Native Ligands: Controlling Valence without Ligand Exchange.* Chemistry of Materials, 2012. **24**(21): p. 4231-4241.

216. Vannoy, C.H., et al., *A competitive displacement assay with quantum dots as fluorescence resonance energy transfer donors.* Analytica Chimica Acta, 2013. **759**: p. 92-99.
217. Vela, J., *Molecular Chemistry to the Fore: New Insights into the Fascinating World of Photoactive Colloidal Semiconductor Nanocrystals.* Journal of Physical Chemistry Letters, 2013. **4**(4): p. 653-668.
218. Nepal, D., et al., *Large Scale Solution Assembly of Quantum Dot-Gold Nanorod Architectures with Plasmon Enhanced Fluorescence.* Acs Nano, 2013. **7**(10): p. 9064-9074.
219. Skripka, A., et al., *Two-photon excited quantum dots as energy donors for photosensitizer chlorin e(6).* Journal of Biomedical Optics, 2013. **18**(7).
220. Steponkiene, S., et al., *Cellular Uptake and Photosensitizing Properties of Quantum Dot-Chlorin e(6) Complex: In Vitro Study.* Journal of Biomedical Nanotechnology, 2014. **10**(4): p. 679-686.
221. Tyrakowski, C.M. and P.T. Snee, *A primer on the synthesis, water-solubilization, and functionalization of quantum dots, their use as biological sensing agents, and present status.* Physical Chemistry Chemical Physics, 2014. **16**(3): p. 837-855.
222. Wegner, K.D., et al., *Quantum-Dot-Based Forster Resonance Energy Transfer Immunoassay for Sensitive Clinical Diagnostics of Low-Volume Serum Samples.* Acs Nano, 2013. **7**(8): p. 7411-7419.
223. Probst, C.E., et al., *Quantum dots as a platform for nanoparticle drug delivery vehicle design.* Advanced Drug Delivery Reviews, 2013. **65**(5): p. 703-718.
224. Yu, D.H., et al., *Biosensors in drug discovery and drug analysis.* Analytical Letters, 2005. **38**(11): p. 1687-1701.
225. Surinova, S., et al., *On the development of plasma protein biomarkers.* Journal of proteome research, 2010. **10**(1): p. 5-16.